DETERMINATION OF MIX PROPORTION OF HARDENED CONCRETE CONTAINING FLY ASH OR LIMESTONE POWDER

Miss Thidaporn Chuosavasdi

A Dissertation Submitted in Partial Fulfillment of the Requirements
for the Degree of Doctor of Philosophy Program in Civil Engineering
Department of Civil Engineering
Faculty of Engineering
Chulalongkorn University
Academic Year 2014

การประเมินสัดส่วนผสมของคอนกรีตผสมเถ้าลอย และคอนกรีตผสมฝุ่นหินปูนในคอนกรีตที่แข็งตัวแล้ว

นางสาวธิดาพร เชื้อสวัสดิ์

วิทยานิพนธ์นี้เป็นส่วนหนึ่งของการศึกษาตามหลักสูตรปริญญาวิศวกรรมศาสตรดุษฎีบัณฑิต
สาขาวิชาวิศวกรรมโยธา ภาควิชาวิศวกรรมโยธา
คณะวิศวกรรมศาสตร์ จุฬาลงกรณ์มหาวิทยาลัย
ปีการศึกษา 2557

Thesis Title	DETERMINATION OF MIX PROPORTION OF HARDENED CONCRETE CONTAINING FLY ASH OR LIMESTONE POWDER
By	Miss Thidaporn Chuosavasdi
Field of Study	Civil Engineering
Thesis Advisor	Associate Professor Boonchai Stitmannaithum, D.Eng.
Thesis Co-Advisor	Assistant Professor Taweechai Sumranwanich, Ph.D.

Accepted by the Faculty of Engineering, Chulalongkorn University in Partial Fulfillment of the Requirements for the Doctoral Degree

.....Dean of the Faculty of Engineering
(Professor Bundhit Eua-arporn, Ph.D.)

THESIS COMMITTEE

.....Chairman
(Professor Teerapong Senjuntichai, Ph.D.)

.....Thesis Advisor
(Associate Professor Boonchai Stitmannaithum, D.Eng.)

.....Thesis Co-Advisor
(Assistant Professor Taweechai Sumranwanich, Ph.D.)

.....Examiner
(Assistant Professor Withit Pansuk, Ph.D.)

.....Examiner
(Associate Professor Phoonsak Pheinsusom, D.Eng.)

.....External Examiner
(Assistant Professor Warangkana Saengsoy, Ph.D.)

ธิดาพร เชื้อสวัสดิ์ : การประเมินสัดส่วนผสมของคอนกรีตผสมเถ้าลอยและคอนกรีตผสมฝุ่นหินปูนในคอนกรีตที่แข็งตัวแล้ว (DETERMINATION OF MIX PROPORTION OF HARDENED CONCRETE CONTAINING FLY ASH OR LIMESTONE POWDER) อ.ที่ปรึกษาวิทยานิพนธ์หลัก: รศ. ดร.บุญไชย สถิตมั่นในธรรม, อ.ที่ปรึกษาวิทยานิพนธ์ร่วม: ผศ. ดร.ทวีชัย สำราญวานิช, หน้า.

ในปัจจุบันได้มีการพัฒนาการตรวจสอบหาสัดส่วนผสมคอนกรีตที่หลากหลาย แต่ยังไม่มีวิธีการหาสัดส่วนผสมคอนกรีตใดที่แม่นยำและเป็นมาตรฐานการตรวจสอบที่เป็นที่ยอมรับกันโดยทั่วไป ทั้งนี้เนื่องจากวัสดุที่ใช้ในการทำคอนกรีตนั้นมีหลากหลาย อีกทั้งการวิเคราะห์ก็จะมีความยุ่งยากและซับซ้อนมากขึ้นเมื่อมีการใช้เถ้าลอยหรือสารผสมเพิ่มอื่นในคอนกรีตด้วย ทำให้วิธีการที่มีอยู่ในปัจจุบัน ส่วนใหญ่สามารถนำมาใช้ได้กับคอนกรีตที่ใช้ปูนซีเมนต์ล้วนเท่านั้น ไม่สามารถนำมาใช้ได้กับคอนกรีตที่มีเถ้าลอยหรือฝุ่นหินปูนเป็นส่วนผสม ซึ่งในปัจจุบันนี้ได้มีการนำเถ้าลอยและฝุ่นหินปูนมาใช้ในงานคอนกรีตกันอย่างแพร่หลาย ดังนั้น งานวิจัยนี้จึงมีวัตถุประสงค์เพื่อพัฒนาวิธีการวิเคราะห์หาสัดส่วนผสมของคอนกรีตที่แข็งตัวแล้วทั้งคอนกรีตใช้ปูนซีเมนต์ล้วน คอนกรีตผสมเถ้าลอยและคอนกรีตผสมฝุ่นหินปูน โดยได้คำนึงถึงคุณสมบัติที่หลากหลายของเถ้าลอยและฝุ่นหินปูนที่ใช้กันอย่างแพร่หลายในเมืองไทย รวมถึงการนำอัตราการเกิดปฏิกิริยาไฮเดรชันของปูนซีเมนต์และปฏิกิริยาปอสโซลานิคของเถ้าลอยมาใช้ในการวิเคราะห์ด้วยเพื่อให้สามารถหาสัดส่วนผสมของคอนกรีตที่แข็งตัวแล้วที่อายุใดๆได้ โดยงานวิจัยนี้ได้นำเสนอวิธีการวิเคราะห์หาสัดส่วนผสมคอนกรีต ได้แก่ อัตราส่วนน้ำต่อวัสดุประสาน ร้อยละการแทนที่เถ้าลอย ร้อยละการแทนที่ฝุ่นหินปูน ปริมาณปูนซีเมนต์ เถ้าลอย ฝุ่นหินปูน น้ำ มวลรวมละเอียดและมวลรวมหยาบ ซึ่งได้นำทั้งวิธีวิเคราะห์ทางกายภาพและทางเคมีมาใช้ในการวิเคราะห์โดยปริมาณมวลรวมหยาบสามารถหาได้จากการวิเคราะห์ทางภาพถ่าย (Image analysis) ส่วนอัตราส่วนน้ำต่อวัสดุประสาน สามารถหาได้จากการคำนวณย้อนกลับจากค่ากำลังรับแรงอัดโดยใช้คอมพิวเตอร์ซอร์ฟแวร์ “FACOMP” สำหรับปริมาณปูนซีเมนต์ เถ้าลอย ฝุ่นหินปูน และมวลรวมละเอียด จะคำนวณจากสมการสมดุลมวล (Mass balance equations) ร่วมกับการวิเคราะห์ทางเคมี ซึ่งสมการเหล่านี้จะถูกนำไปใช้ในการวิเคราะห์หาสัดส่วนผสมของคอนกรีตที่เตรียมในห้องปฏิบัติการที่ทราบสัดส่วนผสมคอนกรีตที่แท้จริงเพื่อตรวจสอบประสิทธิภาพของวิธีการที่ได้พัฒนาขึ้น ซึ่งจากผลการตรวจสอบ พบว่า วิธีการที่ได้นำเสนอสามารถนำมาใช้ในการวิเคราะห์หาสัดส่วนผสมคอนกรีตที่แข็งตัวแล้วได้อย่างแม่นยำ ทั้งคอนกรีตที่ใช้ปูนซีเมนต์ล้วน คอนกรีตผสมเถ้าลอยและคอนกรีตผสมฝุ่นหินปูน

ภาควิชา วิศวกรรมโยธา	ลายมือชื่อนิสิต .....
สาขาวิชา วิศวกรรมโยธา	ลายมือชื่อ อ.ที่ปรึกษาหลัก .....
ปีการศึกษา 2557	ลายมือชื่อ อ.ที่ปรึกษาร่วม .....

5071850121 : MAJOR CIVIL ENGINEERING
KEYWORDS: MIX PROPORTION / WATER TO BINDER RATIO / HARDENED CONCRETE / FLY ASH / LIMESTONE POWDER / IMAGE ANALYSIS / SELECTIVE DISSOLUTION

THIDAPORN CHUOSAVASDI: DETERMINATION OF MIX PROPORTION OF HARDENED CONCRETE CONTAINING FLY ASH OR LIMESTONE POWDER. ADVISOR: ASSOC. PROF. BOONCHAI STITMANNAITHUM, D.Eng., CO-ADVISOR: ASST. PROF. TAWEECHAI SUMRANWANICH, Ph.D., pp.

Nowadays, several techniques have been developed to identify mix proportion of hardened concrete. However, there is no universally applicable method for accurately determining mix proportion of hardened concrete because of the wide variety of materials from which concrete is made and the conditions to which it may have been subjected. The analysis is more complicated if fly ash or other admixtures are used in the concrete. Moreover, a promising method developed to identify the concrete mix design encompassing binder type, w/b, binder content and aggregate content does not exist. Even though standards such as ASTM C1084 and BS 1881: Part 124 described the methods for determining the cement content and other concrete compositions in the hardened concrete, they are applicable only for OPC concrete but not appropriate for concrete containing fly ash or limestone powder. In this study, a method for estimating mix proportion of hardened OPC concrete, fly ash concrete, and limestone powder concrete is proposed. Both physical and chemical methods were adopted for the analysis. The varying properties of fly ashes and limestone powders generally used in Thailand were taken into consideration. The degree of hydration of cement and the degree of pozzolanic reaction of fly ash were also taken into account in the analysis in order to cover the effect of age of concrete. The analytical procedures for evaluating fly ash and limestone powder existence and determination of water to binder ratio, fly ash replacement ratio, limestone powder replacement ratio and content of concrete compositions are described. In the analysis, three major investigation techniques are implemented. Image processing technique is used for determination of coarse aggregate content. Water to binder ratio can be calculated from data back analysis of the compressive strength by using the computer software, “FACOMP”. Cement, fly ash, limestone powder and sand contents are obtained from a set of mass balance equations. The proposed equations were applied to estimate mix proportions of concrete prepared in the laboratory with known mix design in order to verify efficiency of the proposed method. From the analytical results, it was found that the proposed method could be used to precisely estimate mix proportion of concrete with different types and replacement ratios of binder, different water to binder ratios, and different aggregate contents, at any age of concrete. The effect of age of concrete on determination of mix proportion of hardened concrete can be covered by taking into account the time-dependent degree of hydration in the analysis.

Department:	Civil Engineering	Student's Signature	.....
Field of Study:	Civil Engineering	Advisor's Signature	.....
Academic Year:	2014	Co-Advisor's Signature	.....

ACKNOWLEDGEMENTS

The author wishes to express her profound gratitude and sincerest appreciation to her advisor, Associate Professor Dr. Boonchai Stitmannaithum, and her Co-advisor, Assistant Professor Dr. Taweechai Sumranwanich, for their invaluable guidance, encouragement and support during my research.

The author also wishes to express her appreciation and gratitude to the external committee member Dr. Warangkana Saengsoy for her invaluable guidance, encouragement, interesting suggestions and fruitful information throughout the thesis work; and devoting her valuable time to serve as the external examiner of the thesis committee.

Great appreciations are conveyed to the committee members, Professor Dr. Teerapong Senjuntichai, Associate Professor Dr. Phoonsak Pheinsusom, and Assistant Professor Dr. Withit Pansuk for their valuable advices and devoting their valuable time to serve as members of the thesis committee. And the author wishes to acknowledge Professor Dr. Somnuk Tangtermsirikul for his helps and suggestions during the thesis work

Grateful acknowledgements are conveyed to Construction and Maintenance Technology Research Center (CONTEC), Sirindhorn International Institute of Technology (SIIT), National Metal and Materials Technology Center (MTEC), and Burapha University for instrument support of doing research in their Laboratory; and the office of the higher education commission (OHEC) for the scholarship support to the author for funding Ph.D. project through Burapha University. Acknowledgement is also extended to the BLCP Power Company and the Mae Moh power plant for supporting fly ash for her experimental research.

Furthermore, the author would like to thank her sending institution – Burapha University (BUU) and host institution - Chulalongkorn University (CU) for giving me the opportunity to study Ph.D degree under AUN/SEED-Net program.

Finally, yet importantly, the author sincerely and gratefully dedicates this work to her beloved parents for their tremendous encouragement, support and sacrifice to her study and all of her life.

CONTENTS

Page

Page

Page

LIST OF TABLES

LIST OF FIGURES

CHAPTER 1
INTRODUCTION

1.1 General

In the past, major materials used in concrete mix proportion are cement, fine aggregate, coarse aggregate and water. Nowadays, other materials are additionally used in producing concrete to improve many properties of the concrete and to reduce cost of the concrete by either adding or replacing cement with some materials such as limestone powder, fly ash, bottom ash, silica flume and slag. However, these materials should be put in the concrete with the right proportion because applying them without prior studies may cause unexpected results. Mix proportion of concrete has influences on mechanical and durability properties of the concrete. For example, the water to binder ratio is one of the factors that are important to concrete properties, especially strength and durability of the concrete. Water is significant for the concrete reaction, which affects the properties and internal structure of concrete. If water is added in a high proportion, there might be too much porosity in the concrete. Conversely, if it is too little, the concrete might have low workability. Thus, all the materials used in producing concrete should be proportioned properly with specified construction and environment. As the concrete is an important component of reinforced concrete structures which are used widespread today, the concrete should have a good quality and be properly used for structures.

When the concrete problems occur, such as poor strength development occurred after casting in early age or the concrete is deteriorated before specified age, it is being suspicious of the concrete quality and it should be evaluated by some ways such as by construction records (both of procedures and materials), destructive and non-destructive tests, etc. If the examination turns out that the concrete is under qualified or does not follow the required design, a conflict between the owner and contractor may occur. Moreover, once the concrete structure is damaged, its concrete mix proportion is required to evaluate the durability and estimate the service life of the structure in order to assess the optimized repair technique. Then, the mix proportion is concerned as mentioned reasons. However, the record of concrete mix design is often unavailable in especially the structure was built for long time ago, leading to a difficulty in predicting the condition of the concrete structures.

1.2 Statement of Problem

To identify mix proportion of hardened concrete, several techniques have been developed. However, there is no universally applicable method for accurately determining mix proportion of hardened concrete because of the wide variety of materials from which concrete is made and the conditions to which it may have been subjected. The analysis is more complicated if fly ash or other admixtures are used in the concrete. Many different approaches are therefore necessary in those situations. Moreover, a promising method developed to identify the concrete mix design

encompassing binder type, w/c, cement content and aggregate content does not exist. Even though standards such as ASTM C1084 and BS 1881: Part 124 described the methods for determining the cement content and other concrete compositions in the hardened concrete, they are applicable only for OPC concrete but not appropriate for concrete containing fly ash or limestone powder. Moreover, the existing methods are applicable merely for determining mix proportion of hardened concrete at long age (mature concrete) or at a specified age (Jung, Shin et al. 2012). When these methods are applied for estimating mix proportion of hardened concrete at an arbitrarily early age, it may result in an inaccurate estimation. Accordingly, a method for estimating mix proportion of hardened OPC concrete, fly ash concrete, and limestone powder concrete is proposed in this study. The varying properties of fly ashes and limestone powders generally used in Thailand were taken into consideration. The degree of hydration of cement and the degree of pozzolanic reaction of fly ash were also taken into account in the analysis in order to cover the effect of age of concrete.

1.3 Objective of study

In the process of determination of mix proportion of hardened concrete, the existence and type of fly ash or limestone powder are needed to be investigated before determining the mix proportion.

The objectives of this research are as follows:

1. To develop an accurate and appropriate procedure for determining fly ash or limestone powder existence in hardened concrete and identifying their type.
2. To develop an accurate and appropriate procedure for determining the mix proportion of hardened concrete at different ages i.e. the mix proportion of plain cement concrete, concrete containing fly ash, and concrete containing limestone powder.
3. To apply the developed procedure for determining the mix proportion of hardened concrete exposed to real environment.

1.4 Scope of study

This study aims to determine the mix proportion of cement-only concretes, cement-fly ash concretes and cement-limestone powder concretes which are cast and cured in laboratory and also to find the mix proportion of cement-only concretes which are cast and cured in laboratory and then exposed in the marine environment of Thailand for four years. This study emphasizes to find the process of determination of fly ash or limestone powder, which widely used in Thailand, in concrete. The chemical admixtures affecting to chemical and physical properties of hardened concrete, such as accelerator and retarder admixtures, water-reducing admixture and shrinkage-reducing admixture and so on, are not taken into account in this study.

CHAPTER 2
THEORETICAL BACKGROUND AND LITERATURE REVIEWS

2.1 Introduction

In this chapter, the theoretical backgrounds of the determination of concrete materials and the estimation of the mix proportion of hardened concrete are presented. The methods of the previous researches related to this study are summarized.

2.2 Properties of Portland cement, fly ash and limestone powder

The abbreviation of chemical oxide components of binder are as following CaO(C), SiO_2 (S), Al_2O_3 (A), Fe_2O_3 (F), SO_3 ($\overline{S}$) and CO_3 ($\overline{C}$).

2.2.1 Portland cement

In general, Portland cement clinker is typically made from a combination of lime, silica, alumina, iron oxide and other minor constituents as magnesia, sodium, and potassium; and normally contains four major phases called alite (C_2S), belite (C_3S), aluminate (C_3A), and ferrite (C_4AF). Portland cement clinker emerges from a dry process kiln as rounded pellets, or from a wet process kiln as irregularly shaped lumps, in either case is typically dimension of 3-20 mm. Then cement powder is produced by crushing and grinding brittle clinker, therefore cement particles are angular and its size of an irregular particle cannot be given exactly by one number (Taylor 1997).

2.2.2 Fly ash

Fly ashes consist of finely divided ashes produced by burning pulverized coal in power stations. Owing to the high temperature reached during the instantaneous burning of coal, most of the mineral component contained in the coal melts and forms small fused drops. The subsequent sudden cooling transforms them partly or entirely into spherical glass particles. So, their chemical and phase compositions depend on those of the minerals associated with the coal and on the burning condition. Most of the fly ash particles are solid spheres, which are called precipitator, and some particles are hollow, which are called cenospheres. While, plerospheres are hollow particles of large diameter filled with smaller size precipitator and cenospheres. The particle sizes in fly ash vary from less than 1 μm to more the 100 μm. and typical morphologies of fly ash is shown in Figure 2.1

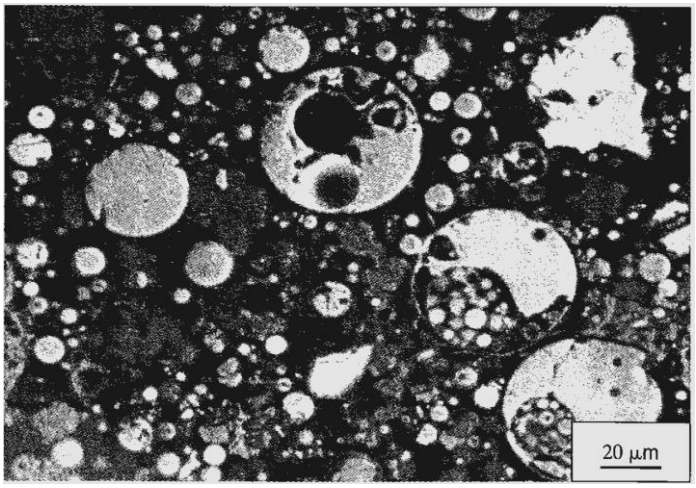

Figure 2.1Particle morphologies of fly ash
(Sidney, J. Francis et al. 2003) pp.101

Fly ash is considered to be a composition of relatively few mineral phases, since the coal mineral does not contain more components. Generally, fly ash is primarily glass containing silica, alumina, iron, and calcium. The American designations of Class F and Class C fly ashes which based on contents of (SiO_2 + $A1_2O_3$ + Fe_2O_3) are above and below 70%, respectively and corresponding to low CaO and high-CaO fly ashes. Minor constituents are magnesium, sulfur, sodium, potassium, and carbon. The good quality of Class F fly ashes have 70-90% glass, with quarzt, mullite, hematite and magnetite as the principle phases that crystallize from the glass during cooling. Almost of the iron is contained in the latter two phases. The crystalline phase occurring in class F fly ash are few, whereas many phases can be found in class C fly ash as a consequence of more variable chemical composition. Analysis of XRD has evidenced another crystalline phases: free lime (uncombined CaO), periclase, anhydrite, ferrite, spinel, merwinite and melilite. Some of these fly ash also may contain$C_4A_3\bar{S}$, C_3A and C_2S; these fly ashes will show cementitious tendencies and will become hard on the addition of water, whereas other pozzolans do not react with water only.

Booher, Martello et al. (1994) studied spherical particulates in fly ash from two bituminous coals, two subbituminous coals and one lignite by interference contrast polarized light microscopy (ICT-PLM) and scanning electron microscopy with energy dispersive spectroscopy (SEM-EDS). Different sphere sizes from each source fly ash were selected for observation by ICT-PLM. Most of the glassy spheres were between 8 and 50 µm in diameter. Second phase material was seen on many of the solid sphere surfaces. The potential for crystal formation in lignitic fly ash appears to be greater than in fly ashes from other coals.

Barzin, Aboozar et al. (2007) studied characteristic fly ash sample from nine PC power plants, using scanning electron microscope (SEM) and energy dispersive spectroscopy (EDS). The investigating found that the chemical and physical properties of fly ash particles are a function of the mineral in the coal, the combustion conditions, and post-combustion cooling. The fly ash samples consisted mostly of amorphous alumino-silicate spheres with a lesser number of iron-rich spheres. The majority of the iron-rich spheres consisted of two phases: an iron oxide mixed with

amorphous alumino-silicate (mullite). This mixing of phases is consistent throughoutthe amount of mixing varies with each fly ash particle, and several internal and surface textures were identified. This analysis indicated that the primary mineral/morphological structures are fairly common. Quartz and alumino-silicates are found as crystals and as amorphous particles, as the XRD data indicate that over 65% of the material in each of the sample analyzed was amorphous. The iron-rich phases identified by XRD are magnetite and hematite.

2.2.3 Limestone powder

Limestone is from sedimentary rock, which calcium carbonate is a primary component. The limestone is commonly interground with the clinker, and because of its softness becomes considerably finer. The limestone powder is the product of crushing and grinding, so its particle is likely angular shape of cement.

2.3 Hydration reaction and microstructure of cement-fly ash system

2.3.1 Hydration reaction of cement-fly ash system

Hydration reaction of cement-fly ash system can be divided into 2 main parts as hydration reaction of cement and pozzolanic reaction of fly ash.

Hydration reaction of cement:

When Portland cement is mixed with water, chemical compounds of cement will have chemical reaction and results in the hardening of concrete. Reactions of cement with water are called as hydration, and the new solids from hydration reaction are referred as hydration products.

Cement hydration is a complex reaction and it is appropriate to be considered as the reactions of the silicate phases (C_3S and C_2S) and the aluminate phases (C_3A and C_4AF) separately (Taylor 1997).Then, the hydration reaction of cement can be divided into 4 main reactions as follows:

Hydration of silicates

$$\boldsymbol{CS} + \boldsymbol{H} \rightarrow \boldsymbol{CSH} + \boldsymbol{CH}$$

Both C_3S and C_2S react with water to produce an amorphous calcium silicate hydrate known as C-S-H gel which is the main ‘glue’ which binds sand and aggregate particles together in concrete. The reaction of C_3S is much more reactive than C_2S.In the standard temperature condition of 20°C, approximately 50% of the C_3S presented in typical cement will be hydrated by 3 days and 80% by 28 days. In contrast, the hydration of C_2S does not normally show a significant reaction until approximately 14 days.

Hydration of C_3A and C_4AF

The reaction of C_3A with water is immediate. Crystalline hydrates, such as C_3AH_6, C_4AH_{19}, and C_2AH_8, are formed quickly, with liberation of a large amount of heat of hydration. Unless the rapid hydration of C_3A is slowed down by some method, Portland cement cannot be used for construction applications. This method is

generally accomplished by the addition of gypsum. Therefore, hydration reaction of C_3A with gypsum is in practical purpose.

$$\underset{}{C_3A} + \underset{\textit{(Gypsum)}}{3C\bar{S}H_2} + 26H \rightarrow \underset{\textit{(Ettringite or calcium sulfoaluminate hydrate)}}{C_6A\bar{S}_3H_{32}}$$

$$\underset{\textit{(Ettringite)}}{C_6A\bar{S}_3H_{32}} + 2C_3A + 4H \rightarrow \underset{\textit{(Calcium Monosulfoaluminate)}}{3C_4A\bar{S}H_{12}}$$

In the hydration of Portland cement, it is convenient to discuss the hydration reactions of C_3A and ferroaluminate together because when the ferroaluminate reacts with water in the presence of sulfate, the products formed are structurally similar to those formed in the hydration of C_3A. For instance, depending on the sulfate concentration, the hydration of C_4AF produces either $C_6A(F)\bar{S}H_{32}$ or $C_4A(F)\bar{S}H_{18}$, which are different in chemical composition, have crystal structures and are similar to ettringite and low sulfate, respectively. However, the ferroaluminate compound results in the early setting and hardening reaction which depends mainly on its chemical composition and temperature of formation. Generally, the reactivity of the ferrite phase is somewhat slower than C_3A, but it increases with increasing alumina content and with decreasing temperature of formation during the clinkering process. In any case, it may be noted that the hydration reaction of the aluminates described below are applicable to both the C_3A phase and the ferrite phase in Portland cement although.

Pozzolanic Reaction of Fly Ash:

When fly ash is added to concrete, the pozzolanic reaction occurs between the silica glass (SiO_2) and the calcium hydroxide ($Ca(OH)_2$) or hydrated lime, which is a by-product of the hydration of Portland cement.

The amorphous or glassy silica, which is the major component of a pozzolan, reacts with calcium hydroxide formed from the hydration of the calcium silicates. The principal reaction is

$$\underset{\textit{(Hydration Product)}}{CH} + \underset{\textit{(Silica in fly ash)}}{S} + H \rightarrow C-S-H$$

Small quantities of reactive alumina in a pozzolan generally substitute for silica as part of the C-S-H. When a pozzolan has appreciable quantities of reactive alumina, a separate set of secondary reactions can occur, leading to the formation of calcium aluminate hydrates C-A-H

$$\underset{\textit{(Hydration Product)}}{CH} + \underset{\textit{(Alumina in fly ash)}}{A} + H \rightarrow C-A-H$$

Then, the reactions of cement fly ash system which consist of both hydration reaction of cement and pozzolanic reaction of fly ash can be shown as:

$$\textbf{Portland cement} + \textbf{water} \rightarrow C-S-H, C-(A,F)-H + CH$$

$$\underset{(SiO_2,\ Al_2O_3)}{\textbf{Pozzolan}} + CH + \textbf{water} \rightarrow C-S-H, C-A-H$$

Thus, the reactions of cement-fly ash system produce the same compounds as those found upon hydration of Portland cement since the overall chemical compositions of the Portland cement and the fly ash are similar.

Hydration Mechanism

The effect of fly ash on the hydration of cement and clinker minerals appear to be complex, and may depend greatly on the chemical and physical nature of the fly ash. The observed changes may also depend on the water to cement ratio of the system. There appears to be retardation of the very early hydration of both C_3S and C_3A, as shown by heat evolution profiles over time. After the induction period, however, this is followed by increased formation of $Ca(OH)_2$ and C-S-H and also by increased formation of ettringite and its subsequent transformation to monosulphoaluminates. The prolongation of the induction period in C_3S hydration is probably due to the species dissolved from the fly ash into the aqueous phase of the hydrating system such as aluminate ions and organics which could delay the nucleation and crystallization of $Ca(OH)_2$ and/or C-S-H. There may also be a physical effect in which the fine fly-ash particles adhere to the surface of cement grain and thus hinder its interaction with water. Once the nucleation and crystallization of hydration products end the induction period, hydration is accelerated by the presence of fly ash. The fly-ash particles provide additional surfaces for the precipitation of the hydration products which would otherwise be formed on the surface of the C_3S, and hinder its interaction with water. Similar arguments may apply to the hydration of C_3A, where the initial retardation is probably due to calcium sulphate and alkalis (in addition to organics) dissolved from the fly ash. The precipitation of the hydration products on the fly-ash spheres may hinder the pozzolanic reaction. However, the alkaline solution may attack the glassy phase of the spheres beneath the coating of hydration products, leaving a clear space between the coating and the sphere

2.3.2 Microstructure of cement-fly ash system

The microstructure structure of cement-fly ash system is developed as result of chemical reaction between cement, fly ash and water. They are consists of many phases in paste as solids, voids and water (P. Kumar and Paulo J.M. 2006).

2.3.2.1. Solids in paste

The types, amounts, and characteristics of the four principal solid phases in the hydrated cement paste are as follows.

- Calcium silicate hydrate (C-S-H)

The calcium silicate hydrate phase makes up 50 to 60 percent of the volume of solids in a completely hydrated Portland cement paste and is, therefore, the most important phase determining the properties of the paste. The fact that the term C-S-H is hyphenated signifies that C-S-H is not a well-defined compound; the C/S ratio varies between 1.5 and 2.0 and the structural water content varies even more. The morphology of C-S-H also varies from poorly crystalline fibers to reticular network.

Due to their colloidal dimensions and a tendency to cluster, C-S-H crystals could only be resolved with the advent of electron microscopy. In older literature, the material is often referred to as *C-S-H gel*. The internal crystal structure of C-S-H also remains unresolved; previously it was assumed to resemble the natural mineral tobermorite and that is why C-S-H was sometimes called *tobermorite gel*.

Although the exact structure of C-S-H is not known, several models have been proposed to explain the properties of the materials. According to the *Powers-Brunauer model,* the material has a layer structure with a very high surface area. Depending on the measurement technique, surface areas on the order of 100 to 700 m^2/g have been proposed for C-S-H, and the strength of the material is attributed mainly to van der Waals' forces. The size of *gel pores*, or the solid-to-solid distance, is reported to be about 18 Å. The *Feldman-Sereda model*[2] visualizes the C-S-H structure as being composed of an irregular or kinked array of layers which are randomly arranged to create interlayer spaces of different shapes and sizes (5 to 25 Å).

- Calcium hydroxide. (CH)

Calcium hydroxide crystals (also called portlandite) constitute 20 to 25 percent of the volume of solids in the hydrated paste. In contrast to the C-S-H, calcium hydroxide is a compound with a definite stoichiometry, $Ca(OH)_2$. It tends to form large crystals with distinctive hexagonal-prism morphology. The morphology usually varies from nondescript to stacks of large plates, and is affected by the available space, temperature of hydration, and impurities present in the system. Compared with C-S-H, the strength-contributing potential of calcium hydroxide is limited as a result of considerably lower surface area.

- Calcium sulfoaluminates hydrates.

Calcium sulfoaluminate hydrates occupy 15 to 20 percent of the solid volume in the hydrated paste and, therefore, play only a minor role in the microstructure-property relationships. It has already been stated that during the early stages of hydration the sulfate/alumina ionic ratio of the solution phase generally favors the formation of trisulfate hydrate, $C_6A\bar{S}_3H_{32}$, also called *ettringite*, which forms needle-shaped prismatic crystals. In pastes of ordinary portland cement, ettringite eventually transforms to the monosulfate hydrate,$C_4A\bar{S}H_{12}$, which forms hexagonal-plate crystals. The presence of the monosulfate hydrate in portland cement concrete makes the concrete vulnerable to sulfate attack. It should be noted that both ettringite and the monosulfate contain small amounts of iron, which can substitute for the aluminum ions in the crystal structure.

- Unhydrated clinker grains and fly ash.

Depending on the particle size distribution of the anhydrous cement and the degree of hydration, some unhydrated clinker grains may be found in the microstructure of hydrated cement pastes, even long after hydration. As stated earlier, the clinker particles in modern portland cement generally conform to the size range 1 to 50μm. With the progress of the hydration process, the smaller particles dissolve first and disappear from the system, then the larger particles become smaller. Because of the limited available space between the particles, the hydration products tend to crystallize in close proximity to the hydrating clinker particles, which gives the appearance of a coating formation around them. At later ages, due to the lack of available space, *in situ* hydration of clinker particles results in the formation of a very

dense hydration product, the morphology of which may resemble the original clinker particle. In part of unhydrated fly ash, the glass in one fly ash cement was heavily etched after 7 days and that many of the particles up to 1-2μm in size were consumed within 28 days. The crystalline phases appeared to be inert.

2.3.2.2. Voids in paste

The hydrated cement paste contains several types of voids which have an important influence on its properties. The various types of voids and their amount and significance are discussed next

- Interlayer space in C-S-H.

Powers-Brunauer assumed the width of the interlayer space within the C-S-H structure to be 18 A° and determined that it accounts for 28 percent porosity in solid C-S-H; however, Feldman and Sereda suggested that the space may vary from 5 to 25 A°. This void size is too small to have an adverse effect on the strength and permeability of the hydrated cement paste. However, as discussed below, water in these small voids can be held by hydrogen bonding, and its removal under certain conditions may contribute to drying shrinkage and creep. In some old literature, the solid-to-solid distances between C-S-H layers were called *gel pores*.

- Capillary voids.

The total volume of capillary voids, popularly known as *porosity*, in Portland cement pastes, the capillary voids represent the space not filled by the solid components of the hydrated cement paste. The total volume of a typical cement-water mixture remains essentially unchanged during the hydration process. The average bulk density of the hydration products is considerably lower than the density of anhydrous Portland cement; it is estimated that 1 cm^3 of cement, on complete hydration, requires about 2 cm^3 of space to accommodate the products of hydration. Thus, cement hydration may be looked upon as a process during which the space originally occupied by cement and water is being replaced more and more by the space filled by hydration products. The space not taken up by the cement or the hydration products consists of capillary voids, the volume and size of the capillary voids being determined by the original distance between the anhydrous cement particles in the freshly mixed cement paste (i.e., water cement ratio).

In well-hydrated, low water-cement ratio pastes, the capillary voids may range from 10 to 50 nm; in high water-cement ratio pastes, at early ages of hydration, the capillary voids may be as large as 3 to 5μm. Capillary voids larger than 50 nm, referred to as *macropores*in modern literature, are probably more influential in determining the strength and impermeability characteristics, whereas voids smaller than 50 nm, referred to as *micropores*, play an important part in drying shrinkage and creep.

- Air voids.

Whereas capillary voids are irregular in shape, air voids are generally spherical. A small amount of air usually gets trapped in the cement paste during concrete mixing. For various reasons, admixtures may be added to concrete to entrain purposely tiny air voids. Entrapped air voids may be as large as 3 mm; entrained air voids usually range from 50 to 200 μm. Therefore, both the entrapped and entrained air voids in the hydrated cement paste are much bigger than the capillary voids, and are capable of adversely affecting the strength.

2.3.2.3. Water in paste

Actually, depending on the environmental humidity and the porosity of the paste, the untreated cement paste is capable of holding a large amount of water. Like the solid and the void phases discussed above, water can exist in the hydrated cement paste in many forms. The classification of water into several types is based on the degree of difficulty or ease with which it can be removed from the hydrated cement paste. As there is a continuous loss of water from a saturated cement paste when the relative humidity of the environment is reduced, the dividing line between the different states of water is not rigid. In spite of this, the classification is useful for understanding the properties of the hydrated cement paste. In addition to vapor in empty or partially water-filled voids, water exists in the hydrated cement paste in the following states:

- Capillary water

This is the water present in voids larger than about 50 A°. It may be pictured as the bulk water that is free from the influence of the attractive forces exerted by the solid surface. Actually, from the standpoint of the behavior of capillary water in the hydrated cement paste, it is desirable to divide the capillary water into two categories: the water in large voids of the order of >50 nm (0.05μm), which may be called *free water* (because its removal does not cause any volume change), and the water held by capillary tension in small capillaries (5 to 50 nm), the removal of which may cause shrinkage of the system.

- Adsorbed water

This is the water that is close to the solid surface. Under the influence of attractive forces, water molecules are physically adsorbed onto the surface of solids in the hydrated cement paste. It has been suggested that up to six molecular layers of water (15 A°) can be physically held by hydrogen bonding. Because the bond energies of the individual water molecules decrease with distance from the solid surface, a major portion of the adsorbed water can be lost when hydrated cement paste is dried to 30 percent relative humidity. The loss of adsorbed water is responsible for the shrinkage of the hydrated cement paste.

- Interlayer water

This is the water associated with the C-S-H structure. It has been suggested that a monomolecular water layer between the layers of C-S-H is strongly held by hydrogen bonding. The interlayer water is lost only on strong drying (i.e., below 11 percent relative humidity). The C-S-H structure shrinks considerably when the interlayer water is lost.

- Chemically combined water

This is the water that is an integral part of the microstructure of various cement hydration products. This water is not lost on drying; it is evolved when the hydrates decompose on heating. Based on the Feldman-Sereda model, different types of water associated with the C-S-H are illustrated in Figure 2.2.

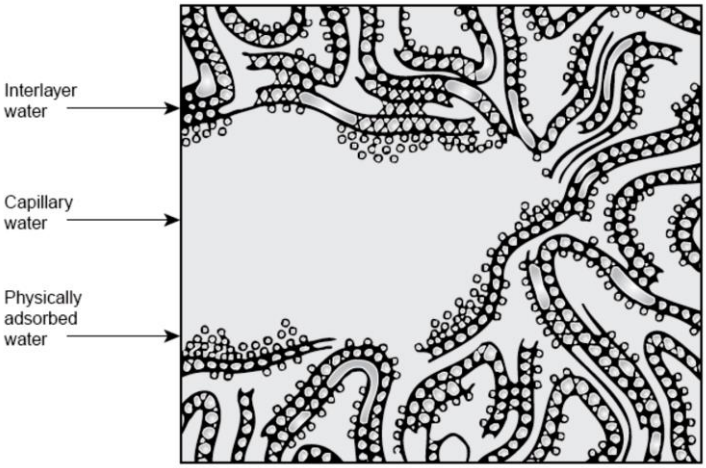

Figure 2.2 Diagrammatic model of the types of water associated with calcium silicate hydrate
(P. Kumar and Paulo J.M. 2006) pp.35.

As with calcium silicate pastes, the gelatinous nature of the principal reaction product renders any definition of chemically bound water somewhat arbitrary. The three definitions of water content for calcium silicate pastes are relevant to cement pastes that are essential water to the formation of the hydration products in a saturated paste as mention above. Water retained after D-drying, known as non-evaporable water, has often been wrongly identified with chemically bound water. It excludes much of the interlayer water in C-S-H, AFm (alumino-ferrite monosulfate hydrate) and hydrotalcite-type phases and much of the water contained in the crystal structures of Aft (alumino-ferrite trisulfate hydrate) phases. It is often used as a measure of the fraction of the cement that has reacted, but can only be approximate in this respect, because the clinker phases react at different rates and yield products containing different amounts of non-evaporable water.

In addition, the extent of a pozzolanic reaction can be followed by monitoring the decrease in calcium hydroxide over time. In theory, it is possible to completely react all the calcium hydroxide formed by regular hydration, but this seldom happens in practice. In fact, it is important to realize that the slow rate of the pozzolanic reaction requires a prolonged period of moist curing if the full benefits of adding a pozzolan are to be realized. Without sufficient moist curing, a pozzolan will act mainly as a noncementitious filler. The pozzolanic reaction is more temperature sensitive than regular hydration and can proceed quite rapidly under steam curing. Although the hydration mechanisms of cement-fly ash system are well understood, the hydration extent quantification for cement and fly ash is not yet clarified, neither by experimental means nor on theoretical basis, the non-evaporable water and the content of calcium hydroxide is investigated the cement hydration and fly ash pozzolanic reaction extents. Fully hydrated cement pastes typically contain about 23% of non-evaporable water, referred to the ignited mass (Taylor 1997). And for fly ash hydrated, it seems that the amount of water fixed by the reaction of a pozzolana is related to the CaO content. Uchikawa quoted that for a fly ash cement containing a high-calcium fly ash, the reaction rate, estimated from the amount of combined water, was higher than that of a fly ash containing an ordinary fly ash. Thus, the

determination of non-evaporable water in blended cement should be cautions and with consideration of the chemical composition of the replacement material or mineral admixture.

The fly ashes modify the microstructure of the hydrated matrix quite significantly. The increased fraction of C-S-H leads to a more homogenous microstructure, particularly when highly reactive, finely divided pozzolans are used. Residual $Ca(OH)_2$ crystals are usually smaller and can have altered morphology. The principal effect on the microstructure is the change in pore structure. Admixture reactions will reduce the overall porosity (the specific gravity of C-S-H is lower than calcium hydroxide) and the pore size. However, reduction of porosity requires extensive pozzolanic reaction produced by prolonged moist curing. Reductions in the water to binder ratio will produce larger reductions in porosity.

Figures 2.3 (a)-(c) show that $Ca(OH)_2$ (hydrated lime) is produced by the reaction of the Portland cement and water. Due to its limited solubility, particles of hydrated lime form within interstitial spaces. With a continuing supply of moisture, the lime reacts with the fly ash pozzolanically, producing additional hydration products of a fine pore structure.

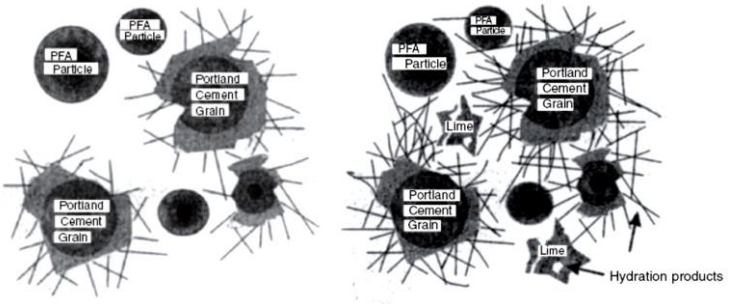

(a) Hydration products of Portland cement

(b): Lime is formed as a by-product of hydration

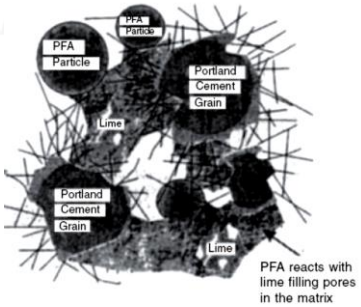

(c) The pozzolanic reaction products fill the interstitial spaces

Figure 2.3 The stage of pozzolanic reaction products
(John and B. S. 2003) pp.3/4-3/5

Vagelis (1999) studied effect of high-calcium fly ash (FH, 23% total CaO) on cement fly ash system. The development of the strength, porosity, bound water, and calcium hydroxide content was measured. Typical SEM image of 20% FH-cement paste at different times of hydration are presented. From the beginning (3 days), reaction products are observed on the surface of the FH particles. However, after 2-3

week, FH particles are difficult to identify in the concrete microstructure. After a longer time (6 months), a dense structure has formed.

Antiohos and Tsimas (2005) studied on the influence of active silica of two high-lime fly ashes on their behavior during hydration. The new blends were examined in terms of compressive strength, remaining calcium hydroxide, generation of hydration products and microstructural development. It was found that soluble silica of fly ashes holds a predominant role especially after the first month of the hardening process. In figure2.4, after 90 days the paste structure has further densified, a fact that corresponds to its higher strength. Silica from the ash particles is increasingly dissolved, joins the pore solution, reacts with still available calcium hydroxide, and provides additional pozzolanic C–S–H. The binding properties of this gel supplement the filling effect of the ashes than remain intact, leading in a subsequent decrease of the pores in the paste.

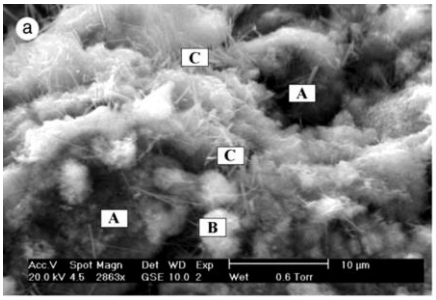

(a) ESEM image of the blend with 30% Tf addition after 2 days of hydration.

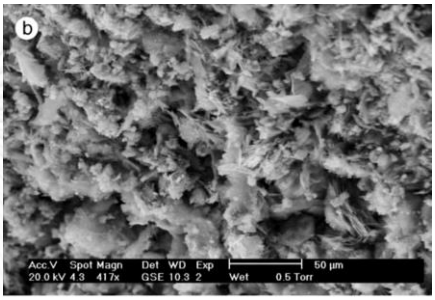

(b) Seven days of hydration

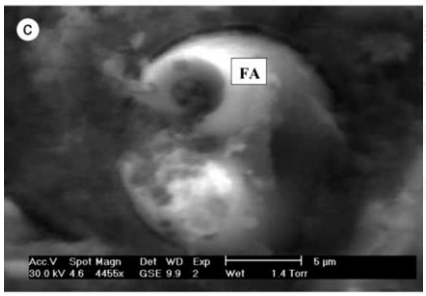

(c) Reacted fly ash particle at 7 days

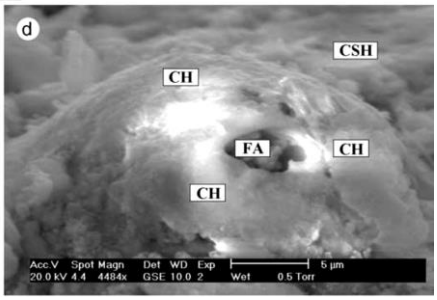

(d) 28 days of hydration of hydration

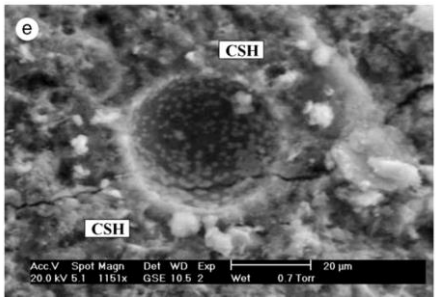

(e) 90 days of hydration

Figure 2.4 Fly ash hydrated on pozzolanic reaction after 2 days to 90 days (Antiohos and Tsimas 2005)

Chindaprasirt, Jaturapitakkul et al. (2007) demonstrated the effect of fly ash fineness on pore size and microstructure of hardened blended cement pastes. Test results indicated that the pore size of hardened blended cement paste were significantly affected by the rate of replacement and the incorporation of classified fly ash results in a further decrease in pore size of blended cement paste. The SEM results revealed that the hardened blended cement paste containing finer fly ash produced a denser structure than the one containing coarser fly ash. In Figure2.5, the microstructure of fractured surface pastes at 7, 28 and 90 days are shown. At 90 days, etched fly ash particles and hydrated rims with fly ash surfaces were quite common. A lot of fly ash particles were substituted by hydrates. For finer fly ash pastes, as shown in Figure.2.6, the results are similar to that obtained from coarser fly ash. In addition, the finer fly ash paste had a denser structure.

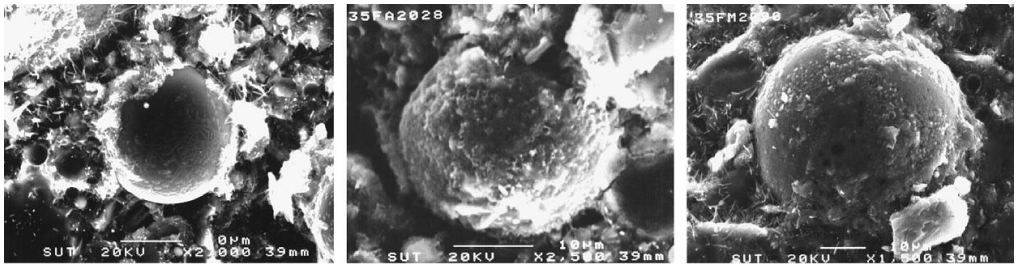

(a) 7 days (b) 28 days (c) 90 days

Figure 2.5 Fractured surface of OFA20 (coarser fly ash) paste by SEM (Chindaprasirt, Jaturapitakkul et al. 2007)

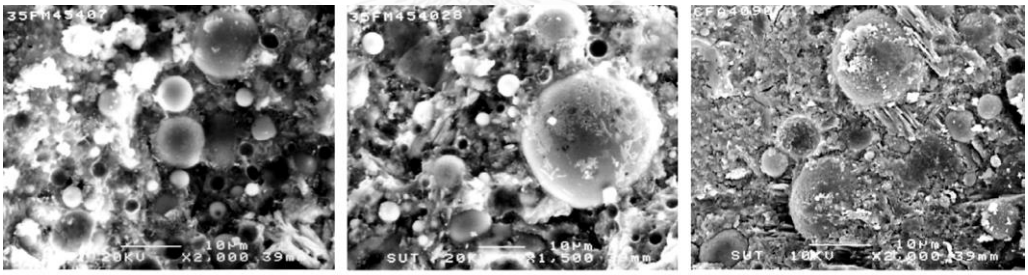

(a) 7 days (b) 28 days (c) 90 days

Figure 2.6 Fractured surface of CFA20 (finer fly ash) paste by SEM (Chindaprasirt, Jaturapitakkul et al. 2007)

2.3.3 Determination of degree of hydration and degree of pozzolanic reaction

The research about the determination of degree of reaction in cement-fly ash concrete rarely exists due to difficulty in investigation. Thus, majority of the researches have been conducted by using cement paste.

Lam, Wong et al. (2000) studied the degree of hydration of the cement in Portland cement (PC) paste by determining the non-evaporable water (Wn) content. The degree of reaction of the fly ash in high-volume fly ash/cement (FC) pastes was determined using a selective dissolution method. Based on the relation between the degree of cement hydration and effective water-to-cement (w/c) ratio, the degree of hydration of the cement in FC pastes was also estimated. It was found that high-volume fly ash pastes underwent a lower degree of fly ash reaction than a paste with

less fly ash while the hydration of the cement in high-volume fly ash pastes was enhanced because of the higher effective w/c ratio for the paste. This effect was more significant for the pastes with lower water-to-binder (w/b) ratios. Thus, preparing high-volume fly ash concrete at lower w/b ratios can result in less strength losses.

Zhang, Sun et al. (2000) investigated the hydration processes of high-volume fly ash cement paste by examining the non-evaporable water content, the CH content, the pH of pore solution and the fraction of reacted fly ash. The results revealed that the non-evaporable water content in high-volume fly ash cement pastes does not develop as plain cement pastes does, so it may be improper to apply the non-evaporable water content to evaluate the hydration process in high-volume fly ash cement matrix. The reduction in CH content increases with the hydration progress and it varies linearly with the logarithm of curing age. The higher the content of fly ash is, the more the reduction in CH is. The pH of pore solution of high-volume fly ash cement paste was reduced to a great extent at early ages and it continued to decline at later ages due to the inclusion of large amount of fly ashes. At elevated temperatures, however, this trend was not found. The fraction of reacted fly ash directly reflects the pozzolanic reactivity of fly ash both at normal and elevated temperatures. There is some inherent correlation between the reduction in CH content, the pH of pore solution and the fraction of reacted fly ash. For specified matrix, the consumption of CH and the pH of pore solutions change linearly with the increase of the fraction of reacted fly ash

Shunsuke, Fuminori et al. (2001) investigated the effects of the mix proportion and curing temperature on the pozzolanic reaction of fly ash in cement paste by examining the productions of calcium hydroxide and the pozzolanic reaction ratio of fly ash. It is possible to accurately determine the reaction ratio of fly ash in cement paste from the insoluble residue and the quantity of dissolved Al_2O_3. The result revealed that the curing at higher temperature or the higher the water/powder ratio is, the higher the reaction ratio of fly ash. The starting time of the pozzolanic reaction at the curing temperature of 20°C is at the age of 28 days or more because the reaction ratio at 28 days is nearly 0%. The pozzolanic reaction of fly ash in cement paste highly depends upon the curing temperature. The reaction ratio of fly ash decreases with an increasing fly ash substitution rate.

Feng, Garboczi et al. (2004) studied the hydration of plain portland and blended cement pastes containing fly ash or slag by using a scanning electron microscope (SEM) point-counting technique. For plain portland cement pastes, the results for the degree of cement hydration obtained by the SEM point-counting technique were consistent with the results from the traditional loss-on-ignition (LOI) of non-evaporable water-content measurements; agreement was within ±10%. The standard deviation in the determination of the degree of cement hydration via point counting ranged from ±1.5% to ±1.8% (one operator, one sample). For the blended cement pastes, it is the first time that the degree of hydration of cement in blended systems has been studied directly. The standard deviation for the degree of hydration of cement in the blended cement pastes ranged from ±1.4% to ±2.2%. Additionally, the degrees of reaction of the mineral admixtures (MAs) were also measured. The results were comparable with previous results obtained using a selective dissolution method. The standard deviation for the degree of fly ash reaction was ±4.6% to ±5.0%. Results of the present study indicate that the SEM point-counting technique

can be a reliable and effective analysis tool for use in studies of the hydration of the MAs in blended cement paste.

Sakai, Miyahara et al. (2005) studied the influences of the glass content and the basicity of glass phase on the hydration of fly ash cement. The hydration of fly ash cement was clarified and the hydration over a long curing time was characterized. Two kinds of fly ash with different glass contents, one with 38.2% and another with 76.6%, were used. The hydration ratio of fly ash was increased by increasing the glass content in fly ash in the specimens cured for 270 days. When the glass content of fly ash is low, the basicity of glass phase tends to decrease. Reactivity of fly ash is controlled by the basicity of the glass phase in fly ash during a period from 28 to 270 days. However, at an age of 360 days, the reaction ratios of fly ash show almost identical values with different glass contents. Fly ash also affected the hydration of cement clinker minerals in fly ash cement. In the long –term hydration of alite was accelerated, while that of belite and C_4AF was retarded.

Haha, De Weerdt et al. (2010) studied the FA reaction in two different blended OPC-FA systems was studied using a selective dissolution technique based on EDTA/NaOH, diluted NaOH solution, the portlandite content and by backscattered electron image analysis. The amount of FA determined by selective dissolution using EDTA/NaOH is found to be associated with a significant possible error as different assumptions lead to large difference in the estimate of FA reacted. In addition, at longer hydration times, the reaction of the FA is underestimated by this methods due to the presence of non-dissolved hydrated and MgO rich particles. The dissolution of FA in diluted NaOH solution agreed during the first days well with the dissolution as observed by image analysis. At 28 days and longer, the formation of hydrates in the diluted solutions leads to an underestimation. Finally, image analysis appeared to give consistent results and to be most reliable technique.

Zeng, Li et al. (2012) proposed a synthetic model for cement hydration extent in blended pastes is established taking into account the dilution effect, local w/c augmentation effect as well as heterogeneous nucleation effect of FA particles. The non-evaporable water content (w_n) and calcium hydroxide content (CH) were measured by thermal gravity analysis (TGA) and the FA reaction extent was quantified by the selective dissolution method. From the results, it is observed that local w/c, heterogeneous nucleation effects and FA hydration have comparable contribution to the total w_n content in blended pastes while the FA hydration dominates in CH content. The cement hydration extent is determined through experimental approach as well as model-based approach and the α_c values from two approaches are linearly correlated. The pozzolanic reaction extent of FA hydration is also determined through experimental approach and model-based approach. The FA hydration extent is found to be much influenced by curing age, i.e. $\alpha_p \approx 0.1$ for 7d and $\alpha_p \approx 0.2-0.4$ for 90 days.

2.4 Hydration reaction and microstructure of cement-limestone powder system

Composite cements may contain mineral additions other than, or as well as, ones with pozzolanic or latent hydraulic properties. These are widely described as 'fillers' but, at least in the case of limestone, which is the most important; this term is

misleading because chemical reaction occurs. For an overall specific surface area (Blaine) of 420 m^2/kg, 50% of the limestone can be below 700 nm, compared with $3\mu m$ for the clinker. The effect on 28-day strength of partial replacement of clinker can be compensated by finer grinding of the clinker, and for equal 28-day strengths, the 1 day strength of cement containing limestone powder can exceed that of one not containing it. This is due to the greater fineness of the clinker and the effects of the limestone.

The limestone filler was considered by many as inert filler, but it has been gradually accepted as contributing to the hydration process by the formation of calcium mono-carboaluminates ($C_3A•CaCO_3•11H_2O$).

The effects of the limestone are partly physical and partly chemical as with many other finely divided admixtures. Because of its fineness, the material also acts as a filler between the grains of clinker, though it is unlikely to be as effective in this respect as silica fume. Chemically, the formation of monocarbonate ($C_4A\bar{C}H_{11}$) is well established. One would also expect that the replacement of ettringite by monosulfate would be inhibited. Monocarbonate was detected after periods of 7-127 days, in amounts that appeared to depend on the amount and reactivity of the $CaCO_3$ present. This observation suggests that the assemblage of AFm (ettringite) and Aft (monosulfate) phases produced may depend on the relative rates at which SO_4^{-2}, $Al(OH)_4^-$ and CO_3^{-2} ions become available.

Heikal, El-Didamony et al. (2000) studied the effect of substitution of limestone for Homra in pozzolanic cement. The effect of limestone replacement was studied by the determination of the combined water, free lime contents, bulk density, total porosity and compressive strength. The results show that the addition of limestone reduces the initial and final setting time, as well as total porosity, whereas the free lime and combined water increase with limestone content. It can be concluded that limestone fills the pores between cement particles due to formation of carboaluminate, which may accelerate the setting of cement pastes.

Kakali, Tsivilis et al. (2000) studied the effect of calcium carbonate on the hydration products of C_3A, C_3S and cement. Pastes made from C_3A and C_3S containing 0%, 10%, 20% and 35% w/w of chemical grade $CaCO_3$, as well as pastes made from Portland cement containing 0%, 10%, 20% and 35% w/w limestone, were examined after 1, 2, 7 and 28 days of hydration. The hydration products in C_3S and C_3A pastes containing $CaCO_3$, as well as in limestone cement pastes, were identified by means of powder diffraction. The effect of calcium carbonate on the hydration procedure was also recorded. It is concluded that in pastes containing $CaCO_3$, either as a chemical reagent or as a limestone constituent, the ettringite's transformation to monosulfate is delayed, while calcium aluminate monocarbonate is preferably formed instead of monosulfate even at early ages. In addition, the hydration of C_3S is accelerated and formation of some carbosilicate is observed

Bonavetti, Rahhal et al. (2001) studied about the hydration of pure C_3A phase with $CaCO_3$ in the presence or not of gypsum and in a calcium hydroxide solution is related to the hydration products of Portland and limestone-blended cements. Results show the formation of monocarboaluminate in systems containing C_3A and $CaCO_3$ while the tricaboaluminate was not found. Calcium hydroxide intervenes in these systems to form a calcium hemicaraluminate hydroxide. In limestone-blended cements, calcium monocarboaluminate is immediately detected after hydration begun

and the transformation of monosulfoaluminate to monocarboaluminate occurs at 28 days while the conversion of ettringite to monosulfoaluminate is deferred.

Lothenbach, Le Saout et al. (2008) investigated the influence of the presence of limestone on the hydration of Portland cement. Blending of Portland cement with limestone was found to influence the hydrate assemblage of the hydrated cement. Thermodynamic calculations as well as experimental observations indicated that in the presence of limestone, monocarbonate instead of monosulfate was stable. The quantities of ettringite, portlandite and amorphous phase as determined by TGA and XRD agreed well with the calculated amounts of these phases after different periods of time. The findings in this paper show that changes in the bulk composition of hydrating cements can be followed by coupled thermodynamic models. Comparison between experimental and modelled data helps to understand in more detail the dominating processes during cement hydration.

Ramezanianpour, Ghiasvand et al. (2009) described the effect of various amounts of limestone on compressive strength, water penetration, sorptivity, electrical resistivity and rapid chloride permeability on concretes produced by using a combination of PC and limestone at 28, 90 and 180 days. The percentages of limestone that replace PC in this research are 0%, 5%, 10%, 15% and 20% by mass. The water/(clinker + limestone) or (w/b) ratios are 0.37, 0.45 and 0.55 having a constant total binder content of 350 kg/m3. Generally, results show that the Portland limestone cement (PLC) concretes having up to 10% limestone provide competitive properties with PC concretes. In addition, Figure 2.7 (a)–(f) the microstructures of the cementitious paste with normal consistency of hydraulic cement (ASTM C187), containing 0%, 10% and 20% limestone replacement are shown at 3 and 28 days after hydration. Moreover, a typical SEM photograph of the limestone is presented in Figure 2.7 (g). The morphology in cement pastes with and without limestone is different. The pore structures (tortuosity and constriction or disconnection) are improved with increasing the curing time.

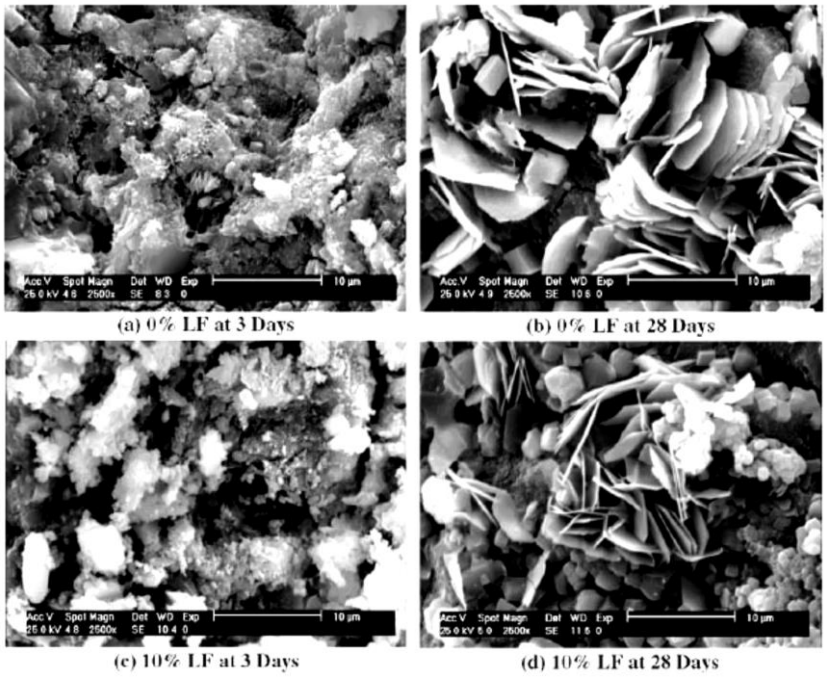

(a) 0% LF at 3 Days (b) 0% LF at 28 Days

(c) 10% LF at 3 Days (d) 10% LF at 28 Days

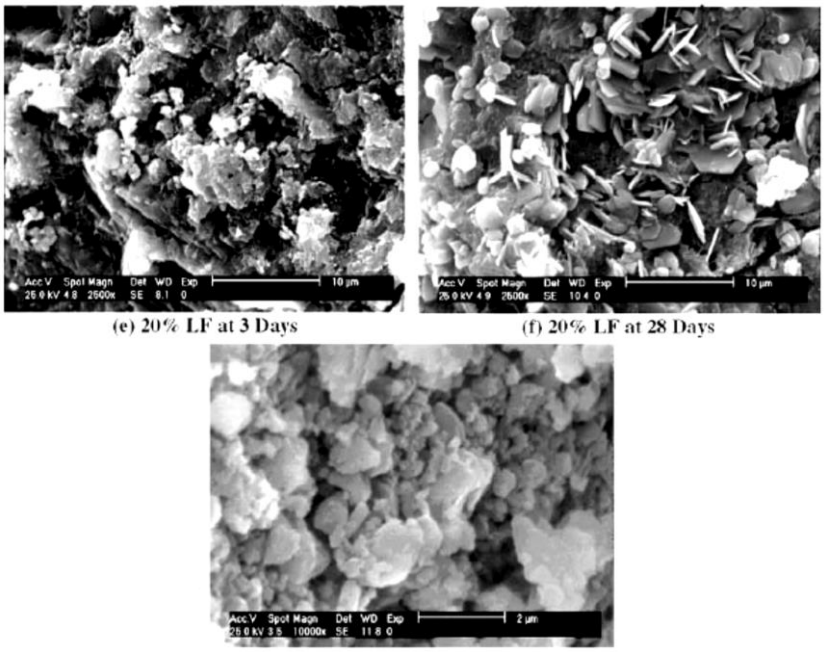

Figure 2.7 SEM photograph of cement pastes and typical limestone.
(Ramezanianpour, Ghiasvand et al. 2009)

Shuhua and Peiyu (2010) studied the effect of limestone powder on microstructure of concrete by using mercury intrusion porosimetry (MIP), backscattering scanning electron (BSE), scanning electron microscopy (SEM) and X-ray diffraction (XRD) techniques. The experimental results show that the compressive strength of concrete containing 100 kg/m3 limestone powder can meet the strength requirement. The filling effect can make the paste matrix and the interfacial transition zone between matrix and aggregate denser, which will improve the performance of concrete. BSE was used to determine the microstructure and the phase distribution of the samples. In order to get a high contrast images for image analysis, the grey-scale histogram of original image was used to distinguish the different phases. Within the grey-scale from 0 (black) to 256 (white), the pores, C-S-H gel, CH, limestone powder and anhydrous cement are identified respectively as shown in Figure2.8. It can be seen that small limestone particles exist in the pastes even after 28 days of hydration, the total amount of limestone powder is almost not changing during 28 days hydration. The limestone powders fill in the interfacial transition zone between the matrix and aggregate, and make it become much denser, which is the reason why the porosity of concretes containing limestone powder is lower than that of traditional concrete.

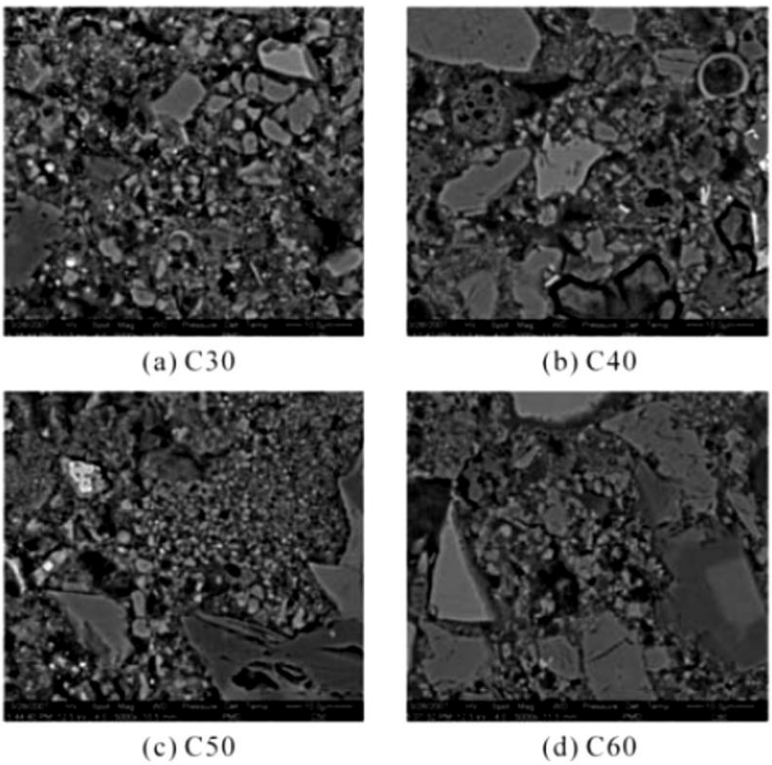

Figure 2.8 BSE images of the four samples at the age of 28 days
(Shuhua and Peiyu 2010)

Ye, Liu et al. (2007) studied the development of the microstructure of SCC, the microstructural parameters of the paste including porosity, pore size distribution and phase distribution by means of mercury intrusion porosimetry (MIP) and scanning electron microscopy (SEM). The thermogravimetric analysis (TGA) and the derivative thermogravimetric analysis (DTG) are used to identify the phase constituents. The result of this research shows that the pore structure, including the total pore volume, pore size distribution and critical pore diameter, in the SCCP (self-compacting cement paste) is very similar to that of HPCP (high performance cement paste). The fact that limestone powder does not participate in the chemical reaction was confirmed both from thermal analysis and BSE image analysis.

2.5 Existing test methods for estimating mix proportion of hardened concrete

Nowadays, there are a few methods to analyze for mix proportion of hardened concrete. Several standards such as BS1881: Part124 described the methods for determining the cement content and other concrete compositions in hardened concrete, but they are applied for the OPC concrete but not appropriate for the concrete with some mineral admixtures.

Jung, Shin et al. (2012) presented a new technique of analyzing the acid neutralization capacity (ANC) data to identify a concrete mix design which had been developed to be applied for examining cement and other mixture in the hardened concrete at 200 days. The suspension of concrete was formed in still water and nitric acid to produce the variation in the pH. As a result, the pH of the suspension for

concrete at a given concentration of the nitric acid was dramatically decreased at around 10 in the pH, depending on the aggregate content, of which characteristics was used to determine the aggregate content in a concrete mix. Simultaneously, an increase in the w/c resulted in decrease pH, of which the empirical equation was adopted to determine the w/c. As the there is no difference in the ANC characteristics between coarse and fine aggregate, aggregate content encompassing coarse and fine aggregates was determined in this study. This method is limited in applying for all unknown concrete mixes, because the fitted equation (the aggregate content vs acid concentration) may be dependent on binder type. Thus, the variation in binder type must be preliminary known, although information for determining the aggregate content was applicable to only OPC in this study.

British Standard Institution (BSI) BS1881: Part124: 1988 is a standard test method for analysis of hardened concrete. This method appropriately applies to concrete sample at age over 28 days. They describes the sampling procedures, treatment of sample, and analytical methods to be used on a sample of concrete to determine the cement content, aggregate content and other concrete compositions in hardened concrete. The techniques used in this standard are such as oxide analysis, extracting soluble silica or loss on ignition method. Subsequently, those data are indirectly used to calculate percentage of cement or other compositions. However, some procedures have limitation such as aggregate grading test is only applicable to concrete containing essentially insoluble in dilute hydrochloric acid. Moreover, this standard can be applied to concrete made with Portland cements and, in favorable circumstances, contained ground granulated blast-furnace slag, but the determination of pulverized-fuel ash content are outside the scope of this standard. Moreover, each procedure requires a substantial degree of chemical skill and relatively complicated chemical instrumentation as show in Figure 2.9 which is typical apparatus for determination of water content, and for determination of carbon dioxide content.

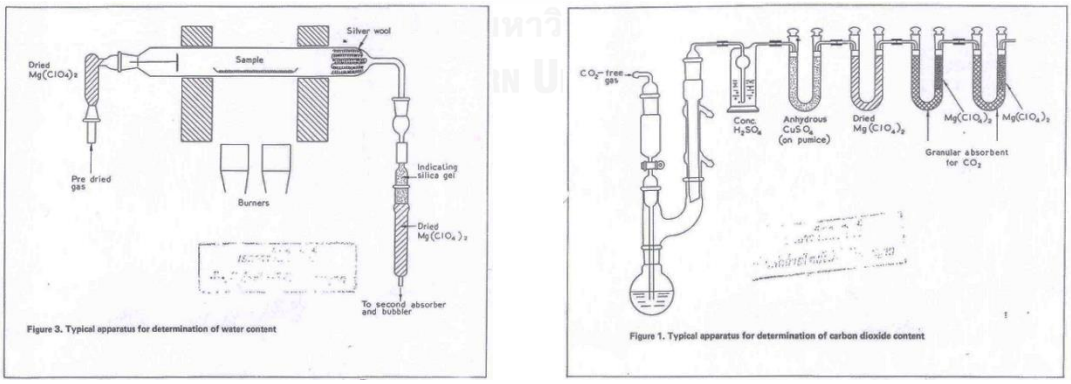

(a) Typical apparatus for determination of water content

(b) Typical apparatus for determination carbon dioxide content

Figure 2.9 Typical apparatus in BS1881 standard method

2.6 Determination of cement content in hardened concrete

Clemeiia (1972) evaluated the method of selective dissolution by methanolic maleic acid, developed by Tabikh et al. for the determination of cement content in

hardened concrete. It was found to be relatively simple and inexpensive, and is accurate to within ±1% point cement at the 95% confidence level with the use of calibration curve. Such factors as aggregate and cement compositions, curing time, and water-cement ratio were investigated as to their effects on the method. Among these factors, aggregate composition was the only one found to have a significant effect on the analytical results. In addition, the determination of cement content by the measurement of the specific gravity increase in a methanolic maleic acid solution was also investigated, but was found to have unsatisfactory precision.

American Society for Testing and Materials (ASTM) C1084-02 is standard test method for determination of Portland cement content of a sample of hardened hydraulic-cement concrete. This test method consists of two independent procedures: an oxide-analysis procedure and an extraction procedure. Nevertheless, the procedure is also applicable estimating the combined content of Portland cement and pozzolan or slag in concrete made with blended hydraulic cement and blends of Portland cement with pozzolans or slag. But, the test method should be applied to determination of the blended cement content of the pozzolanic content only by use of calibration concrete samples on other information. Then, indirectly calculating the percentage of cement by assuming from analyses of silica and calcium oxide in the original cement used; consequently, it is not applicable to concrete that contains aggregates that yield simultaneously significant amounts of silica and calcium oxide under the conditions of the test.

Linares, López-Atalaya et al. (2009) proposed the stain method for determining cement content in hardened concrete by image capture and treatment of the stained specimen images. The samples resulting from this process are stained the cement paste through immersion in a solution of tannic acid (3%in weight) acidified with tartaric acid (3% in weight). This stain process is equally valid for young concretes with an abundant alkaline reserve and for old concretes with an advanced carbonation degree and it can be used for concretes manufactured using cements with admixture as long as there is a calibration curve prepared with this type of cement. The result obtained with this method is similar to those achieved by the ASTM reference method. In addition, the method developed has no dependence on the composition of the coarse aggregates, whereas the ASTM method.

Wong and Buenfeld (2009) proposed a new method to estimate the initial cement content, water content and free water/cement ratio (w/c) of hardened cement-based materials made with Portland cements that have unknown mixture proportions and degree of hydration. This method first measures the volume fractions of the unreacted cement, hydration products and capillary pores, using high resolution field emission scanning electron microscopy (FE-SEM) in the backscattered electron (BSE) mode and image analysis. From the obtained data and the volumetric increase of solids during cement hydration, we can calculate the degree of hydration. The proposed method has the advantage that it is quantitative and does not require comparison with calibration graphs or reference samples made with the same materials and cured to the same degree of hydration as the tested sample. The resulting of the estimate degree of hydration is compared against the measured value from the LOI test and conventional image analysis. A relative good agreement between the estimated and measured values is observed. However, the preliminary

results show that the proposed method is applicable to ordinary Portland cement pastes with a range of w/c ratios (0.25–0.50) and curing ages (3–90 days).

2.7 Determination of fly ash content in hardened concrete

Ohsawa, Asaga et al. (1985) studied the quantitative determination of fly ash in hydrated fly ash-$CaSO_4$-$2H_2O$ -$Ca(OH)_2$ system, various kinds of selective dissolution were evaluated using pastes made from a single representative fly ash. Selective dissolution using picric acid - methanol solution was found to be adequate. Selective dissolution using picric acid - methanol + water can also be used, when it is necessary to save time, although rather bigger corrections are needed. Reproducibility of the determination by both methods was found to be satisfactory, as the standard deviation of the measurement was within 0.23 - 0.55%. Several dissolution experiments were also carried out to obtain the basic information related to this technique.

R. Doug and C. A. (1995) proposed methods developed for determination of slag and fly ash content in hardened concrete. The optical microscopy method involves preparation of thin sections of the concrete and point counting to obtain the number of fly ash grains for estimating fly ash content substitution in Portland cements. These are compared to a set of calibration standard sections. This technique is satisfactory where the engineer wishes to know rough proportions on the scale used, and the importance of knowing the particle size distribution of the fly ash is crucial to obtaining an estimate

Presuel-Moreno and Sagüés (2009) investigated of conduction to assess the applicability of magnetic methods for determining FA presence and content in hardened concrete. Reproducible measurements of magnetic susceptibility χm of laboratory and field extracted concrete core samples were achieved with simple instrumentation. There was a nearly linear relationship between χm and the mass of fly ash per unit volume, or its volume fraction. The magnetic response of a given FA was not significantly affected by the process of curing and subsequent evolution of the concrete over two years, or by carbonation of the concrete. Field extracted concrete cores exhibited a wide range of χm values. The group of specimens with the highest values of χm also had the lowest chloride ion diffusivity, consistent with the presence of admixed FA. Conversely, specimens with nil magnetic response included those from concrete with the highest chloride diffusivity. The magnetic measurements provided reasonable order-of-magnitude indications of FA presence in field extracted cores. However, precise determination of FA content from magnetic measurements of field cores does not appear feasible in the absence of additional information.

2.8 Determination of water to cement ratio (w/c) in hardened concrete

Elsen, Lens et al. (1995) presented results of the w/c ratio determination of hardened cement paste and concrete samples on thin sections using automated image analysis techniques. Two series of samples prepared in laboratory conditions have been used as ‘reference samples’ to develop and to evaluate procedures for measuring the w/c ratio by image analysis techniques: a series of pure cement paste samples and one of concrete samples. Three different image analysis methods have been

employed: an interactive, an automatic method with thresholding of grey values by the operator, and a fully automatic method without thresholding. The measurements on the pure cement paste samples confirm the direct relationship between the w/c ratio of the samples and the mean grey value measured on thin sections. The results of the measurements of the thin sections prepared out of the reference concrete series also indicate a clear relationship between the w/c ratio and the mean grey value but these measurements are less reproducible. The main cause of this variability with the concrete samples is the difficulty in selecting threshold level values.

All the measurements here have been performed for cement paste and concrete samples which have been cured under laboratory conditions for 28 days. The results cannot of course be transferred in a simple way to field concrete.

Sahu, Badger et al. (2004) developed methodology for the determination of the water–cement ratio (w/c) in hardened concrete using backscattered electron imaging (BEI) by a scanning electron microscope. The method is based on concrete sections that have been vacuum impregnated with epoxy and polished to a flat surface. The backscattered intensity of the epoxy is the lowest compared to all other phases present within a concrete. By using image analysis program and setting an appropriate threshold of the gray scale the capillary porosity of the concrete can be quantified. The technique has been tested for laboratory specimens of known w/c ratio and shows good linear correlation. w/c ratios determined on field concretes show very good correlation with results obtained on the same specimens using the standardized fluorescence microscopy Nordtest method (NT Build 361-1999) except in the range of extremely high water–cement ratios exceeding 1.

2.9 Coarse aggregates analysis by image processing

Wang (1999) studied a local thresholding algorithm for binarizing gray scale images of aggregates from gravitational flow-falling particles. The algorithm repeatedly thresholds an aggregate image until no object can be thresholded any further. Before thresholding an object, in each iteration of the thresholding process, the algorithm calculates the size, shape and range of gray levels of the object. The algorithm has been implemented in an on-line system and the field test result show that it works under certain conditions.

Banta, Cheng et al. (2003) described to approach for predicting particle mass based on 2D electronic images. Crushed limestone aggregates, similar to those used in asphalt pavement mixtures were placed on a light table and imaged using a CCD video camera and frame grabber. The images were processed to separate touching and overlapping particles, define the edges of the particles and to calculate certain features of the particle silhouettes, such as area, centroid and shape-related features. A multiple linear regression model was created, using the dimensionless parameters as regress or variables to predict particle mass. Regress or coefficients were found by fitting to a sample of 501 particles ranging in size from 4.75 mm< particle sieve size < 25 mm. When tested against a different aggregate sample, the model predicted the mass of the batch to within ±2%. The approach was based on a low cost vision system and image analysis. The algorithms were tested on a limited number of samples, and have produced encouraging results.

Fernlund (2005) proposed a 3-D method for particle shape determination of coarse aggregates using image analysis, IA, is presented. It is based on the measures the axial length of all three axis of every particle in a coarse aggregate sample. Two images of the entire aggregate sample are taken, in lying and standing positions. Since the particle's intermediate axes are measured in both images they can be used to couple the shortest and longest axial dimensions for each particle. The method allows an interpretation of length/thickness, length/width and width/thickness ratios of all the particles and is thus comparable to the flakiness and shape index tests. This method for shape determination gives a very good measure of both the size distribution and shape distribution of all the particles in the aggregate sample. The reproducibility of results is good. As previously stated sieving does not directly measure any particle in the sample. In contrast the IA measures every particle. This new IA method can be used to evaluate the results of other aggregate tests that use sieving in the methodology.

Abbas, Fathifazl et al. (2009) developed method to determine the residual mortar content of recycled concrete, to serve as a quality control tool for such aggregates. In order to validate the results obtained by that laboratory test procedure, image analysis was used to quantify the residual mortar content in the different size fractions of the recycled concrete aggregates tested. The results confirmed that the quick laboratory test provides an accurate measurement of the residual mortar content in recycled concrete aggregates.

CHAPTER 3
EXPERIMENT

3.1 General

This study aims to develop an estimation method of mix proportion of hardened concrete. In order to verify the accuracy of the developed method, the concrete samples were prepared in laboratory for the experiment; therefore all material mixtures and their proportions were already known. The concrete samples were then analyzed for investigating fly ash and limestone powder and determining the mix proportion. If the developed method can be verified with cored concrete samples under exposed environment, this estimation method of the mix proportion can be applied for the determination of mix proportion of hardened concrete in real environment or in existing structures as shown in Figure 3.1.

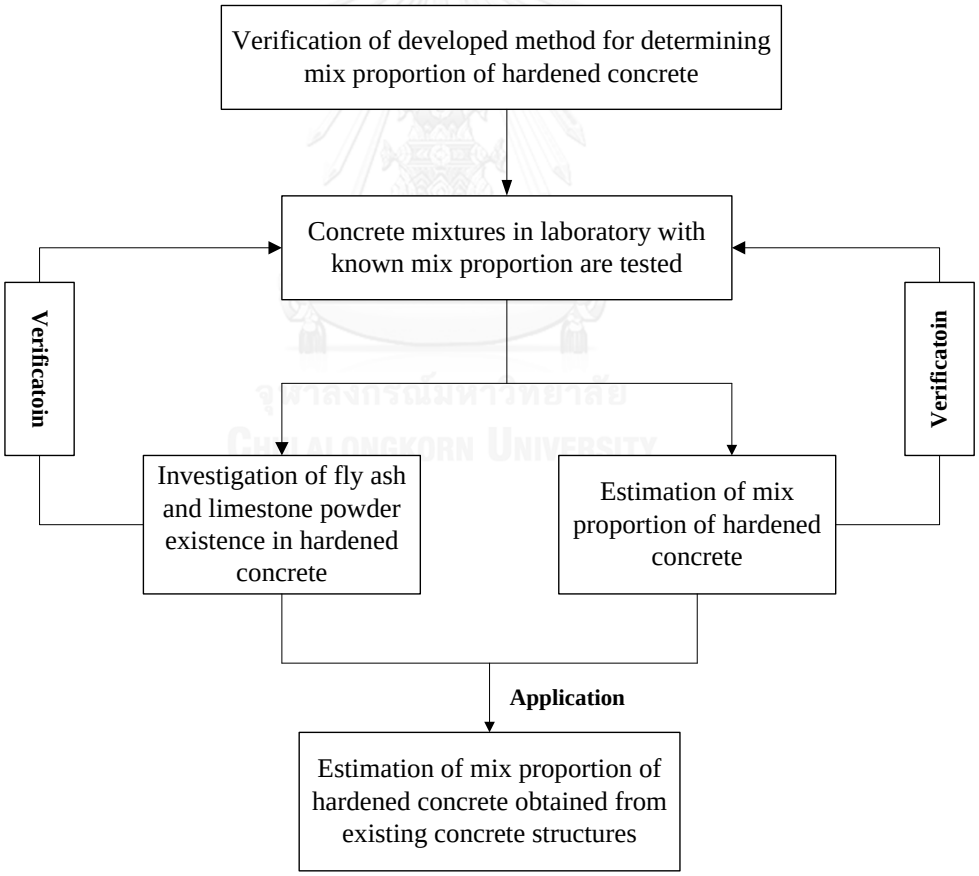

Figure 3.1 Methodology procedure

In the estimation method of mix proportion of hardened concrete, the physical, mechanical and chemical analysis tests were adopted. Many testing methods were used to determine the fly ash or limestone powder in concrete and the mix proportion

of hardened concrete, such as Scanning Electron Microscope (SEM), Scanning Electron Microscope on Back-Scattered Electrons (BSE), Scanning Electron microscope equipped with Energy Dispersive X-Ray spectroscopy (EDS), X-Ray Diffraction (XRD), Loss on ignition (LOI), X-Ray Fluorescent (XRF), Compressive strength test by Universal Testing Machine (UTM), Selective dissolution and Image processing. Hence, in this chapter describes details of the sample preparation and the experimental procedure of each method.

3.2 Materials

Materials used in the preparation of concrete sample in laboratory are as follows:

1) Cement

Ordinary Portland Cement Type I (OPC1), which is manufactured by Siam Cement Co., Ltd., Thailand, was used in this study. The chemical compositions and physical properties of cement are shown in Table 3.1.

2) Fly ash

Two types of fly ash were used in this study. The Mae Moh fly ash (FA1), which was collected from Mae Moh electric power plant of Electricity Generating Authority in Lampang province of Thailand, is Class C fly ash corresponding to high-CaO fly ash. The FA1 is a by-product from the burning of lignite coal as fuel in the power plant. The BLCP fly ash (FA2), which was collected from BLCP power station in Maptaphut Industrial Estate, is Class F fly ash corresponding to low-CaO fly ash. The FA2 is a by-product from burning of bituminous coal. The chemical compositions and physical properties of fly ash are presented in Table 3.1.

3) Limestone powder

Two types of limestone powder from Surint Omya Chemicals (Thailand) Co.,Ltd. were used in this study. They were different in particle size, which were 4.46 μm of LP1 and 16.93 μm of LP2, analyzed by laser diffraction technique test. The chemical compositions and physical properties of limestone powder are shown in Table 3.1.

4) Aggregates

Three types of fine aggregates (A, B, and C) were used in the mixture. Fine aggregates were pit sand that passed sieve No.4 (4.75 mm). Specific gravity of the fine aggregates A, B and C based on saturated surface dry (SSD) conditions test in accordance with ASTM C128 were 2.59, 2.60, and 2.60, respectively. Coarse aggregates, which were crushed limestone with nominal size from 25.0 to 4.75 mm (1 in. to No.4) were used in this study. Specific gravity of coarse aggregate A, B, and C based on saturated surface dry (SSD) conditions test in accordance with ASTM C127 were 2.70, 2.73, and 2.70, respectively.

The gradations of fine and coarse aggregates were complied with ASTM C33. Compacted void contents of aggregates were performed according to ASTM C29. They were designed as ratio between volume of paste to volume of void (γ) of 1.4.

Table 3.1 Chemical composition and physical properties of materials

Chemical compositions	OPC1	FA1	FA2	LP1	LP2
SiO_2 (%)	19.36	31.56	65.15	0.09	0.26
Al_2O_3 (%)	5.10	18.18	22.06	0.03	0.01
Fe_2O_3 (%)	3.35	15.86	4.17	0.03	0.07
CaO (%)	64.36	20.91	1.25	57.19	55.93
MgO (%)	0.81	3.38	0.68	0.39	0.55
SO_3 (%)	2.83	4.70	0.18	0.08	0.01
Na_2O (%)	0.15	2.35	0.02	0.01	0.01
K_2O (%)	0.51	1.92	1.09	0.01	0.01
TiO_2 (%)	0.25	0.37	1.00	0.01	0.01
P_2O_5 (%)	0.08	0.23	0.35	0.01	0.01
LOI (%)	3.01	0.14	3.78	42.10	43.17
Physical and Chemical properties					
Specific gravity	3.15	2.29	2.24	2.74	2.69
Blaine fineness (cm^2/g)	3480	2836	2997	4443	3252

3.3 Specimens preparation and testing procedure

In the specimen preparation, the concrete samples were cast in cylindrical mold with a dimension of 10 cm in diameter and 20 cm in height. It is noted that length-to-diameter ratio (L/D) of the specimen is equal to 2 which is conforming to the standard test method for compressive strength of cylindrical concrete specimens (ASTM C39) The specimen diameter is more than three times of the nominal maximum aggregate size, corresponding to the standards (ASTM C42).

After the concrete samples were cast, they were cured in the molds and covered with plastic sheet at room temperature for 24 hours. Then, they were demolded and cured in water at room temperature until the specified test age. Pictures of the concrete sample preparation are shown in Figure 3.2.

At each test age, the samples were prepared for the tests. Three cylindrical specimens were prepared for the compressive strength test by Universal Testing Machine (UTM). The broken specimens from the compressive strength test were subsequently used for the tests of SEM, XRD, selective dissolution, and XRF. Other two specimens were prepared for the tests of BSE, image processing method and unit weight of concrete.

Figure 3.2 Concrete sample preparation

After the test of compressive strength; the specimens were splitted into small pieces as shown in Figure 3.3 (a). The small piece samples were sieved. The retained samples on sieve No.4, 8 and 16 were shown as in Figure 3.3 (b) and then immersed in acetone for 24 hours in order to stop the hydration reaction as shown in Figure 3.3 (c). Next, the acetone was decanted as much as possible from the samples and the samples were kept in the oven at 50 ºC for 24 hours. In Figure 3.3 (d), the small piece samples with coarse aggregate were removed and the remaining sample content was expected at least 100-150 gram. Approximate 5 gram of sample was used for the SEM. About 100 gram of sample was finely ground for XRD test, XRF test and selective dissolution test. The ball mill jar and pulverizer were used for grinding samples as seen in Figure 3.3 (e) and (f). The powder particles must be passed sieve No.200 (74 µm).

(a) Small piece sample b) Sieving (c) Sample immerse acetone

(d) Removing contaminated coarse aggregate

(e) Ball mill jar

(f) Pulverizer machine

Figure 3.3 Equipment and sample preparation procedure of the first part

Other two cylinders of each mix were cut by using diamond saw into many sliced specimens as shown in Figure 3.4 (a) and (b). The slices were then cut into cube specimens of 1x1x1 cm^3 size as shown in Figure 3.4 (c). Then, they were performed the stop of hydration reaction by using acetone. Approximate 3-5 slice specimens were used for the preparation of BSE and mapping tests. Another piece of slice was determining coarse aggregate content by image processing method and examining unit weight of concrete according to ASTM C642

(a) Cutting machine

(b) Slice samples

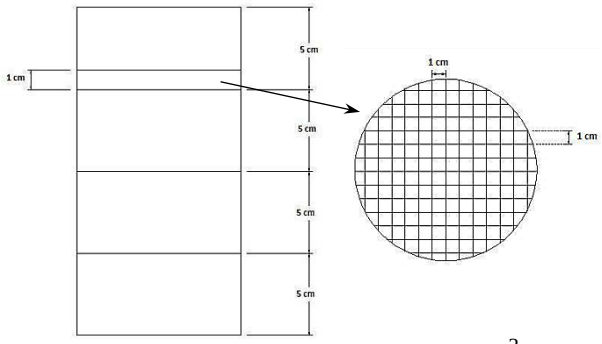

(c) Cube sample size 1x1x1 cm^3

(d) Cube sample immersed in acetone

Figure 3.4 Equipment and sample preparation procedure of the second part

3.3.1 Scanning Electron Microscope (SEM) technique

About 3-4 small pieces of specimens taken from the mortar of concrete were used for the test of SEM technique. The small piece samples were kept in oven at 100 ºC for 24 hours before they were coated by carbon (C) before SEM testing. The equipment and sample preparation is shown in Figure 3.5. The SEM model JEOL JSM-6301F equipped with an Oxford-INCA 350 energy dispersive spectrometer was used with the accelerating voltage of 20 kV.

Figure 3.5 Equipment and sample preparation for SEM testing

3.3.2 Scanning Electron Microscope on Back-Scattered Electrons (BSE) and Mapping technique

The 3-4 piece cube specimens of 1x1x1 cm^3 were kept in oven at 100 ºC for 24 hours. Then, they were mounted by epoxy resin, and sucked air by vacuumed pump. After that, their surfaces were polished by sand paper No. 240, 400, 800, and 1000, respectively. Then, they were polished by diamond powder 3, 1, and ¼ µm, respectively. In addition, the lubricant of polishing is ethanol. The polished samples were cleaned by the ultrasonic cleaner bath with ethanol for 20 minutes. The polished samples were kept in oven at 100 ºC for 24 hours before they were coated by carbon (C), before testing. The equipment for BSE and Mapping testing was same model of the SEM testing. The equipment and sample preparation is shown in Figure 3.6.

Figure 3.6 Equipment and sample preparation for BSE testing

3.3.3 Scanning Electron Microscope equip with Energy Dispersive X-Ray spectroscopy (EDS) technique

When, the SEM or BSE were found some suspected particles or areas that they may be mineral admixtures, the energy dispersive X-ray spectroscopy (EDS) and mapping were applied to the sample for more investigation. So, the same samples done with SEM and BSE were used for EDS/Mapping testing.

3.3.4 X-Ray Diffraction (XRD) technique

About 5 gram of powder samples were used for XRD testing. The powder samples were kept in oven at 50 ºC for 24 hours before blending with corundum. The 10% of the corundum was replaced by weight of sample. They were blended by the pounder. The X-Ray diffraction equipment was a Bruker-D8 Discover, CuKα X-Ray type. The experiment was performed in the 2θ range start at 5-80º with increment 0.01º/sec step scan. The equipment and sample preparation is shown in Figure 3.7.

Figure 3.7 Equipment and sample preparation for XRD testing

3.3.5 Loss on ignition (LOI) technique

About 3 gram of powder samples were used for LOI testing. The testing method was conformed with ASTM C114 (2004). The sample was ignited in a muffle furnace at a controlled temperature of 950 ± 50˚C.

3.3.6 X-Ray Fluorescent (XRF) technique

About 30 gram of powder was used for XRF technique. The powder samples were kept in oven at 100 ºC for 24 hours.

3.3.7 Selective dissolution technique

The powder samples were kept in oven at 100 ºC for 24 hours. Then, they were kept in desiccator before testing. For testing procedure of selective dissolution method, A 1 gram of sample was precisely weighed and put in a centrifuge tube. The 2N HCl solution 30 milliliter was added in the tube, and stirred by using a glass rod. Then, the tube was placed in a water bath and shacking with 125 rpm and heated to 60 ºC for 15 minutes. The solution was stirred occasionally by using a glass rod. The tube were removed from the bath and centrifuged for 2 minute at 4500 rpm. The acid was decanted as much as possible without disturbing the solid residue in the bottom. The tube was then filled with hot water, centrifuged again and decanted. This operation was repeated 3 times. The tube was then filled with a 5% Na_2CO_3 solution, stirred placed in the water bath shacking with 125 rpm at 80 ºC for 20 minutes. The tube was then centrifuged for 2 minutes at 4500 rpm. The liquid was decanted and the

residue was washed with hot water, centrifuged again and decanted. This washing was repeated 3 times. The tube with residue was dried at 100 ºC for 24-48 hours, and weighted (Ohsawa, Asaga et al. 1985). The equipment and testing are shown in Figure 3.8

Figure 3.8 Equipment and testing for Selective dissolution

3.3.8 Strength of concrete by Universal Testing Machine (UTM) technique

For compressive strength test of concrete, three cylindrical concrete samples were used for each test age. The universal testing machine (UTM) was used in the test. The samples and testing are shown in Figure 3.9.

Figure 3.9 Compressive strength testing

3.3.9 Image processing technique

The slice samples from two cylindrical concrete specimens were used for determining coarse aggregate by image processing. In the test procedure, the concrete disc samples were brought to take photos of their cut faces with sufficient resolution. The pictures of cut faces were processed to investigate by using image processing software. The image size and quality of the photographs were adjusted for the easiness to identify the boundaries of coarse aggregate as shown in Figure 3.10 (a) and (b). Afterward, the boundaries of the coarse aggregate were identified as shown in Figure 3.10 (c). The areas of the selected boundaries of the coarse aggregate were determined by programming in MATLAB as shown in Figure 3.10 (d).

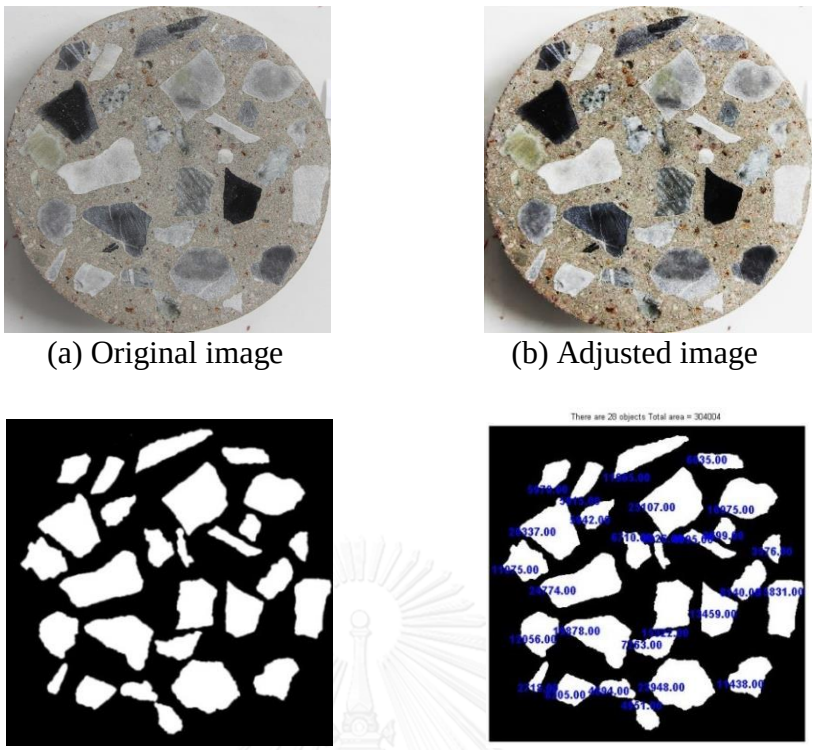

(a) Original image (b) Adjusted image

(c) Boundaries of coarse aggregate identified (d) Aggregate area determined by MATLAB

Figure 3.10 Determination of coarse aggregate content by image analysis

Fine aggregate particles passed through sieve No.4 (4.75 mm.) were not coarse aggregate. Hence, the area smaller than 0.17 cm^2 or 1700 pixels, were not considered as coarse aggregate.

The ratio of cross-sectional area of coarse aggregate to total cross-sectional area of concrete slices was then converted to volumetric ratio of the coarse aggregate. This was modified from ASTM C1356 (1996), which is standard test method for quantitative determination of phases in Portland cement clinker by microscopical point-count procedure. Moreover, the principle of conversion of area to volume was also used in other researches such as Feng, Garboczi et al. (2004), Linares, López-Atalaya et al. (2009), Wong and Buenfeld (2009), and Banta, Cheng et al. (2003). Then, the weight content of coarse aggregate in concrete can be obtained by multiplying its volume by the specific gravity. It is noted that gradation of coarse aggregate could not be evaluated by this method.

3.3.10 Unit weight of concrete by ASTM C642

The slice specimens were used for the test of unit weight of concrete by ASTM C642 (1997). They were the same specimens used in the image processing test.

CHAPTER 4
DETERMINATION OF MIX PROPORTION OF HARDENED CEMENT CONCRETE

4.1 General

The estimation method of mix proportion of hardened concrete has been developed in this study. The physical, mechanical and chemical analysis tests were adopted in the estimation method. The analytical procedures for the determination of water to cement ratio, and mix proportion of concrete including water, cement, sand, and coarse aggregate are described in this chapter.

4.2 Material and Mix proportion

Concrete samples were prepared at water to cement ratios (w/c) of 0.45, 0.55, and 0.65. For concrete with w/c of 0.45, three types of coarse aggregates (A, B and C) were used. The concrete samples were tested for the determination of mix proportion at 14, 28 and 91 days. The ratio by volume of sand to total aggregate (s/a) of A, B and C was 0.42, 0.42 and 0.44. The void ratio of sample at aggregate set A, B and C was 0.237, 0.230 and 0.230, respectively. Five mix designs of concrete specimens are shown in Table 4.1. The sample preparations were mentioned in Chapter 3.

Table 4.1 Mix proportion for the determination of mix proportion of hardened cement concrete

Sample	w/c	Cement (kg/m^3)	Water (kg/m^3)	s/a	Sand (kg/m^3)	Coarse aggregate (kg/m^3)	Age (days)
W45C-A	0.45	419	188	0.42	727	1047	28,91
W45C-B	0.45	407	183	0.42	737	1061	28,91
W45C-C	0.45	407	183	0.44	776	1025	14,91
W55C-C	0.55	360	198	0.44	776	1025	14,91
W65C-C	0.65	322	210	0.44	776	1025	14,91

4.3 Methodology of determination of mix proportion of hardened concrete

The procedure for determining mix proportion of hardened cement concrete was divided as three parts and was implemented techniques as shown in Figure 4.1. Firstly, image processing technique was used for determination of coarse aggregate content. Secondly, water to cement ratio can be calculated from data back analysis of the compressive strength by using the computer software, "FACOMP". Thirdly, cement and sand contents were obtained based on the residues from the selective dissolution of sample. All compositions of concrete per 1 m^3can be derived from the mass balance equations.

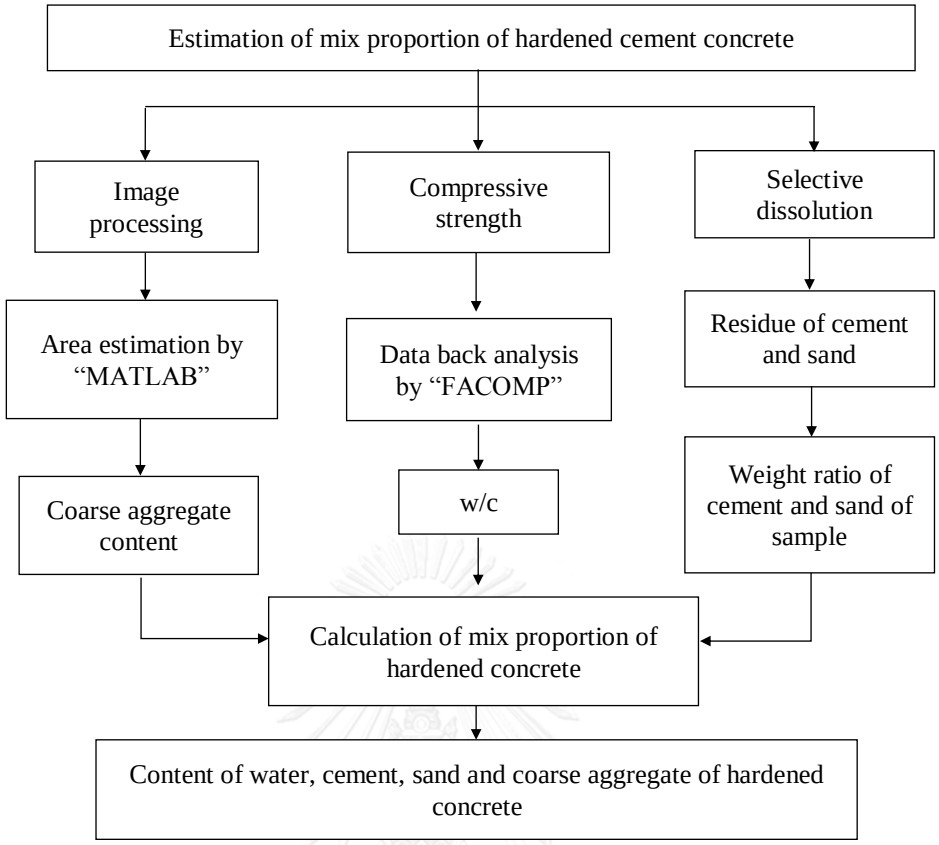

Figure 4.1 Method for determination of mix proportion of hardened cement concrete

The developed method was applied to estimate the mix proportion of concrete prepared in laboratory in order to verify its efficiency. The details of procedure for determining the mix proportion of hardened concrete are described below.

4.3.1 Determination of coarse aggregate by image processing

Image analysis method was used to determine coarse aggregate content of hardened concrete. The chemical composition of coarse aggregate was disregarded in the analysis. The randomly selection of concrete slices were performed; consequently, the analysis method was organized and defined by statistical analysis. Hence, image analysis was verified by sample preparation in laboratory.

Twelve concrete samples were analyzed for coarse aggregate content by using image processing with appropriately statistics. In order to determine the reliability of the determination of coarse aggregate, a statistical method by using standard score (Z-score) was used. It means that a set of data between $\bar{x} - \mu$ to $\bar{x} + \mu$, where $\bar{x}$ is the mean of the population and μ is the standard deviation of the population, was considered.

4.3.2 Determination of water to cement ratio

The compressive strength of concrete sample was obtained by using the universal testing machine. Then, the water to binder ratio can be calculated from the back analysis of compressive strength data by using mathematical model. The model was proposed for predicting compressive strength of no-slump concrete with and

without fly ash, with considering the effect of curing temperature (Tangtermsirikul and LeViet 2007). The model was constructed based on the following Eq.(4.1)

$$f_c^{'}(t,T) = f_c^{'}(28days, 30°C) \times \phi(t,T) \tag{4.1}$$

Where $f_c^{'}(t,T)$ is compressive strength of concrete at t days cured under a constant temperature T ˚C. $f_c^{'}(28days, 30°C)$ is the 28 day compressive strength of concrete cured at 30˚C that it considered many parameters affecting strength of concrete such as w/b, γ, density of concrete, filling effect, properties of binder, and so on as shown in Eq. (4.2). $\phi(t,T)$ is the strength development ratio at t days and at a constant curing temperature T ˚C as shown in Eq. (4.3).

$$f_c^{'}(28days, 30°C) = [\alpha_1 \log(CaO_{eff}) + \lambda_f \alpha_2]\chi_{LOI}\chi_{density} \tag{4.2}$$

$$\phi(t,T) = \varepsilon_p \varepsilon_t X^{\nu} \tag{4.3}$$

where CaO_{eff} is the effective calcium oxide content in concrete which depends on amount of CaO content of binder and fineness of fly ash. α_1 and α_2 are coefficients affected by w/b, λ_f represents the filling effect of fly ash. χ_{LOI} and $\chi_{density}$ are coefficients affected by loss on ignition in fly ash and density of concrete mixture, respectively. These parameters can be obtained from Tangtermsirikul, Jitvutikrai et al. (2004). $\varepsilon_t, \varepsilon_p$ and ν are the effects of curing temperature, the effect of quantity of the ingredients of pastes and the effect of concrete age on structure formation of paste, respectively. X is the gel/space ratio of paste.

$\varepsilon_p, \varepsilon_t$ and ν in Eq.(4.3) were derived based on test results together with those obtained from works of Julnipitawong (2003) and Tahir (1998) as follows:

$$\varepsilon_p = 0.574 + 0.504\frac{w}{b}r \tag{4.4}$$

$$\varepsilon_t = 1.217 + 0.142t^{0.389} + 0.015\left(\frac{T}{30}\right)^{-4.766}\left(\frac{t}{28}\right)^{-1.325} \tag{4.5}$$

$$\nu = -0.982 + 0.0012t + 1.326\left(\frac{T}{30}\right)^{-0.418}\left(\frac{t}{28}\right)^{-0.243} \tag{4.6}$$

where w/b is the ratio of water to total binder by weight. r is the replacement ratio of fly ash in total binder by weight. t (days) and T(˚C) are the age and curing temperature of concrete, respectively.

The gel/space ratio (X) can be computed from Eq. (4.7) together with Eqs. ((4.8)-(4.11)). It is defined as the ratio of the volume of solid products of reactions of

binders to the volume of space occupied by the reacted binders and unit water content (mixing water).

$$X = \frac{gel\ volume}{gel\ volume + volume\ of\ cappilary\ pores}$$

$$= \frac{volume\ of\ products\ of\ reactions\ of\ binders}{volume\ of\ (reacted\ binders + mixing\ water)}$$

$$= \frac{V_0 \times v_b \times b \times \alpha_b}{v_b \times b \times \alpha_b + w} \qquad = \frac{V_0 \times v_b \times \alpha_b}{v_b \times \alpha_b + w/b} \tag{4.7}$$

Then,

$$v_b = 1/\rho_b \tag{4.8}$$

$$\rho_b = (1-r)\rho_c + r\rho_f \tag{4.9}$$

$$\alpha_b = (1-r)\alpha_{hy} + r\alpha_{poz} \tag{4.10}$$

$$b = c + f \tag{4.11}$$

where X is the gel/space ratio of fly ash-cement paste; V_0 is the ratio of the volume of gel at complete reactions of the binder to the original volume of the binder; v_b is the average specific volume of binder; ρ_c, ρ_f and ρ_b are the specific gravity of cement, fly ash and binder, respectively; b, c and f are the weight of binder, cement and fly ash in a unit volume of paste (g), respectively; r is the replacement ratio of fly ash by weight of total binder, and w is the unit water content of paste (g). α_b, α_{hy} and α_{poz} are the average degree of reaction of binder, the degree of hydration of cement and degree of pozzolanic reaction of fly ash, respectively.

Degree of hydration of cement is adopted from the work of Saengsoy (2002). In the Saengsoy's study, degree of hydration of cement was considered mainly depending upon the following factors: age of concrete, cement compositions, water to binder ratio and concrete temperature. The degree of pozzolanic reaction was considered affected by water to binder ratio, properties of fly ash, temperature and age of concrete.

The degree of hydration of cement was obtained from mathematical models constructed based on experimental data as in Eqs. (4.12) to (4.18). The models were implemented in a computer software (FACOMP 2006). The degree of hydration of cement was defined as the weight average of the degree of hydration of all compounds of the cement as shown in Eq. (4.12).

$$\alpha_{hy}(t) = \frac{\sum_{i=1}^{4} m_i \alpha_i(t)}{\sum_{i=1}^{4} m_i} \tag{4.12}$$

Where $\alpha_{hy(t)}$ is the degree of hydration of cement (%). i is the mineral compound of cement $(C_3S, C_2S, C_3A, C_4AF)$. m_i is the mass of each compound per cubic meter of concrete (kg/m^3). $\alpha_i(t)$ is the degree of hydration (%) of each compound in cement (Tangtermsirikul and Saengsoy 2002). And, the degree of hydration of each cement compound at each constant concrete temperature can be formulated as a function of water to binder ratio and age as shown in Eq. (4.13) to Eq. (4.16). A, B, C, D, E, F, G and H in these equations are the constant values (Saengsoy 2002). The physical acceleration at early age mainly affects the hydration reaction at early age of C_3A and C_3S. The effect of physical acceleration of C_3A and C_3S is represented by η_{C3A} and η_{C3S}, respectively (Choktaweekarn 2008). The factors are shown in Eq. (4.17) and Eq. (4.18).

$$\alpha_{C_3A}(t) = \eta_{C_3A} \cdot \frac{1-\exp\left[A\cdot\tan^{-1}\left\{B\cdot(w/b)^{C}\cdot t\right\}\right]}{1+\exp\left[\left\{D\cdot(w/b)^3+E\cdot(w/b)^2+F\cdot(w/b)+G\right\}\cdot\tan^{-1}(H\cdot t)\right]}\times 100 \tag{4.13}$$

$$\alpha_{C_3S}(t) = \eta_{C_3S} \cdot \frac{1-\exp\left[\left\{A/\left(B+\exp(C\cdot w/b)\right)\right\}\cdot\tan^{-1}\{D\cdot t\}\right]}{1+\exp\left[\left\{E\cdot(w/b)^3+F\cdot(w/b)^2+G\cdot(w/b)+H\right\}\cdot t^{\{I/(J+\exp(K\cdot w/b))\}}\right]}\times 100 \tag{4.14}$$

$$\alpha_{C_2S}(t) = \frac{1-\exp\left[\left\{A/\left(B+\exp(C\cdot w/b)\right)\right\}\cdot\tan^{-1}\left\{D\cdot(w/b)^{E}\cdot t\right\}\right]}{1+\exp\left[F\cdot t^{G}\right]}\times 100 \tag{4.15}$$

$$\alpha_{C_4AF}(t) = \frac{1-\exp\left[A\cdot\tan^{-1}\left\{B\cdot(w/b)^{C}\cdot t\right\}\right]}{1+\exp\left[\left\{D\cdot(w/b)^3+E\cdot(w/b)^2+F\cdot(w/b)+G\right\}\cdot\tan^{-1}\left(H\cdot(w/b)^{I}\cdot t\right)\right]}\times 100 \tag{4.16}$$

$$\eta_{C_3S} = 0.2\alpha_{C_3S}(t-1)^4 - 0.4\alpha_{C_3S}(t-1)^3 + 0.2\alpha_{C_3S}(t-1)^2 - 0.05\alpha_{C_3S}(t-1) + \left(\left(\frac{w}{b}\times\frac{W_c+W_f}{UW}\right)+0.97\right) \tag{4.17}$$

$$\eta_{C_3A} = -0.18\alpha_{C_3A}(t-1)^4 + 0.24\alpha_{C_3A}(t-1)^3 - 0.15\alpha_{C_3A}(t-1)^2 + 0.01\alpha_{C_3A}(t-1) + \left(\left(\frac{w}{b}\times\frac{W_c+W_f}{UW}\right)+1\right) \tag{4.18}$$

where $\alpha_{C3A}(t)$, $\alpha_{C3S}(t)$, $\alpha_{C2S}(t)$ and $\alpha_{C4AF}(t)$ are degrees of hydration at the considered age of C_3A, C_3S, C_2S and C_4AF, respectively (%). $\alpha_{C_3A}(t-1)$ and $\alpha_{C_3S}(t-1)$ are degrees of hydration at the hour before the considered age of C_3A and C_3S (%). W_c and W_f are the weights of cement and fly ash in a cubic meter of concrete, respectively (kg). UW is unit weight of concrete (kg/m^3).

The degree of pozzolanic reaction was considered affected by water to binder ratio, properties of fly ash, temperature, and age of the concrete. The equations of degree of pozzolanic reaction used in this study are shown in Eq. (4.19) to Eq. (4.24).

$$\alpha_{poz}(t) = \frac{\tan^{-1}[(0.049 \cdot T^{0.496} - 0.186 \cdot w/b - 0.135) \cdot t}{\tan^{-1}[(0.049 \cdot T^{0.496} - 0.186 \cdot w/b - 0.135) \cdot 365} \cdot \alpha_{poz}(365) \tag{4.19}$$

$$\alpha_{poz}(365) = \left[100 - \left\{ \tan^{-1} \left\{ \begin{array}{l} (102 - 0.1 \cdot T) \cdot (0.416 + 0.0088 \cdot w/b^{-1.822}) \cdot \\ (7.927 \cdot w/b^{-1.546} - 15.699) \cdot \left(\frac{SiO_2}{CaO_{eff}} - \frac{\%SiO_{2C}}{\%CaO_C} \right) \end{array} \right\} \right\} \right] \cdot \left[\left(1 - \%LOI/100\right) \cdot \left\{ 0.948 \cdot \tan^{-1} \cdot \left(7.227 \times 10^{-4} \cdot F_f \right) \right\} \right] \tag{4.20}$$

$$SiO_2 = \left[\left(W_c \cdot \%SiO_{2c} \right) + \left(W_f \cdot SiO_{2f} \right) \right] / 100 \tag{4.21}$$

$$CaO_{eff} = \left[\left(W_c \cdot \%CaO_c \right) + \varphi \cdot \left(W_f \cdot CaO_f \right) \right] / 100 \tag{4.22}$$

$$\varphi = \frac{1 - \exp\left(-a \cdot \%CaO_f\right)}{1 + \exp\left(-a \cdot \%CaO_f\right)} \tag{4.23}$$

$$a = 0.0048 \cdot \left(F_r / 3000 \right)^{3.0734} + 0.0245 \tag{4.24}$$

where $\alpha_{poz(t)}$ and $\alpha_{poz(365)}$ are the degree of pozzolanic reaction at any age of paste and at 365 days of paste, respectively (%). t is the considered age of paste (days), T is concrete temperature (ºC), and w/b is the water to binder ratio. $\%CaO_c$, and $\%SiO_{2c}$ are calcium oxide content and silicon dioxide content in cement, respectively (% by weight of cement). $\%CaO_f$, and $\%SiO_{2f}$ are calcium oxide content and silicon dioxide content in fly ash, respectively (% by weight of fly ash). CaO_{eff} is the effective unit calcium oxide content in paste (kg/m^3). φ is effectiveness of calcium oxide in fly ash, and F_f is Blaine's fineness of fly ash (cm^2/g)

This model was complied to generate the computer software "FACOMP", which was developed at Sirindhorn International Institute of Technology (SIIT), Thammasat University, Thailand. The model for predicting compressive strength in the FACOMP was constructed based on experimental data. It has been proven that the prediction model can be used to accurately predict the compressive strength of concrete within acceptable limits. In addition, the accurately prediction of compressive strength is shown in Figure 4.2, comparing the compressive strength from tested results and compressive strength from predicted results of FACOMP.

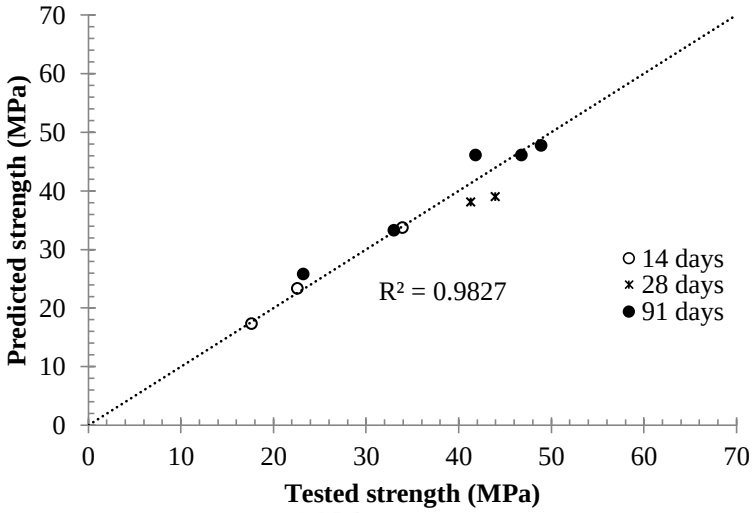

Figure 4.2 Comparison of the predicted and the tested compressive strength

The determination procedure of water to cement ratio is seen in Figure 4.3. Water to cement ratio was primarily assumed for calculating mix proportion of concrete. The compressive strength of the calculated mixture proportion was subsequently simulated by FACOMP. The valid water to cement ratio can be determined by means of trial and error until the compressive strength obtained from the FACOMP is nearly equal to the compressive strength obtained from the test.

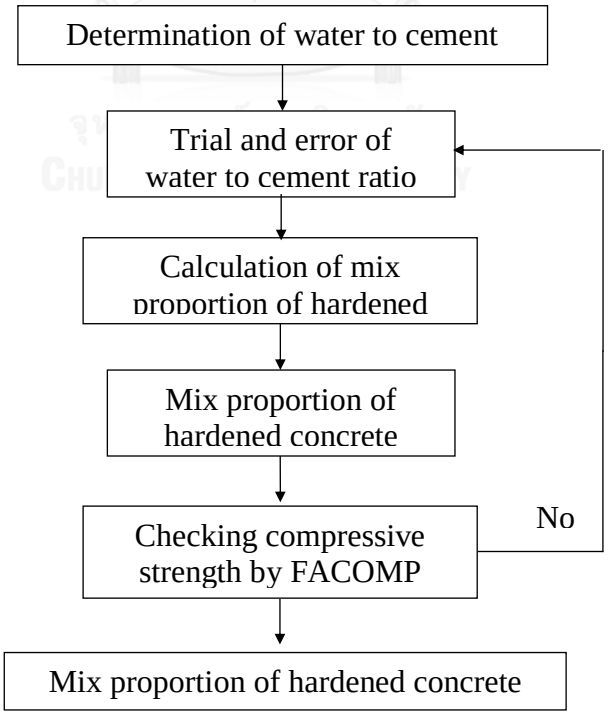

Figure 4.3 Procedure for determination of water to cement ratio

4.3.3 Determination of weight ratio of cement and sand by residual weight

The selective dissolution method was used to investigate residues left from the dissolved sample. The powder sample was dissolved by the hydrochloric acid (HCl). The 2N HCl was used to dissolve calcium components in cement and hydrated product. Further, the 5% Na_2CO_3 was used to dissolve silica gel. However, a few amount of cement was still insoluble. Therefore, the residues left from the dissolution were sand and little amount of cement. The concrete material and concrete sample were tested by selective dissolution. The sample preparation and testing procedure was mentioned in Chapter 3.

In order to determine contents of cement and sand in the sample, they were estimated primarily based on their oven-dried weight ratio. Eq. (4.25) and Eq. (4.27) were formed based on the mass balance condition of sample without coarse aggregate. The equations were used to determine the weight ratio of cement and sand since two unknowns (w_{cs} and w_{ss}) could be solved by two equations.

$$w_{ts} = w_{cs} + w_{ss} + w_{ns} \tag{4.25}$$

$$w_{ns} = 0.23(\alpha_{hy} w_{cs}) \tag{4.26}$$

$$r_{ts} w_{ts} = r_c w_{cs} + r_s w_{ss} \tag{4.27}$$

Where r_{ts} is residual weights of sample (g/g of sample), r_c is residual weights of the cement (g/g of cement). r_s is residual weights of sand (g/g) of sand. w_{ts} , w_{cs} w_{ss} and w_{ns} are oven-dried weight ratio of sample, cement, sand, and combined water of the sample to oven-dried weight ratio of sample without coarse aggregate (mortar in concrete) , respectively. w_{ts} is equal 1. α_{hy} is degree of hydration of cement. In this study, the degree of hydration of cement at 14, 28 and 91 days of each sample can be obtained by mathematical models from a computer software (FACOMP 2006). 0.23 is assumed for the combined water in cement hydration with full degree of reaction (Taylor 1997).

4.3.4 Calculation of mix proportion of hardened concrete

The water to cement ratio, coarse aggregate content, and weight ratio of cement and sand in sample without coarse aggregate can be obtained as mentioned earlier. They were used to determine the mix proportion of concrete as following.

The oven-dried weight ratio of coarse aggregate can be obtained by Eq. (4.28). Then, the oven-dried weight ratio of cement and sand of concrete can be modified as Eq. (4.29).

$$w_G = \frac{W_G}{(1 + a_G) \times UW_d} \tag{4.28}$$

$$w_{tc} = w_{cc} + w_{sc} + w_{nc} + w_G \tag{4.29}$$

Where $w_{tc}, w_{cc}, w_{sc}, w_{nc}$ and w_G are ratio of oven-dried weight of concrete sample cement, sand, combined water, and coarse aggregate to oven-dried weight of concrete, respectively. w_{tc} is equal 1. W_G is aggregate content obtained from the image analysis (kg/m^3). a_G is absorption of coarse aggregate. UW_d is oven-dried unit weight of concrete (kg/m^3) which can be obtained according to ASTM C642.

Then, the oven-dried weight ratios of concrete composition are converted to mass of cement, sand and water at SSD state as shown in Eq. (4.30).

$$\left.\begin{aligned} W_{cc} &= w_{cc} \times UW_d \\ W_{sc} &= w_{sc} \times UW_d \times (1 + a_s) \\ W_{wc} &= W_{cc} \times (w/c) \end{aligned}\right\} \quad (4.30)$$

Where W_{cc}, W_{sc} and W_{wc} are mass of cement, sand, and water of concrete at SSD state, respectively (kg). a_s is absorption of sand. w/c is water to cement ratio.

Generally, the mix design of concrete is estimated for 1 m^3 of volume based on SSD state of the aggregates. Hence, volume of each concrete ingredient per 1,000 liters of concrete is shown in Eq. (4.31). The volume of each concrete ingredient can be obtained from dividing its mass (Eq. (4.30)) by the specific gravity. Then, the content of cement, sand, and water of the mix proportion are obtained from Eq. (4.32).

$$V_t = 1000 = V_c + V_s + V_w + V_G + V_{air} \quad (4.31)$$

$$\left.\begin{aligned} W_c &= V_c \times SG_c \\ W_s &= V_s \times SG_s \\ W_w &= W_c \times (w/c) \end{aligned}\right\} \quad (4.32)$$

Where V_t, V_c, V_s, V_w, V_G and V_{air} are total volume of concrete, cement, sand, water, coarse aggregate and air of concrete for 1,000 liters at SSD condition, respectively (liters/m^3). SG_c, SG_s and SG_G are specific gravity of cement, sand and coarse aggregate, respectively. W_c, W_s and W_w are mass of cement, sand, and water, respectively (kg/m^3).

4.4 Result and Discussion

4.4.1 Determination of coarse aggregate by image processing

The result and percentage error of each mix were defined by Z-score as shown in Figure 4.4. Each sample set was obtained by randoming, then its analytical result cannot be known its distribution that it may not be normal distribution. So the different set of sample was defined by different Z-value (μ) of 0.25, 0.50, 0.75 and 1.00. The analytical results show that the set of sample with Z-value (μ) of 0.50 and 0.75 had some error percentages over 10%. Some results of sample set with Z-value (μ) of 0.25 and 1.00 had fewer error than 10% but over 5%. The mean percentage errors of sample set of Z-score between ±0.25, ±0.50, ±0.75 and ±1.0 are 3.25%, 3.89%, 3.27%, and 2.75%, respectively. It can be observed that the analytical result of coarse aggregate content with Z-score between -1.00 to 1.00 is better mean percentage errors than Z-score between ±0.25, ±0.50 and ±0.75.Moreover, the mean percentage error of each mix at Z-value (μ) of 1.00 is not more distributed when compared with others as shown in Figure 4.4. Thus, the appropriate standard score of this method is a range at ±1.00 of Z-score for this population.

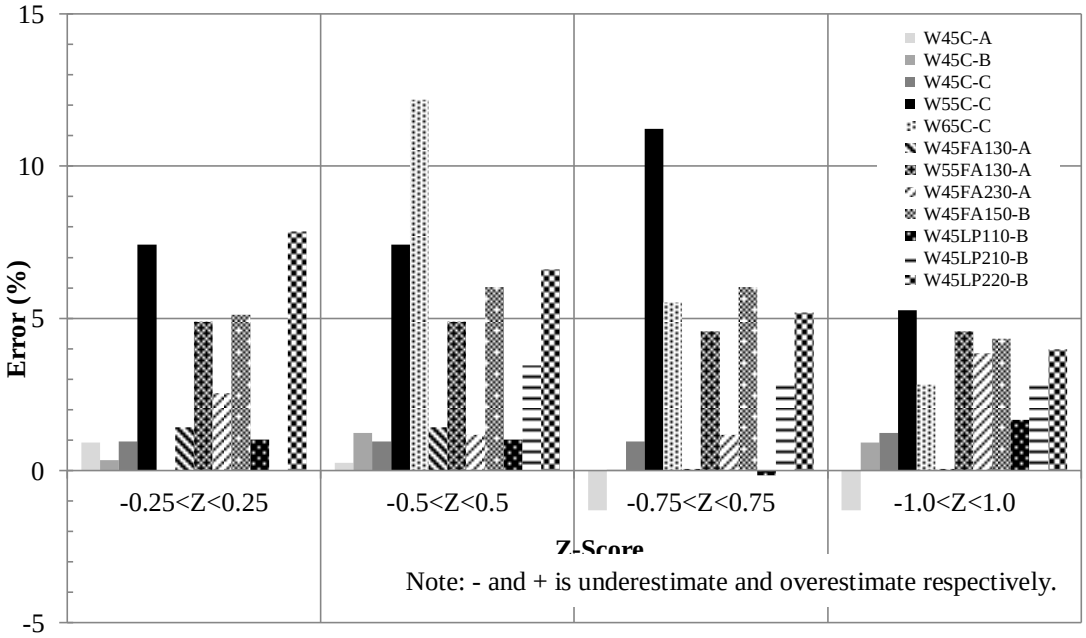

Figure 4.4 Mean error result of coarse aggregate content at each sample set with different Z-Score

Hence, the reasonable Z-score between -1 to 1 (-1 < Z < 1) was applied to analyze the results of the coarse aggregate content of concrete in this study. In addition, the analytical result of Z-score between -1 to 1 (-1 < Z < 1), the maximum error is 5.28% (or 54 kg/m^3) which is within acceptable limits. This can be confirmed that the image processing technique can be efficiently used to determine coarse aggregate content of hardened concrete regardless of source and s/a of aggregate.

In case of the specific gravity of coarse aggregate is unknown, assumed value depending on type of aggregate is used in the analysis. For limestone, assumed specific gravity is 2.7 (the Department of Primary Industries and Mines (2007)). For

other types of aggregate, their specific gravity can be found in ASTM C568 (2003) and ASTM C615 (2003). Since the assumed value of specific gravity of coarse aggregate is used, the error of the determination of coarse aggregate content by this method can be occurred. However, the error is insignificant as 1% of change of specific gravity of coarse aggregate causes 1% of error of the determination of coarse aggregate content.

Table 4.2 Analytical result of coarse aggregate content of cement concrete by image analysis

Sample	Coarse aggregate content (kg/m^3)		% Error.
	By designed	By image analysis	
W45C-A	1047	1033.3	-1.31
W45C-B	1062	1071.6	+0.93
W45C-C	1025	1037.7	+1.24
W55C-C	1025	1079.1	+5.28
W65C-C	1025	1054.1	+2.84

Note: - and + is underestimate and overestimate respectively.

For the cement concrete, the content of coarse aggregate estimated by image processing technique is shown in Table 4.2. From the analytical results, the percentage of error is between 0.93 (or 9.6 kg/m^3) to 5.28%. The maximum error is 5.28% (or 54 kg/m^3) which is acceptable. This result was used to determine mix proportion procedure.

4.4.2 Determination of water to cement ratio

The results of compressive strength of concrete sample are shown in Table 4.3. The water to cement ratios obtained from the back analysis of the compressive strength data by using FACOMP are shown in Table 4.4.

From Table 4.4, it can be seen that the water to cement ratio obtained from back analysis of the compressive strength data by using FACOMP is close to the designed water to cement ratio for all mixtures and test ages. The maximum error is 8.89%. This can also be confirmed that the proposed method can be efficiently used to determine water to cement ratio of hardened concrete.

Table 4.3 Tested compressive strength results of hardened cement concrete by UTM

Sample	Compressive strength (MPa)		
	14 days	28 days	91 days
W45C-A	-	43.99	48.95
W45C-B	-	41.30	46.81
W45C-C	33.96	-	41.87
W55C-C	22.61	-	33.04
W65C-C	17.66	-	23.23

Table 4.4 Analytical result of w/c ratio of cement concrete by FACOMP

Sample	Design	w/c					
		14 days		28 days		91 days	
		Trial	Error (%)	Trial	Error (%)	Trial	Error (%)
W45C-A	0.45	-	-	0.41	-8.89	0.43	-4.44
W45C-B	0.45	-	-	0.43	-4.44	0.45	0
W45C-C	0.45	0.45	0	-	-	0.48	+6.67
W55C-C	0.55	0.57	+3.64	-	-	0.56	+1.82
W65C-C	0.65	0.66	+1.54	-	-	0.70	+7.69
Mean error (%)		**+1.73**		**-6.67**		**+2.35**	
		+0.36					

Note: - and + is underestimate and overestimate, respectively.

4.4.3 Calculation of mix proportion of hardened concrete

4.4.3.1 Calculation of mix proportion with designed value of coarse aggregate content and w/c

In this order, the proposed method for calculation of mix proportion of cement concrete was verified by using design w/c and coarse aggregate content with calculating procedure. This verification was also analyzing efficiently developed method of determination of content of cement and sand by residual weight.

Residual weight of cement and sand with aggregate set A, B and C are shown in Table 4.5. Residual weights of sample by selective dissolution method are shown in Table 4.6. In addition, a few amount of cement was still insoluble. They are subsequently used to calculate weight ratio of cement and sand.

Table 4.5 Residual weight of concrete materials by selective dissolution method

Materials	Residue (%)		
	A	B	C
Cement	0.420	0.417	0.417
Sand	94.935	96.671	96.671

Table 4.6 Residual weight of cement concrete sample by selective dissolution method

Sample	Residue (%)		
	14 days	28 days	91 days
W45C-A	-	55.837	55.442
W45C-B	-	59.437	59.323
W45C-C	61.374	-	60.965
W55C-C	64.380	-	64.011
W65C-C	66.628	-	64.405

The design value of w/c and coarse aggregate content were used to verify proposed equation as presented in Eq. (4.12)-(4.19); hence, the proposed calculation method was evaluated the efficiency. The results of cement, water and sand content and percentage error are shown in Table 4.7 and 4.8, respectively.

Table 4.7 The analytical results of mix proportion of cement concrete with designed w/c and coarse aggregate content.

Sample	w/c	Cement (kg/m^3)	Water (kg/m^3)	Sand (kg/m^3)	Coarse aggregate (kg/m^3)
W45C-A	**Design**	**419**	**188**	**727**	**Design**
28 days	*0.45*	418	188	729	*1047*
91 days	*0.45*	420	189	724	*1047*
W45C-B	**Design**	**407**	**183**	**737**	**Design**
28 days	*0.45*	393	177	769	*1061*
91 days	*0.45*	393	177	769	*1061*
W45C-C	**Design**	**407**	**183**	**776**	**Design**
14 days	*0.45*	386	174	816	*1025*
91 days	*0.45*	388	175	813	*1025*
W55C-C	**Design**	**360**	**198**	**776**	**Design**
14 days	*0.55*	337	186	826	*1025*
91 days	*0.55*	339	187	821	*1025*
W65C-C	**Design**	**322**	**210**	**776**	**Design**
14 days	*0.65*	302	196	826	*1025*
91 days	*0.65*	319	207	786	*1025*

Table 4.8 Percentage error of mix proportion of cement concrete with designed w/b and coarse aggregate content

Sample	Age (days)	% Error		
		Cement	Water	Sand
W45C-A	28	-0.19	-0.19	+0.22
	91	+0.36	+0.36	-0.42
W45C-B	28	-3.53	-3.53	+4.27
	91	-3.56	-3.56	+4.30
W45C-C	14	-4.97	-4.97	+5.20
	91	-4.61	-4.61	+4.82
W55C-C	14	-6.22	-6.22	+6.50
	91	-5.62	-5.62	+5.88
W65C-C	14	-6.26	-6.26	+6.55
	91	-1.22	-1.22	+1.27
Mean error (%)		**-3.58**	**-3.58**	**+3.86**

Note: - and + is underestimate and overestimate respectively.

From the analytical results, it can be seen that the proposed calculating method can be used to estimate cement and sand content of hardened concrete with good accuracy for all mixtures. The maximum errors of the determination of cement and sand content are -6.26 % and +6.55 %, respectively. The mean errors of the determination of content of cement and sand are -3.58 % and +3.86%, respectively. The results show that the proposed calculation method is effectively used to estimate mix proportion of hardened cement concrete. Hence, the analytical results of cement and sand content show that the residue of selective dissolution testing is effectively adopted to estimate mix proportion of hardened cement concrete. Moreover, it can be seen that the analytical result of mix proportion of the same sample at different age is nearly same for all samples, except W65C-C. Hence, the analytical result of mix proportion of the same sample at different age can also be accurately determined since the effect of concrete age is covered by taking into account the degree of hydration inthe analysis. But, the different error between sample W65C-C at 14 and 91 days may be occurred by human error from sample preparation procedure.

4.4.3.2 Calculation of mix proportion with analytical result of coarse aggregate content and trial w/c

Mix proportion of cement concrete estimated by the proposed method and its error percentages are shown in Tables 4.9 and 4.10, respectively.

Table 4.9 The analytical results of mix proportion of cement concrete

Sample	Age (days)	w/c	Cement (kg/m^3)	Water (kg/m^3)	Sand (kg/m^3)	Coarse aggregate (kg/m^3)
W45C-A	**Design**	**0.45**	**419**	**188**	**727**	**1047**
	28	0.41	433	178	756	1033
	91	0.43	430	185	741	1033
W45C-B	**Design**	**0.45**	**407**	**183**	**737**	**1061**
	28	0.43	396	170	775	1072
	91	0.45	390	176	765	1072
W45C-C	**Design**	**0.45**	**407**	**183**	**776**	**1025**
	14	0.45	383	173	810	1038
	91	0.48	378	181	792	1038
W55C-C	**Design**	**0.55**	**360**	**198**	**776**	**1025**
	14	0.57	323	184	790	1079
	91	0.56	327	183	790	1079
W65C-C	**Design**	**0.65**	**322**	**210**	**776**	**1025**
	14	0.66	296	195	808	1054
	91	0.70	305	214	752	1054

Table 4.10 Percentage error of mix proportion of cement concrete

Sample	Age (days)	% Error				
		w/c	Cement	Water	Sand	Coarse aggregate
W45C-A	28	-8.89	+3.53	-5.67	+3.95	-1.31
	91	-4.44	+2.65	-1.92	+1.85	-1.31
W45C-B	28	-4.44	-2.84	-7.16	+5.02	+0.93
	91	0	-4.15	-4.15	+3.66	+0.93
W45C-C	14	0	-5.70	-5.69	+4.40	+1.24
	91	+6.67	-7.11	-0.91	+2.08	+1.24
W55C-C	14	+3.64	-10.28	-7.02	+1.89	+5.28
	91	+1.82	-9.22	-7.57	+1.84	+5.28
W65C-C	14	+1.54	-8.36	-6.96	+4.16	+2.84
	91	+7.69	-5.42	+1.85	-3.04	+2.84
Mean error (%)		**+0.36**	**-4.69**	**-4.52**	**+2.58**	**+1.79**

Note: - and + is underestimate and overestimate respectively.

From the analytical results, it can be seen that the proposed method can be used to effectively estimate the mix proportion of hardened concrete for all mixtures. The maximum errors of the determination of content of cement, water, sand, and coarse aggregate are -10.28 %, -7.57 %, +5.02 %, and +5.28 %, respectively. The mean errors of the determination of content of cement, water, sand, and coarse aggregate are -4.69 %, -4.52 %, +2.58 %, and +1.79%, respectively. Although the mean errors of cement, water and sand increase due to many procedures used in the determination of mix proportion, the results show that the proposed method can be used to estimate the mix proportion of hardened concrete at different water to cement ratios and different sources of aggregate.

4.5 Summary

The method for estimating mix proportion of hardened cement concrete has been proposed in this study. The developed method was applied to estimate mix proportions of concrete prepared in laboratory with known mix design in order to verify its efficiency. Moreover, it was found that the proposed calculation method can be used to determine mix proportion of hardened concrete with good accuracy even though different age of concrete sample, since the effect of age of concrete is covered by taking into account the degree of hydration of sample in the analysis.

In addition, the determination of mix proportion of hardened concrete was analyzed by many procedures as shown in Figure 4.1. The error of coarse aggregate content by image processing and w/c ratio was effected analytical result as shown in Figure 4.5 (a) and (b). It was found that the errors of cement, water, and sand were related to result of w/c and coarse aggregate content.

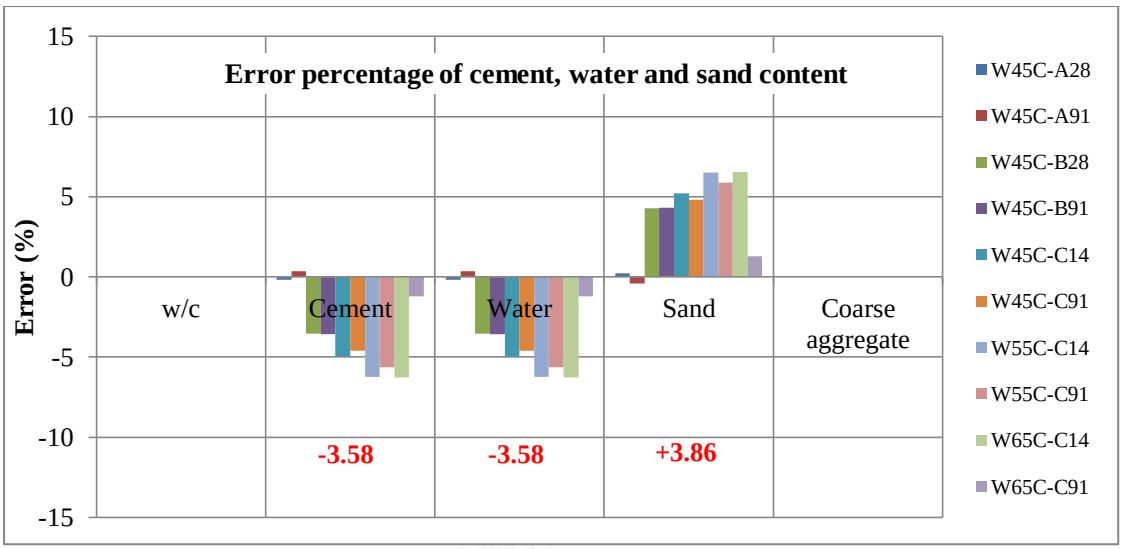

(a) Determining mix proportion with designed w/b and coarse aggregate

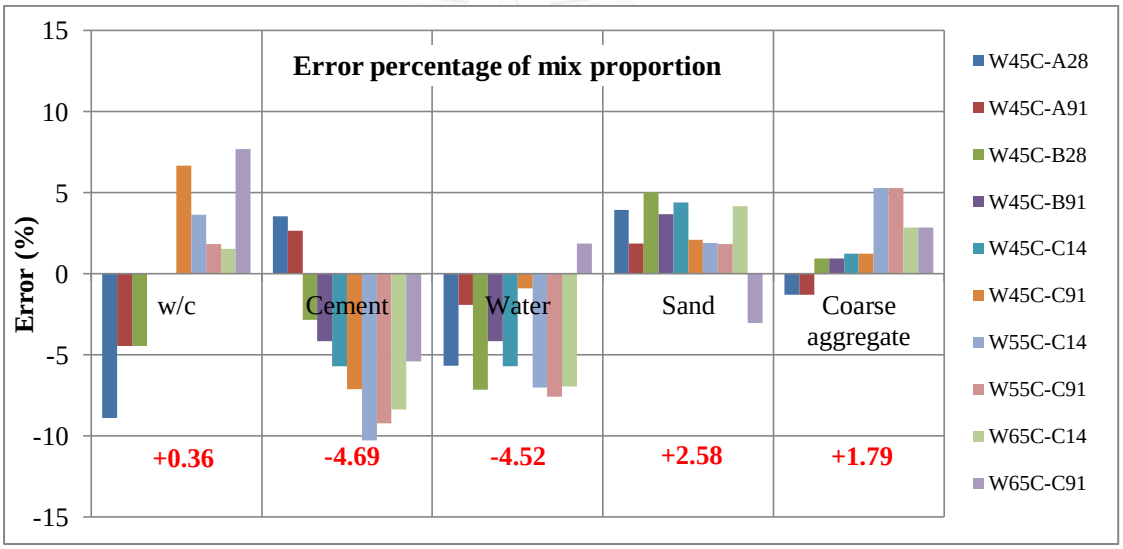

(b) Determining mix proportion with analytical result of w/b and coarse aggregate content

Figure 4.5 The error percentages of analytical result of each material of cement concrete

CHAPTER 5
DETERMINATION OF MIX PROPORTION OF HARDENED CEMENT-FLY ASH CONCRETE

5.1 General

In this chapter, the cement-fly ash concrete (FA concrete) was studied for determining mix proportion. When concrete contains fly ash, its type must be identified first. The methodology of this study can be divided into 2 main procedures: one is the investigation of fly ash existence procedure and the other is the determination of mix proportion of concrete procedure. The methods for evaluating fly ash existence and determining mix proportion of FA concrete have been proposed. The physical, mechanical and chemical analysis methods were adopted for the analysis. The analytical procedures for evaluating fly ash existence and determining water to binder ratio, fly ash replacement ratio and content of concrete compositions including water, cement, fly ash, sand, and coarse aggregate are described in this chapter.

5.2. Material and Mix proportion

FA concrete samples were prepared with water to binder ratio (w/b) of 0.45 and 0.55. The concrete samples were prepared by using different aggregates (A and B). The specific gravity of FA1 and FA2 is 2.29 and 2.24, respectively. The concrete samples at 28 and 91 days were prepared for mix proportion determination. The ratio by volume of sand to total aggregate (s/a) was 0.42 for all mixes, and the void ratio of sample at aggregate set A and B was 0.237 and 0.230, respectively. Four mix designs of concrete specimens are shown in Table 5.1. The sample preparations were mentioned in Chapter 3.

Table 5.1 Mix proportion for determination of mix proportion of hardened FA concrete

Sample	w/b	Cement	Fly ash			Water	Sand	Coarse aggregate
		(kg/m^3)	Type	% rep.	(kg/m^3)	(kg/m^3)	(kg/m^3)	(kg/m^3)
W45FA130-A	0.45	280	FA1	30	120	180	727	1047
W55FA130-A	0.55	249	FA1	30	107	196	727	1047
W45FA230-A	0.45	279	FA2	30	120	179	727	1047
W45FA150-B	0.45	193	FA1	50	193	174	729	1058

5.3 Investigation of Physical and Chemical Properties of Materials

This experiment is aimed to investigate basic properties of materials. Basic information on each type of material including chemical and physical properties will

be investigated. The results will be used as a database for analyzing concrete samples. They will be utilized for analyzing in procedure of investigation of fly ash existence and estimation of mix proportion. The techniques adopted for investigation are consisted of many techniques such as Scanning Electron Microscope (SEM) technique, SEM equipped with Energy Dispersive X-Ray Spectroscopy (EDS) technique, X-Ray Diffraction (XRD) technique, X-Ray Fluorescent (XRF) technique and selective dissolution method.

5.3.1 Physical properties

5.3.1.1 Particle shape and size by Scanning Electron Microscope (SEM) analysis

This technique was used to investigate particle shape of materials. Normally, fly ash has a spherical shape but it is possible that fly ash particle from some sources is in irregular shape (Kutchko and Kim 2006). Moreover, particle shape of cement has irregular shape, too. Therefore, it is necessary to ensure whether the particle shape of fly ash is spherical or not and that different shapes and sizes of these particles can be determined.

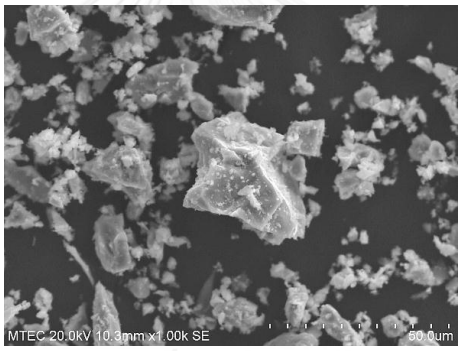

(a) Portland Cement

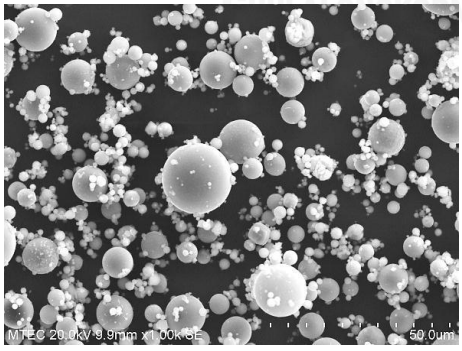

(b) FA1

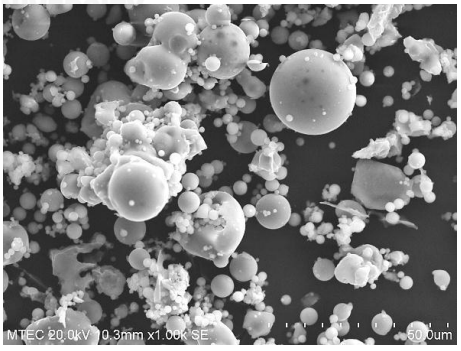

(c) FA2

Figure 5.1 Particle shapes of cement and fly ash by SEM

The results of particle shape of Portland cement, 2 types of fly ash (FA1 and FA2) were shown in Figure 5.1. From the experimental results, the cement particle mostly has irregular shape as shown in Figure 5.1 (a). And the almost particle of FA1 appears in the spherical shape (precipitator) as shown in Figure 5.1 (b). But the

particle shape of FA2 consists both spherical shape (precipitator) and irregular shape (plerospheres) as shown in Figure 5.1 (c). This experimental result was used for analyzing the investigation of fly ash existent procedure.

5.3.2 Chemical properties

5.3.2.1 Elemental composition by Scanning Electron Microscope equipped with Energy Dispersive X-Ray Spectroscopy (SEM-EDS) analysis

This technique was used to measure the spectrum of elements such as Ca, Al, or Si in materials. Moreover, different fly ash particles may have different elemental compositions depending on quality of the fly ash (Barzin, Aboozar et al. 2007). The relationship of the elements such as Ca and Si was investigated. The Ca/Si ratio by weight was used in order to identify some particles that they may be fly ash particle. The results are shown in Figure 5.2.

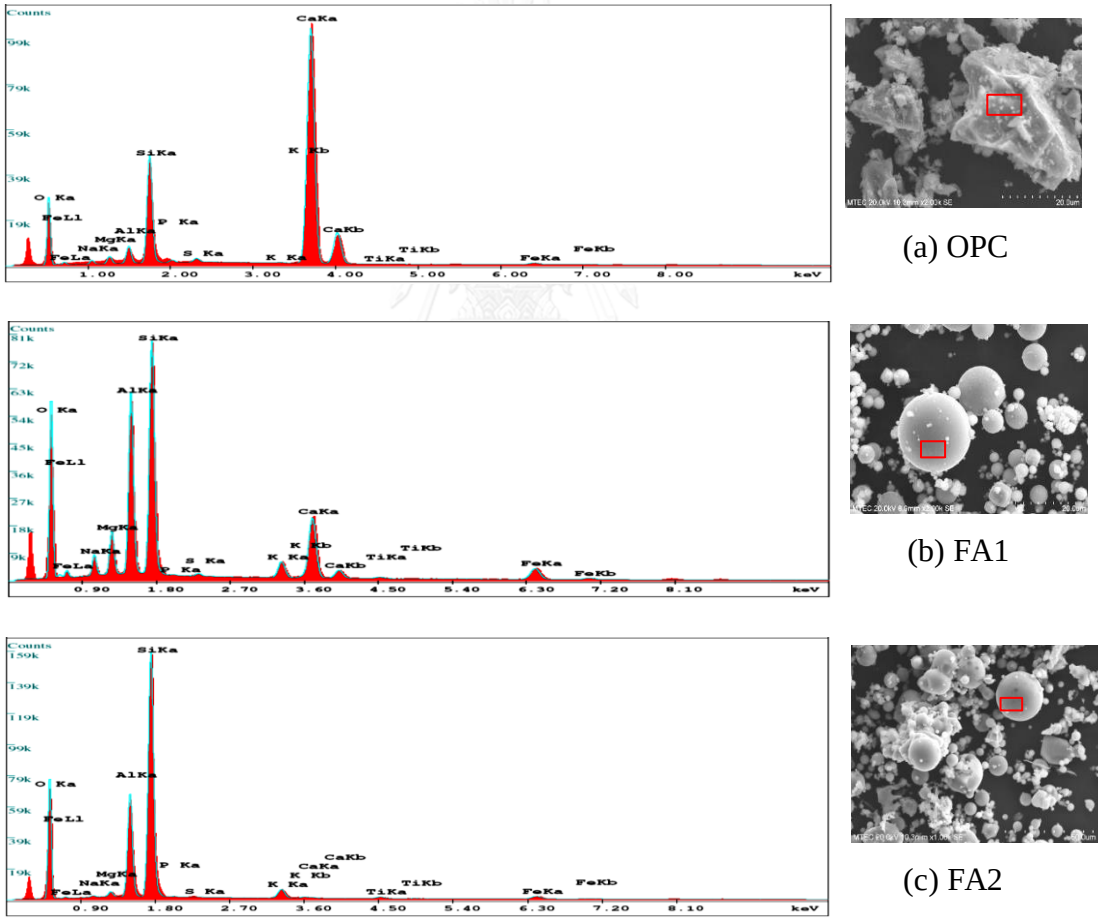

Figure 5.2 Elemental compositions of cement and fly ash by SEM-EDS

Generally, the chemical composition of cement is mainly CaO and SiO_2 while the chemical composition of fly ash is mainly SiO_2 and Al_2O_3. From the experimental results, the greatest elements in cement are Ca and Si, respectively, and fly ash mainly contains Si and Al. The experimental results show that the elemental result of FA1

and FA2 is highest in Si and Al respectively. In addition, the content of Ca in FA1 is higher than FA2.

Hence, the amount of Ca/Si ratio of cement should be more than 1, because they are high Ca as shown in Table 5.2. But, fly ash consists more SiO_2 and Al_2O_3 than CaO. So, the amount of Ca/Si ratio of fly ash should be lower than 1 that Ca/Si ratio of fly ash depends on type of source and production of fly ash as the result shown in Table 5.2 in which the amount of Ca/Si of fly ash is lower than 1. The Ca/Si of FA1 and FA2 is 0.307 and 0.005, respectively. This experimental result was used for analyzing investigation of fly ash existent procedure.

Table 5.2 Ca/Si ratio by weight of elemental composition of materials

Elemental	Cement	FA1	FA2
Ca (%)	39.79	7.34	0.18
Si (%)	13.38	23.93	38.83
Ca/Si Ratio	2.974	0.307	0.005

5.3.2.2 Mineral composition by X-Ray Diffraction (XRD) analysis

This technique is used to the investigate type of mineral composition or crystalline phase in materials. The XRD analysis is used to quantify the mineral compositions of materials. It is known that most of mineral phase in sand is quartz (SiO_2). In case of cement, four major phases of mineral compositions are C_3S, C_2S, C_3A, and C_4AF in which cement is constituted about 50-70 %, 15-30 %, 5-10 % and 5-15 %, respectively (Taylor 1997). In case of fly ash, the mineral phase results can be seen that the fly ash had some mineral phases which were different from those in cement and sand. These minerals are Mullite, Hematite, and Magnetite which are unique phase of fly ash. The amount of each phase is depends on type of fly ash (Booher, Martello et al. 1994).

Table 5.3 The Mineral Composition of fly ash by XRD-Reitveld

Phase	FA1	FA2
Mullite(%)	1.867	10.929
Hematite(%)	0.602	0.455
Periclase(%)	1.574	0.276
Magnetite(%)	3.396	0.651
Lime(%)	0.389	0.039
Thernardite(%)	1.110	0.767
Quartz(%)	0.993	11.887
Anhydrite(%)	3.640	-
Rutile(%)	-	0.098
Arcanite(%)	0.313	0.572
Portlandise(%)	1.118	-
Tobermorite(%)	4.008	-
Amorphous(%)	80.989	74.290

The mineral composition of fly ash was compared with those of cement and sand. The crystalline phases of fly ashes were quantified by XRD technique as shown

in Table 5.3. It can be seen that both of fly ash had unique phase but different in quantity. This experimental result was used for analyzing investigation of fly ash existent procedure.

5.3.2.3 Chemical composition by X-Ray Fluorescent (XRF) analysis

This technique was used to investigate the chemical composition of materials. The XRF analysis was used to quantify the chemical compositions of material such as calcium oxide (CaO), silica (SiO_2) and alumina (Al_2O_3). Generally, it is known that most of the chemical composition in sand is SiO_2 as shown in Table 5.4. The results show that the main chemical compositions of Portland cement type I was CaO. On the other hand, the main chemical composition of fly ash was SiO_2, Al_2O_3 and Fe_2O_3. In addition, the content of each chemical composition depends on the source of fly ash. The FA1 and the FA2 had lower CaO content than the Portland cement as shown in Table 3.1. When both of fly ashes were compared, it was shown that the FA2 had more SiO_2 and Fe_2O_3 contents than the FA1. The FA1 had more CaO content than the FA2. This experimental result was used for determining the mix proportion of hardened concrete procedure.

Table 5.4 The chemical composition of materials

Chemical compositions	Sand-A	Sand-B
SiO_2 %	88.6	96.66
Al_2O_3 %	5.08	1.06
Fe_2O_3 %	1.19	1.16
CaO %	0.51	0.07
MgO %	0.01	0.01
SO_3 %	0.04	0.01
Na_2O %	0.46	0.01
K_2O %	3.01	0.33
TiO_2 %	0.10	0.16
P_2O_5 %	0.01	0.04
LOI %	0.83	0.30

5.3.2.4 Selective Dissolution

The Selective dissolution analysis was used to quantify the residues left of each material. This technique was used to dissolve calcium component into material and hydrated product. The residues left form the dissolvent were unhydrated fly ash, sand and a little amount of cement as shown in Table 5.5. From the experimental results, it was seen that the residual weight of the fly ash is correlated with the CaO content (Table 3.1). The fly ash with lower CaO content had higher residual weight. This investigation was utilized for determining mix proportion.

Table 5.5 Residual weight of materials

Samples	Cement-A	Cement-B	FA1	FA2	Sand-A	Sand-B
Residual weight %	0.420	0.417	60.327	93.345	94.935	96.671

5.4 Procedure for investigation of fly ash existence in hardened concrete

This procedure is aimed to investigate fly ash existence in hardened concrete. The physical and chemical analysis methods, such as SEM technique, SEM-EDS technique, and XRD technique, were adopted. In addition, the concrete samples, which were used for investigation, were mixed in laboratory. Thus, type of fly ash in sample is known, and then this procedure can be verified. The fly ash concrete samples were used to investigate fly ash existence in hardened concrete such as W45FA130-A and W45FA230-A.

5.4.1 Methodology

In order to determine the fly ash existence in sample, the procedure for determining fly ash existence in sample is mapped out, as shown in Figure 5.3.

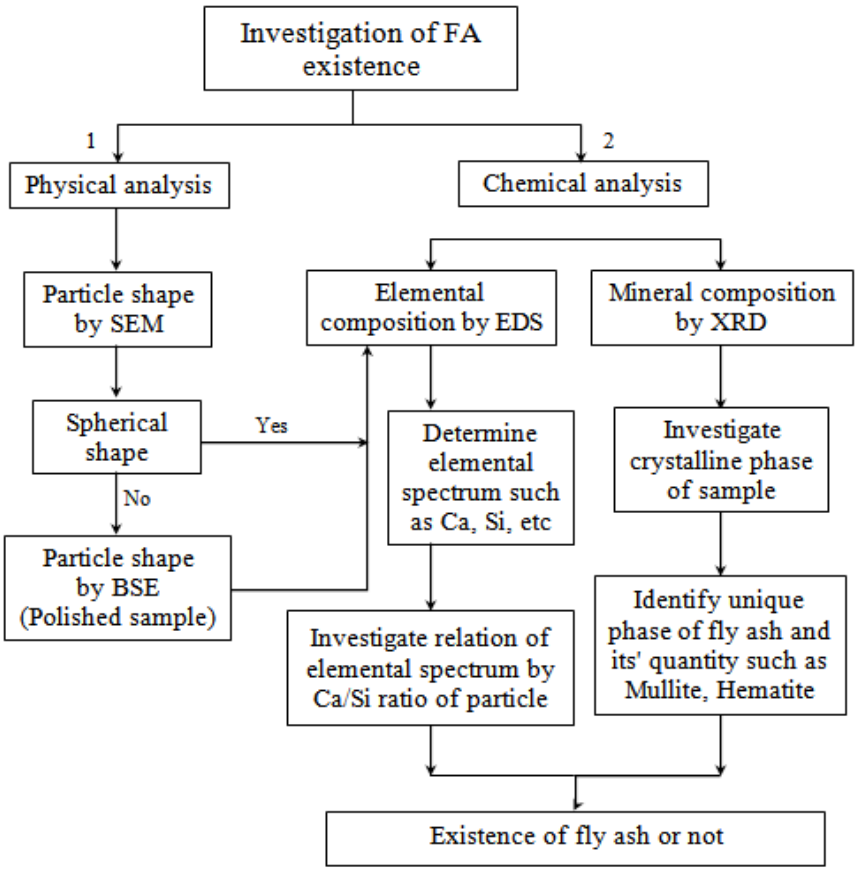

Figure 5.3 Procedure of investigation of fly ash existence

The proposed procedure for investigation of fly ash existence in hardened concrete can be divided into two parts as physical and chemical analysis. The physical analytical technique was to investigate particle shape using SEM techniques and then if they could find some particles that may be fly ash, SEM-EDS technique was used to investigate its elemental composition. In addition, XRD technique was used to investigate unique crystalline phase of fly ash in sample.

5.4.1.1 Physical Analysis by Scanning Electron Microscope (SEM) technique

The small piece of sample as mentioned in Chapter 3 was taken to investigate fly ash existence by SEM. If spherical shape of fly ash is mixed in concrete, its spherical particle should be observed in the concrete samples. However, most fly ash particle might have more pozzolanic reaction if the replacement percent of fly ash in concrete is very low and much time. The fly ash particle may be difficult to find by SEM technique. Hence, the SEM technique was verified by testing mortar sample with low percent of replacement of fly ash and accelerator pozzolanic reaction. This verification is intended to evaluate which is the efficient method. The fly ash-cement mortar was prepared with water to binder (w/b) of 0.45. The various percent replacement of fly ash was 5%, 10%, 15% and 30%. The mortar sample was accelerated, curing by warm water at 50 ºC for 28 days, because the degree of pozzolanic reaction was increased react In addition, mix of mortar was designed by s/b ratio to produce same mix design of concrete, and FA1 was used due to higher amorphous content.

After the SEM was used to investigate fly ash particle, the suspect particle should be evaluated for confirming as fly ash particle. Therefore the sample needs more evaluation on their particle with other techniques. And an additional EDS was adopted.

5.4.1.2 Elemental compositions by Scanning Electron Microscope equipped with Energy Dispersive X-ray Spectrometer (SEM-EDS) technique

This technique was used to measure the spectrum of elements such as Ca, Al, or Si in materials. After the concrete sample had been analyzed by the SEM, the EDS was used to identify the particles in sample that it was suspected to be fly ash particles. The relationship of the spectrum of elements such as Ca, Al or Si of the particles in sample was determined. Normally, the Ca/Si ratio of the cement and hydrated product is higher than 1. In contrast, the Ca/Siratio of the fly ash is lower than 1 due to high SiO_2 content and low CaO. Thus, if the Ca/Si ratio of the suspect particle is lower than 1, it was fly ash particle.

However, the SEM-EDS technique cannot investigate if some particle which may be fly ash cannot be found. Hence the XRD technique was adopted, and the sample needs other techniques to further investigate fly ash existence.

5.4.1.3Mineral compositions by X-Ray Diffraction (XRD) technique

The mineral compositions were quantified the crystalline phase by XRD. The powder sample with corundum as mentioned in Chapter 3, was used to investigate. If the unique phase of fly ash can be observed in the sample, it implies that the concrete contains fly ash.

5.4.2 Result and Discussion

5.4.2.1 Physical Analysis by Scanning Electron Microscope (SEM) technique

To verify the SEM method, the mortar samples were evaluated by the SEM as mentioned earlier. From the experimental result in Figure 5.4, spherical particle was found in all samples although fly ash was replaced 5% as the result shown in Figure

5.4 (a). Hence, this technique was effective for finding some fly ash particle in samples.

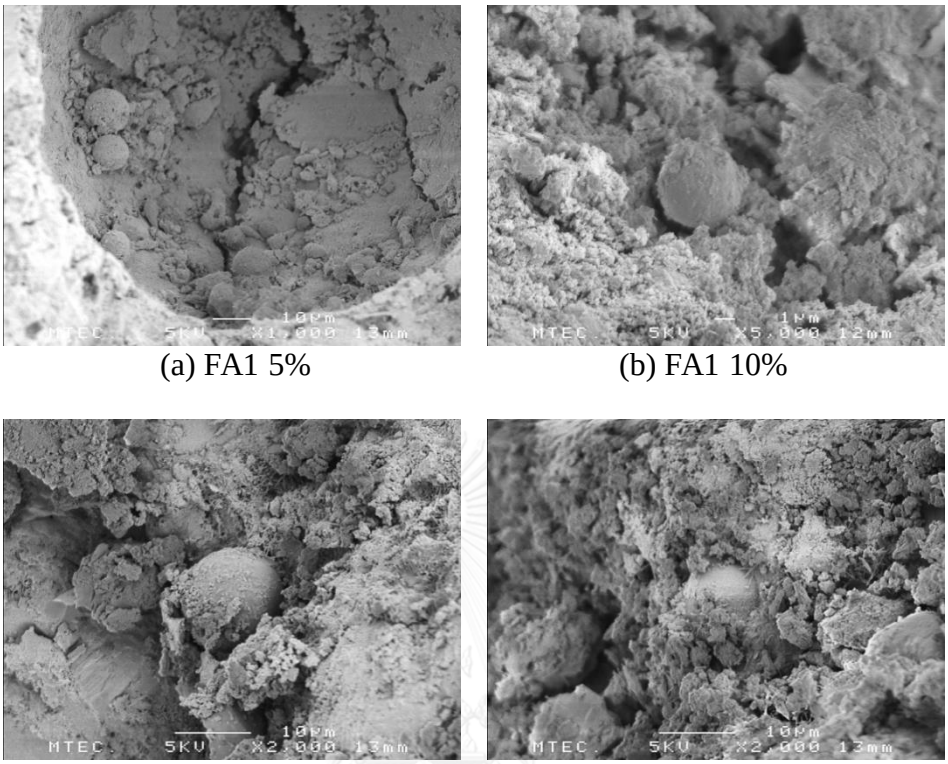

(a) FA1 5% (b) FA1 10%

(c) FA1 15% (d) FA1 30%

Figure 5.4 Investigation fly ash existences in mortar

Then the SEM was applied on concrete samples to investigate fly ash existence, the FA concrete samples W45FA130-A and W45FA230-A were used. The experimental results of FA concrete at 28 days are shown in Figure 5.5 (a) and (b), where spherical particles can be seen to exist in all samples. The experimental results of FA concrete at 91 days are shown in Figure 5.5 (c) and (d), and the spherical particles also exist in all samples of FA concrete. In addition, the FA concrete at 91 days had more degree reaction. It can be seen that the surface of fly ash particles of the sample at 91 days had more reaction than the sample at 28 days.

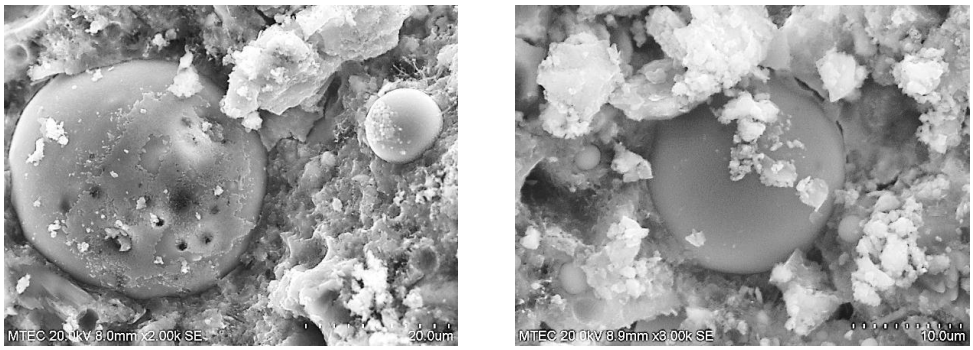

(a) W45FA130-A at 28 days (b) W45FA230-A at 28 days

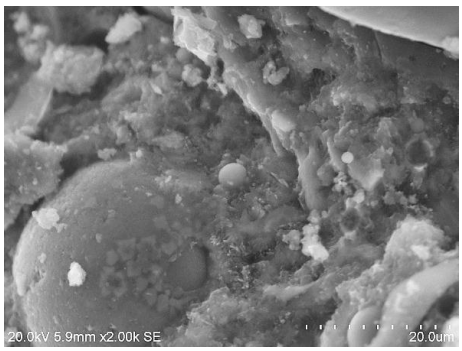

(c) W45FA130-A at 91 days

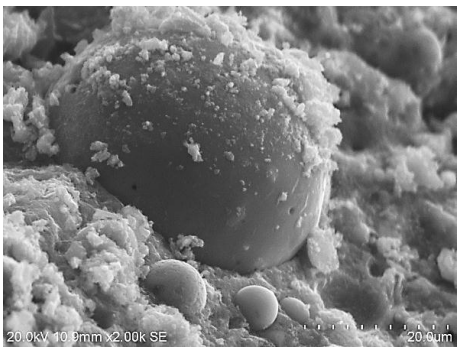

(d) W45FA230-A at 91 days

Figure 5.5 Investigation fly ash existences in hardened concrete

It can be concluded that some spherical particle can be found in the FA concrete samples at 28 and 91 days. This technique is able to investigate fly ash existence in hardened concrete efficiently, still it is not enough to determine the type of fly ash because the experimental result of particle shape of both samples contain spherical particle. Therefore the FA concrete sample needs more testing on their particle with other technique such as SEM-EDS technique.

In addition, the fly ash concrete at long life may be difficult for SEM-EDS testing on surface of particle owing to higher degree of hydration, as shown in Figure 5.5 (c). So, polished sample is needed to be prepared for the SEM-EDS testing. In Figure 5.6 (a), the polished sample was prepared as mentioned in Chapter 3. The experimental result of SEM on polished sample is shown in Figure 5.6 (b). It shows some area of circular shape which indicates to fly ash. Therefore, SEM-EDS were applied to some polished samples.

On the other hand, the samples in which some spherical particle cannot be found cannot be concluded that there is the existence of fly ash. Because some types of fly ash may be in more irregular particle shape which is similar to cement, only SEM technique may be insufficient to distinguish particle of fly ash from other components. Then, the additional XRD technique was adopted to investigate fly ash existence for verification. Moreover this problem is a similar subject of investigation of limestone powder existence, which will be described in the next chapter.

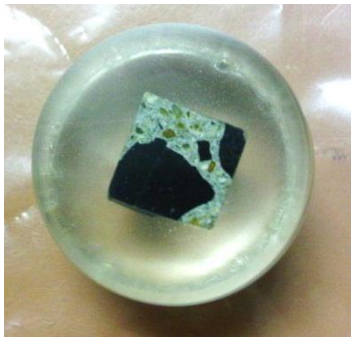

(a) Smooth polished sample

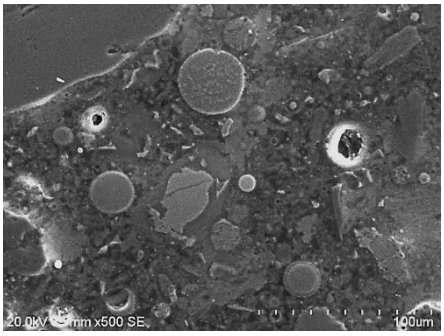

(b) The investigation of the polished sample

Figure 5.6 Investigation of fly ash on polished sample

5.4.2.2 Elemental compositions by Scanning Electron Microscope equipped with Energy Dispersive X-ray Fluorescence Spectrometer (SEM-EDS) technique

This result was used to identify some particles that it may be fly ash. From the experimental results of SEM testing on FA concrete, the fly ash existence in concrete samples was observed. Then, the SEM-EDS technique was applied to investigate its elemental composition of the particles. The SEM-EDS result in Figure 5.7 was investigated to find spherical particles in the sample.

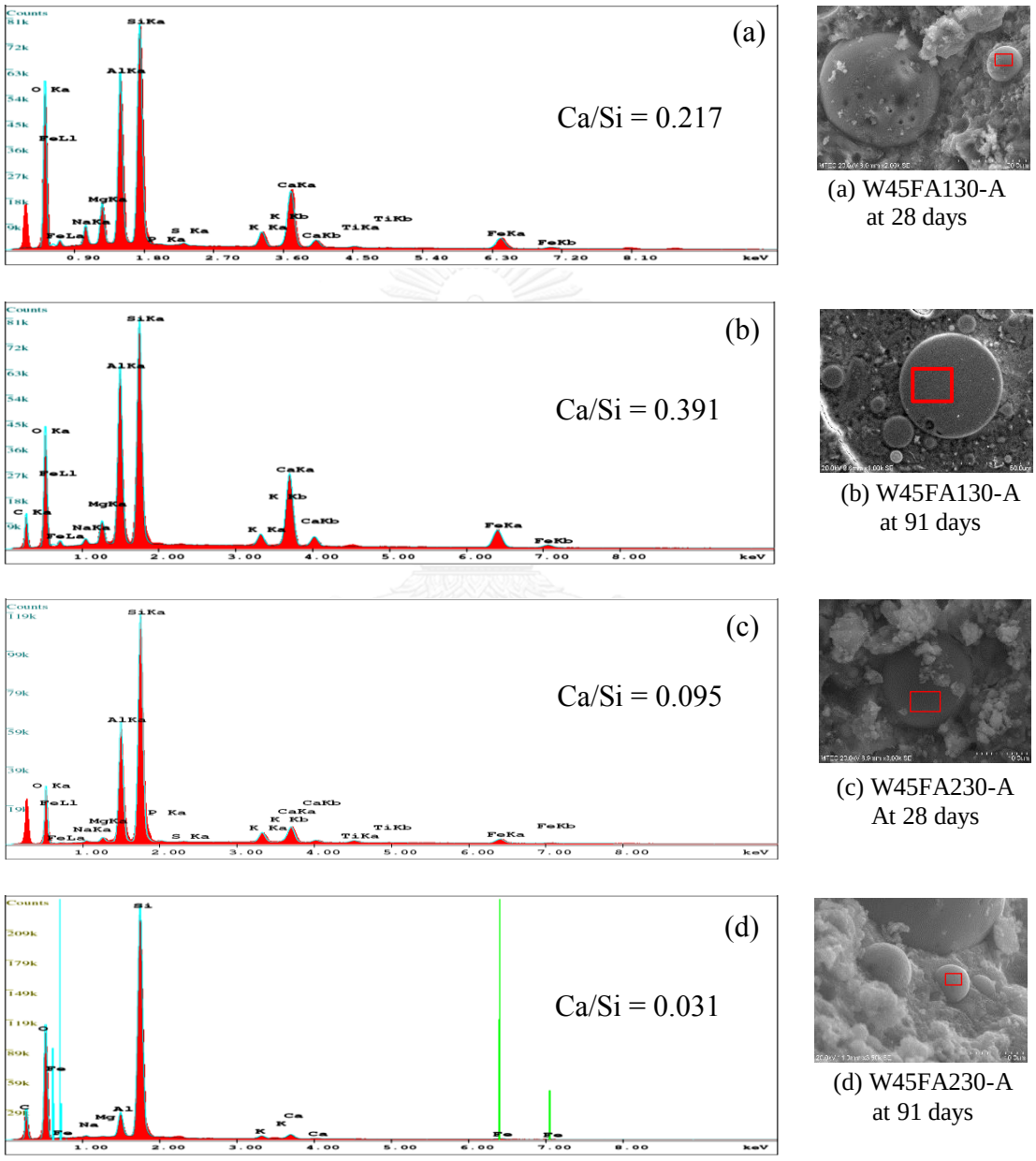

Figure 5.7emental compositions of fly ash particles of samples by SEM-EDS

In the SEM-EDS result in Figure 5.7, the Ca/Si ratio of the observed particle is shown in Table 5.6. This amount of Ca/Si cannot be cement or other hydrated products since Ca/Si ratios are relatively high (normally higher than1). From Figure

5.7 (a) and (b), the Ca/Si ratio of the observed particle is close to that of FA1 that Ca/Si was 0.307. In Figure 5.7 (c) and (d), the Ca/Si ratio is close to that of FA2. Moreover, it can be observed that the pattern of intensity peak of each element in Figure 5.7 (a) and (b) are similar to FA1, as shown in Figure 5.2 (b). And, Figure 5.7 (c) and (d) have similar pattern of intensity peak in Figure 5.2 (c), which is of FA2.

Table 5.6 Ca/Si ratio by weight of elemental composition of fly ash in hardened concrete

Elemental	Cement	FA1	FA2	W45FA130-A		W45FA230-A	
				28 days	91 days	28 days	91 days
Ca (%)	39.79	7.34	0.18	5.25	7.87	4.02	1.31
Si (%)	13.38	23.93	38.83	24.23	20.13	42.31	42.09
Ca/Si Ratio	2.974	0.307	0.005	0.217	0.391	0.095	0.031

From these results, it can be concluded that W45FA130-A contains fly ash, which is FA1, and W45FA230-A contains fly ash, which is FA2. Thus, SEM and EDS procedure was verified, W45FA130-A and W45FA230-A were designing real mix with FA1 and FA2, respectively.

5.4.1.3 Mineral compositions by X-Ray Diffraction (XRD) technique

After investigating SEM and SEM-EDS when fly ash particle cannot be found, the additional XRD technique was adopted to investigate fly ash existence for more information for analysis.

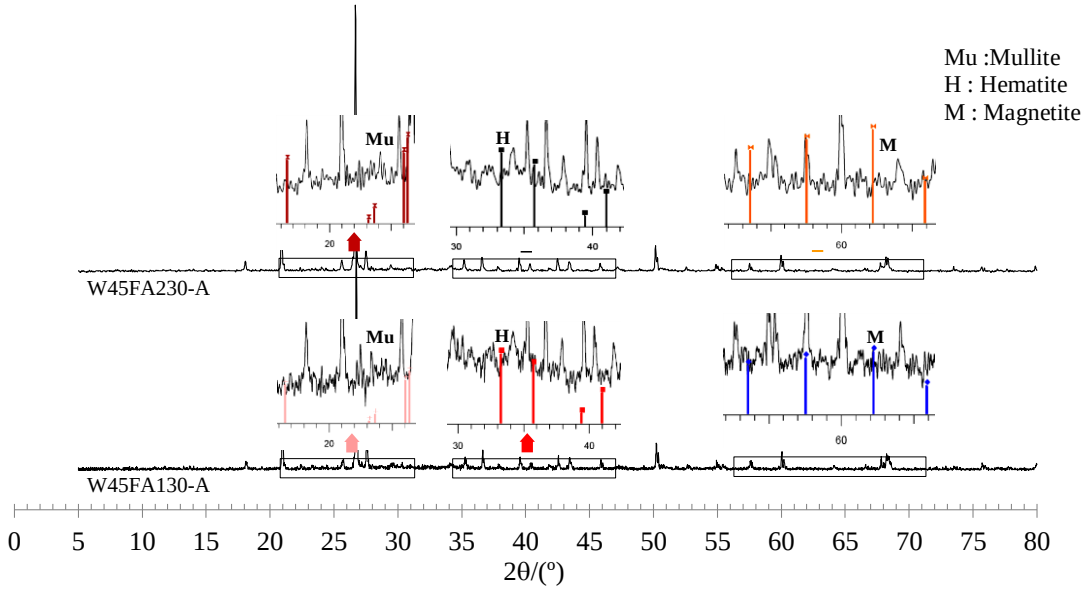

Figure 5.8 XRD pattern of sample W45FA130 and W45FA230 at 28 days

The experimental results show that mineral compositions of the concrete sample were obtained and found that there was determined Mullite, Hematite, and

Magnetite phase in concrete sample of W45FA130-A and W45FA230-A as shown in Figure 5.8. This implies that the concrete contains fly ash.

In addition, the content of crystalline of fly ash in a sample should be the same at each age, because crystalline phase is more inert of a reaction than amorphous phase in concrete system. Thus this experimental result, the only sample at 28 days was investigated. It can be concluded that the sample W45FA130-A and W45FA230-A contained fly ash. But it is noted that this result does not represent fly ash content in the concrete mixture unless additional data of SEM analysis is obtained. Moreover it cannot represent type of fly ash because of the quantitative of each crystalline need be more identified.

5.4.3 Summary

The method for determining fly ash existence in hardened concrete has been proposed in this study. The proposed method was verified by sample prepared in laboratory with known mix design. From the analytical result of SEM technique, it can be concluded that it is efficient to find some spherical particle of fly ash although only 5% fly ash replaced. The SEM-EDS technique was adopted for evaluating their particle after the SEM testing. The analytical result of EDS technique can be concluded that it is also able to identify fly ash particle efficiently. As mentioned above, additional XRD technique was adopted to investigate fly ash existence for ensuring, especially fly ash type with irregular shapes.

5.5 Procedure for estimation of mix proportion of hardened concrete containing fly ash

After the fly ash existence had been evaluated, the mix proportion was determined. In order to estimate the mix proportion of hardened concrete, several testing techniques were adopted such as Universal Testing Machine (UTM), Selective dissolution, X-Ray Fluorescent (XRF) technique, and Image processing. In addition, the concrete samples, which were used for determining mix proportion, were mixed in laboratory. Thus, mix design of sample was known, and then this procedure can be verified. Four FA concretes were determined mix proportion of hardened concrete as shown in Table 5.1.

5.5.1 Methodology

In the order to determine the mix proportion of hardened FA concrete, the experiment for estimating mix proportion of hardened concrete has been proposed. In the analysis, three main parts for determining mix proportion were implemented as shown in Figure 5.9. It is a similar method for estimating mix proportion of hardened cement concrete. But the fly ash content was added to determine the mix proportion. Thus the CaO content was added to analyze procedure for determining weight ratio of cement, fly ash and sand. The developed method was applied to estimate mix proportions of concrete prepared in laboratory with known mix design in order to verify its efficiency. Detail of the procedure for determination of mix proportion of hardened concrete is described below.

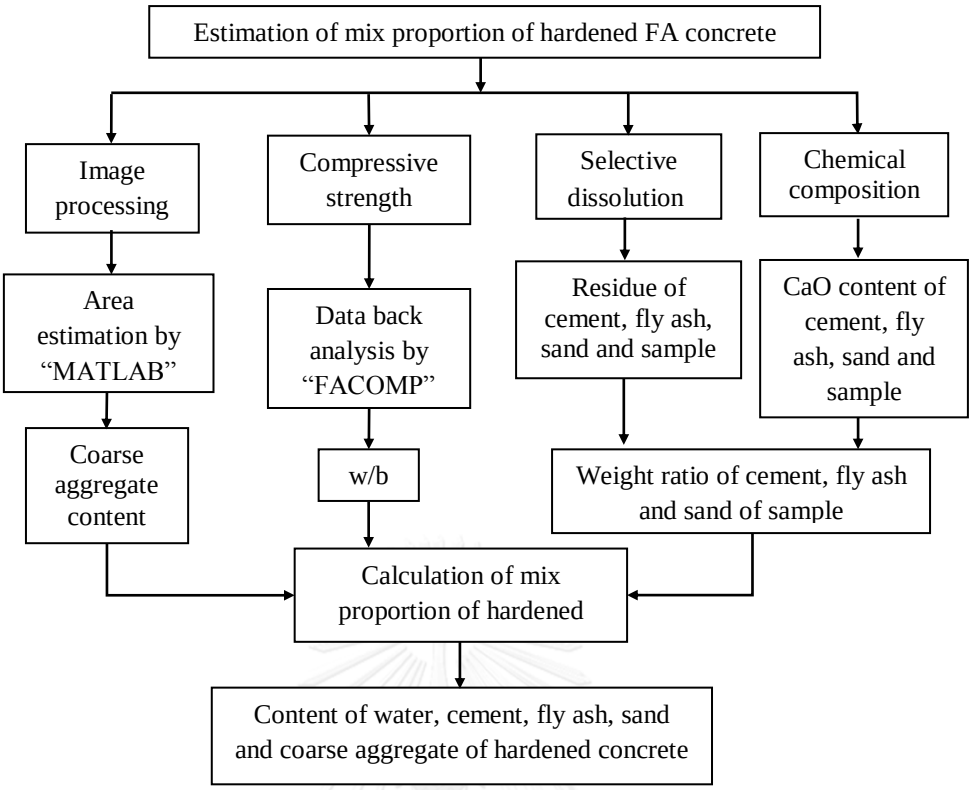

Figure 5.9 Method for determination of mix proportion of hardened FA concrete

5.5.1.1 Determination of coarse aggregate by image processing

The image analysis method was used to determine coarse aggregate content per unit of hardened concrete. The analytical method is the same as mentioned in Chapter 4.

5.5.1.2 Determination of water to binder ratio

The compressive strength of concrete samples was obtained by using the universal testing machine. Then, the water to binder ratio could be calculated from data back analysis of the compressive strength by using the computer software "FACOMP". The procedure for determining water to binder ratio is the same procedure for determining water to cement ratio of cement concrete sample as mentioned in Chapter 4.

5.5.1.3 Determination of weight ratio of cement, fly ash and sand by residual weight and CaO content

In order to determine weight ratio of cement, fly ash and sand in sample, the three unknowns could be solved by three equations. The three primary equations were needed to solve the weight ratio of cement, fly ash and sand. Eq. (5.1) to (5.4) were formed based on the mass balance of sample without coarse aggregate at oven-dried state. The equations were used to determine the weight ratio of cement, fly ash and sand in sample.

First, Eq. (5.1) was formed based on mass balance condition of sample without coarse aggregate (mortar in the concrete), which was cement, fly ash, sand

and water, equal 1. Next, was formed by balance of residue weight between sample and total of each material, which was cement, fly ash and sand, after dissolved by the selective dissolution testing as followed Eq. (5.3). The residues left from being dissolved were sand, unhydrated fly ash and a little amount of cement. Eq. (5.1) and Eq. (5.3) was formed by same principle of equation for cement concrete. Last, the additional equation was formed by balance of CaO content between sample and total of each material, which was cement, fly ash and sand, as follow Eq. (5.4).

$$w_{ts} = w_{cs} + w_{fs} + w_{ss} + w_{ns} \tag{5.1}$$

$$w_{ns} = 0.23(\alpha_{hy} w_{cs}) + w_{nf}(\alpha_{poz} w_{fs}) \tag{5.2}$$

$$r_{ts} w_{fs} = r_c w_{cs} + (1-\alpha_{poz}) r_f w_{fs} + r_s w_{ss} \tag{5.3}$$

$$C_{ts} w_{ts} = C_c w_{cs} + C_f w_{fs} + C_s w_{ss} \tag{5.4}$$

In addition, the CaO content of XRF method was more time consuming and expensive for testing result. And the different science service institutions have difference testing result especially the result of concrete sample without coarse aggregate, since the database of each institution may not be the same or not enough on quantitative analyzing the sample. The database of the sample needs generated calibration standards curves, which can be used for analysis of samples with similar matrices, for best accuracy, but it concerns extensive benefit of new calibration curve to various type of concrete with many factors as it takes more time and expenses to prepare sample and testing for new calibration curve. Consequently, the CaO content was determined by other method that is considered related between residue left and CaO content based on the mass balance principle. The existing data could obtain the relationship between residue left and CaO content as shown in Figure 5.10. They obtained empirical equation as Eq. (5.5)

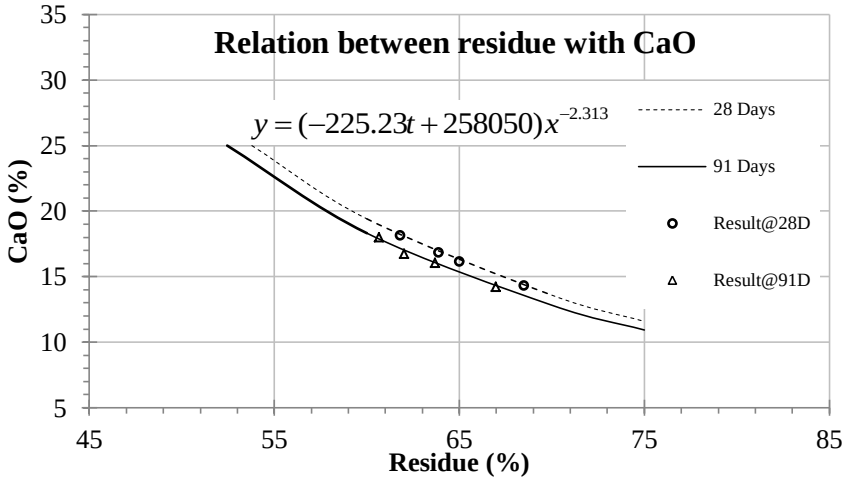

Figure 5.10 Relation of residue and CaO

$$C_{ts} = (-225.23t + 258050) r_{ts}^{-2.313} \quad (5.5)$$

Where r_{ts} is residual weights of sample (g/g of sample), r_c is residual weights of the cement (g/g of cement). r_s is residual weights of sand (g/g) of sand. r_f is residual weights of fly ash (g/g of fly ash). w_{ts}, w_{cs}, w_{fs}, w_{ss} and w_{ns} are oven-dried weight ratio of sample, cement, fly ash, sand, and combined water of the sample to oven-dried weight ratio of sample without coarse aggregate (mortar in concrete) , respectively. w_{ts} is equal 1. α_{hy} and α_{poz} are degree of hydration and pozzolanic reaction of fly ash-cement system. In this study, the degree of hydration and pozzolanic reaction were determined by a computer software (FACOMP 2006). 0.23 is assumed the combined water value of hydration of cement for full degree reaction (Taylor 1997). w_{nf} is 0.20 and 0.18 which are assumed the combined water value of pozzolanic reaction of high CaO fly ash for the percentage fly ash replacement as 30% and 50%, respectively (Saengsoy 2002), and w_{nf} is 0.173 which is assumed the combined water value of pozzolanic reaction of low CaO fly ash (Zeng, Li et al. 2012). t is age of sample (days). C_{ts}, C_c, C_f and C_S are percentage of CaO content of the sample, cement, fly ash and sand, respectively.

5.5.1.4 Calculation of mix proportion of hardened concrete

After the coarse aggregate content and weight ratio of cement, fly ash and sand in sample were previously obtained, they were modified to weight ratio of concrete. The oven-dried weight ratio of coarse aggregate can be obtained by Eq. (4.28). Then, the oven-dried weight ratio of cement, fly ash, sand of concrete can be modified as Eq. (5.6).

$$w_{tc} = w_{cc} + w_{fc} + w_{sc} + w_{nc} + w_G \quad (5.6)$$

Where $w_{tc}, w_{cc}, w_{fc}, w_{sc}, w_{nc}$ and w_G are ratio of oven-dried weight of concrete sample cement, fly ash, sand, combined water, and coarse aggregate to oven-dried weight of concrete, respectively. w_{tc} is equal 1.

Then, the oven-dried weight ratios of concrete compositions are converted to mass of cement, fly ash, sand and water at SSD state as shown in Eq. (5.7).

$$\left.\begin{aligned} W_{cc} &= w_{cc} \times UW_d \\ W_{fc} &= w_{fc} \times UW_d \\ W_{sc} &= w_{sc} \times UW_d \times (1 + a_s) \\ W_{wc} &= (W_{cc} + W_{fc}) \times (w/b) \end{aligned}\right\} \quad (5.7)$$

Where W_{cc}, W_{fc}, W_{sc} and W_{wc} are mass of cement, fly ash, sand and water of concrete at SSD state, respectively (kg). a_s is absorption of sand. w/b is water to binder ratio.

Generally, the mix design of concrete is estimated for 1 m^3 of volume based on SSD state of the aggregates. Hence, volume of each concrete ingredient per 1000 liters of concrete is shown in Eq. (5.8). The volume of each concrete ingredient can be obtained by dividing its mass (Eq. (5.7)) by the specific gravity. Then, the content of cement, fly ash, sand, and water of the mix proportion were obtained by Eq. (5.9).

$$V_t = 1000 = V_c + V_f + V_s + V_w + V_G + V_{air} \tag{5.8}$$

$$\left.\begin{aligned} W_c &= V_c \times SG_c \\ W_f &= V_c \times SG_f \\ W_s &= V_s \times SG_s \\ W_w &= (W_c + W_f) \times (w/b) \end{aligned}\right\} \tag{5.9}$$

Where $V_t, V_c, V_f, V_s, V_w, V_G$ and V_{air} are total volume of concrete, cement, fly ash, sand, water, coarse aggregate and air of concrete for 1000 liters at SSD state, respectively (liters/m^3). SG_c, SG_f, SG_s and SG_G are specific gravity of cement, fly ash, sand and coarse aggregate, respectively. W_c, W_f, W_s and W_w are mass of cement, fly ash, sand, and water, respectively (kg/m^3).

5.5.2 Result and Discussion

5.5.2.1 Determination of coarse aggregate by image processing

The analytical procedure for determining coarse aggregate content is same method as mentioned in Chapter 4. Hence, the concrete sample in this study, the reasonable Z-score between -1 to 1 (-1 < Z < 1) was applied to analyze the results of the coarse aggregate content.

Table 5.7 Analytical result of coarse aggregate content of FA concrete by image analysis

Sample	Design content (kg/m^3)	-1.0 < Z < 1.0	
		kg/m^3	% Error
W45FA130-A	1047	1048	+0.06
W55FA130-A	1047	1095	+4.58
W45FA230-A	1047	1087	+3.86
W45FA150-B	1058	1103	+4.34

Note: - and + is underestimate and overestimate respectively.

For the FA concrete, the content of coarse aggregate estimated by image processing technique is shown in Table 5.7. From the analytical results, the error percentages are between 0.06% (or 0.7 kg/m^3) to 4.58% (or 48 kg/m^3). The maximum error is 4.58 % which is acceptable. This result was used to determine mix proportion analysis.

5.5.2.2 Determination of water to binder ratio

The compressive strength of concrete sample is shown in Table 5.8. The water to cement ratio obtained from the data back analysis of the compressive strength by using FACOMP is shown in Table 5.9.

Table 5.8 Tested compressive strength results of hardened FA concrete by UTM

Sample	Compressive strength (MPa)	
	28 days	91 days
W45FA130-A	38.33	46.30
W55FA130-A	21.24	27.90
W45FA230-A	32.09	46.05
W45FA150-B	27.50	33.56

Table 5.9 Analytical result of w/b ratio of FA concrete by FACOMP

Sample	Design	w/b			
		28 days		91 days	
		Trial	Error (%)	Trial	Error (%)
W45FA130-A	0.45	0.41	-8.89	0.42	-6.67
W55FA130-A	0.55	0.57	+3.64	0.58	+5.45
W45FA230-A	0.45	0.44	-2.22	0.40	-11.11
W45FA150-B	0.45	0.44	-2.22	0.45	0
Mean error (%)		**-2.42**		**-3.08**	
		-2.72			

Note: - and + is underestimate and overestimate, respectively.

From Table 5.9, it can be seen that the water to binder ratio obtained from data back analysis of the compressive strength by using FACOMP is close to the designed water to binder ratio for some sample and age; in contrast, some sample is more be different with the designed w/b. However, the mean error of analytical w/b result of FA concrete not exceed 10% by designed w/b, the mean error of w/b of FA concrete at 28 and 91 days are -2.24 % and -3.08 %, respectively. In addition, the analytical result of water to binder ratio was depended on mix proportion of concrete, so this error may involves analytical result of mix proportion with tested strength result of hardened concrete.

5.5.2.3 Calculation of mix proportion of hardened concrete

5.5.2.3.1 Calculation of mix proportion with designed value of w/b and coarse aggregate content

In this order, the proposed method for calculation of mix proportion of FA concrete was verified by using design w/b and coarse aggregate content with

calculating procedure. This verification was also analyzing efficiently developed method of determination of content of cement, fly ash and sand by residue weight and CaO content.

Residual weights and CaO content of concrete sample are shown in Table 5.10. In addition, the percentage of chemical composition of sample was based on excluding of loss on ignition (LOI), and the CaO content of sample was obtained as mention from relation above. They are subsequently used to calculate weight ratio of cement, fly ash and sand. The analytical result and percentage error of mix proportion by proposed method are obtained as shown in Table 5.11 and 5.12, respectively.

Table 5.10 Residual weight and CaO content of FA concrete sample

Sample	Residue (%)		CaO (%)	
	28 days	91 days	28 days	91 days
W45FA130-A	61.041	59.361	18.665	18.777
W55FA130-A	64.165	62.245	16.621	16.826
W45FA230-A	66.405	65.101	15.353	15.168
W45FA150-B	66.230	66.105	15.447	14.640

Table 5.11 The analytical results of mix proportion of FA concrete with designed w/b and coarse aggregate content

Sample	w/b	Cement (kg/m^3)	Fly ash		Water (kg/m^3)	Sand (kg/m^3)	Coarse aggregate (kg/m^3)
			% rep.	(kg/m^3)			
W45FA130-A	**Design**	**280**	**30**	**120**	**180**	**727**	**Design**
28 days	*0.45*	294	27.3	110	182	722	*1047*
91 days	*0.45*	293	28.5	117	185	708	*1047*
W55FA130-A	**Design**	**249**	**30**	**107**	**196**	**727**	**Design**
28 days	*0.55*	244	31.1	110	195	728	*1047*
91 days	*0.55*	256	27.6	97	194	737	*1047*
W45FA230-A	**Design**	**279**	**30**	**120**	**179**	**727**	**Design**
28 days	*0.45*	268	30.3	117	173	755	*1047*
91 days	*0.45*	264	32.0	124	175	745	*1047*
W45FA150-B	**Design**	**193**	**50**	**193**	**174**	**729**	**Design**
28 days	*0.45*	205	49.8	204	184	680	*1058*
91 days	*0.45*	198	49.9	197	178	711	*1058*

From the analytical results, it can be seen that the calculating procedure can be obtained cement, fly ash, water and sand content of each hardened concrete sample. The maximum errors of the determination of content of cement, fly ash, water, and sand are +6.27 %, -8.83 %, +5.89 %, and -6.71 %, respectively. It shows that the maximum errors of each material are lower than 10 %. The mean errors of analytical result of content of cement, fly ash, water and sand are +1.25 %, -0.85 %, +0.59 %, and -0.60 %, respectively. In addition, the error percentage of water content also

depends on analytical result of cement and fly ash content as followed Eq. (5.8). The mean errors of all concrete material are lower than 5 %.

Table 5.12 Percentage error of mix proportion of FA concrete with designed w/b and coarse aggregate content

Sample	Age (days)	% Error			
		Cement	Fly ash	Water	Sand
W45FA130-A	28	+4.86	-7.99	+1.01	-0.69
	91	+4.75	-2.49	+2.58	-2.69
W55FA130-A	28	-1.88	+3.46	-0.28	+0.15
	91	+2.59	-8.83	-0.83	+1.32
W45FA230-A	28	-3.87	-2.28	-3.39	+3.82
	91	-5.24	+3.93	-2.49	+2.49
W45FA150-B	28	+6.27	+5.51	+5.89	-6.71
	91	+2.48	+1.89	+2.19	-2.48
Mean error (%)		**+1.25**	**-0.85**	**+0.59**	**-0.60**

Note: - and + is underestimate and overestimate respectively.

5.5.2.3.2 Calculation of mix proportion with analytical result of coarse aggregate content and trial w/b

Mix proportion of FA concrete estimated by the proposed method and its error percentages are shown in Tables 5.13 and 5.14, respectively.

Table 5.13 The analytical results of mix proportion of FA concrete

Sample	w/b	Cement (kg/m^3)	Fly ash		Water (kg/m^3)	Sand (kg/m^3)	Coarse aggregate (kg/m^3)
			% rep.	(kg/m^3)			
W45FA130-A	**0.45**	**280**	**30**	**120**	**180**	**727**	**1047**
28 days	0.41	302	27.3	113	170	742	1048
91 days	0.42	299	28.5	119	176	722	1048
W55FA130-A	**0.55**	**249**	**30**	**107**	**196**	**727**	**1047**
28 days	0.57	234	31.1	106	194	699	1095
91 days	0.58	244	27.6	93	195	703	1095
W45FA230-A	**0.45**	**279**	**30**	**120**	**179**	**727**	**1047**
28 days	0.44	263	30.3	115	166	741	1088
91 days	0.40	266	32.0	125	157	751	1088
W45FA150-B	**0.45**	**193**	**50**	**193**	**174**	**729**	**1062**
28 days	0.44	201	49.8	200	176	666	1103
91 days	0.45	193	49.9	192	173	691	1103

From the analytical result was obtained cement, fly ash, sand, water and coarse aggregate content of hardened concrete. The maximum errors of the determination of content of cement, fly ash, water, sand, and coarse aggregate are +7.71 %, -13.05 %, -12.66 %, -8.69 %, and +4.58 %, respectively. The mean errors of the determination of content of cement, fly ash, water, sand, and coarse aggregate are

0.00 %, -2.10 %, -3.52 %, -1.84 %, and +3.21 %, respectively, as shown in Table 5.14. Since, the error of each procedure as coarse aggregate content from image analysis, and w/b from data back analysis of compressive strength, the mean error of cement, fly ash, water and sand is changed. The analytical results show that the proposed method can be used to estimate mix proportion of hardened concrete with different percent replacement of fly ash and type of fly ash. Both early and later age of sample is unrelated to tendency of the error of analytical result; because of the age of concrete is concerned to analyze procedure. Hence, the proposed method can be applied to determine mix proportion although the different age of concrete.

Table 5.14 Percentage error of mix proportion of FA concrete

Sample	Age (days)	% Error					
		w/b	Cement	Fly ash	Water	Sand	Coarse aggregate
W45FA130-A	28	-8.89	+7.71	-5.49	-5.47	+2.01	+0.06
	91	-6.67	+6.89	-0.49	-2.30	-0.70	+0.06
W55FA130-A	28	+3.64	-5.89	-0.77	-0.87	-3.94	+4.85
	91	+5.45	-2.15	-13.05	-0.26	-3.37	+4.85
W45FA230-A	28	-2.22	-5.66	-4.10	-7.30	+1.89	+3.86
	91	-11.11	-4.51	+4.73	-12.66	+3.28	+3.86
W45FA150-B	28	-2.22	+4.01	+3.26	+1.33	-8.69	+4.34
	91	0	-0.38	-0.96	-0.67	-5.20	+4.34
Mean error (%)		**-2.75**	**0.00**	**-2.10**	**-3.52**	**-1.84**	**+3.21**

Note: - and + is underestimate and overestimate respectively.

5.4.3 Summary

The method for estimating mix proportion of hardened FA concrete has been proposed in this study. The proposed method was applied to estimate mix proportions of concrete prepared in laboratory with known mix design in order to verify its efficiency. In addition, the determination of mix proportion of hardened concrete was analyzed by many procedures as shown in Figure 5.9. The error of coarse aggregate content by image processing and w/b ration was effected analytical result as shown in Figure 5.11 (a) and (b). However, some results increase error but some results reduce error owing to the analytical procedure of w/b, and the coarse aggregate content from image analysis.

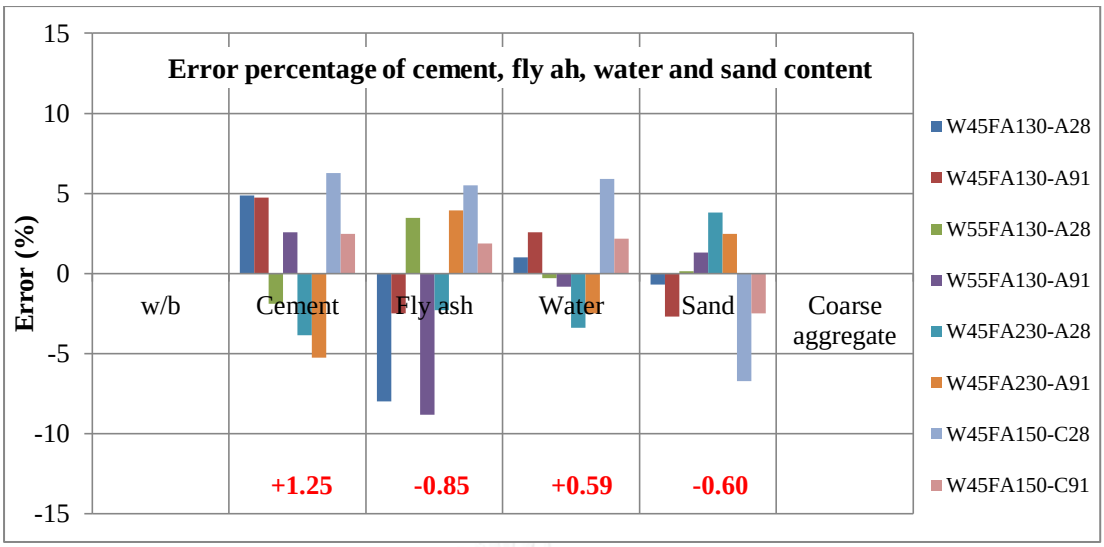

(a) Determining mix proportion with designed w/b and coarse aggregate

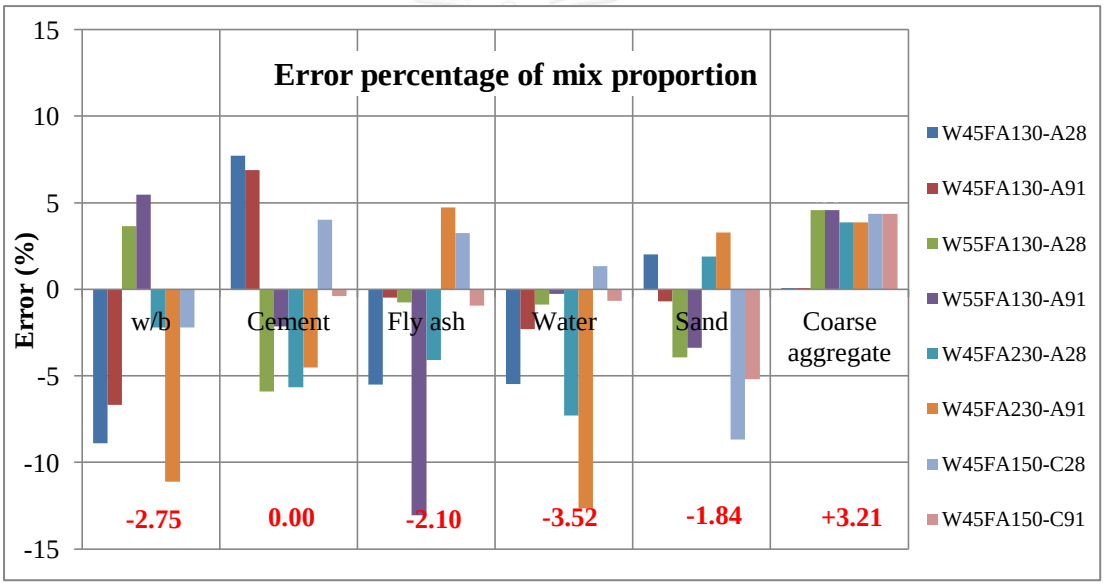

(b) Determining mix proportion with analytical result of w/b and coarse aggregate content

Figure 5.11 The error percentages of analytical result of each materials of FA concrete

CHAPTER 6
DETERMINATION OF MIX PROPORTION OF HARDENED CEMENT–LIMESTONE POWDER CONCRETE

6.1 General

In this chapter, the cement-limestone powder concrete (LP concrete) was studied for determining mix proportion. When concrete contain some admixture, they need to know its type before. Therefore, the methodology of this study is same procedure of FA concrete. It divided into 2 main procedures as investigation of limestone powder existence procedure and determination of mix proportion of concrete procedure. The methods for evaluating limestone powder existence and determining mix proportion of LP concrete have been proposed. The physical, mechanical and chemical analytical methods were adopted for the analysis. The analytical procedures for evaluating limestone powder existence and determination of water to binder ratio, limestone powder replacement ratio, and content of concrete compositions including water, cement, limestone powder, sand, and coarse aggregate are described in this chapter.

6.2 Material and Mix proportion

LP concrete samples were prepared with water to binder ratio (w/b) of 0.45. The specific gravity of LP1 and LP2 is 2.74 and 2.69, respectively. The concrete samples at 28 and 91 days were prepared investigating mix proportion. The ratio by volume of sand to total aggregate (s/a) was 0.42 for all mix that their void ratio was 0.230. Four mix designs of concrete specimens are shown in Table 6.1. The sample preparations were as mentioned in Chapter 3.

Table 6.1 Mix proportion for determination of mix proportion of hardened LP concrete

Sample	w/b	Cement	Limestone powder			Water	Sand	Coarse aggregate
		(kg/m^3)	Type	% rep.	(kg/m^3)	(kg/m^3)	(kg/m^3)	(kg/m^3)
W45LP110-B	0.45	364	LP1	10	40.5	182	740	1072
W45LP210-B	0.45	363	LP2	10	40.4	182	740	1072
W45LP220-B	0.45	321	LP2	20	80.3	181	740	1072

6.3 Investigation of Physical and Chemical Properties of Materials

This experimental is aim to investigate basic properties of materials. Basic information on each type of material including chemical and physical properties will be investigated. The results will be used as a database for analyzing concrete samples. They will be utilized for analyzing in procedure of investigation of limestone powder in hardened concrete and estimation of mix proportion of hardened concrete. The techniques were adopted for investigation consists of many techniques as Scanning Electron Microscope (SEM) on Back-Scattered Electrons (BSE) technique, Mapping and SEM equipped with Energy Dispersive X-Ray Spectroscopy (EDS) technique, Loss on ignition technique (LOI) and selective dissolution method.

6.3.1 Physical properties

6.3.1.1 Particle shape and size by Scanning Electron Microscope (SEM) analysis

This technique was used to investigate particle shape of materials. Normally, particle shape of cement and limestone powder has irregular shape. From the experimental results, the most particle shape of cement and 2 types of limestone powder is irregular shape as shown in Figure 6.1 (a), (b) and (c) respectively.

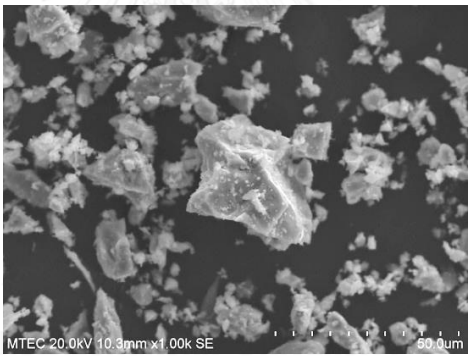

(a) Portland Cement

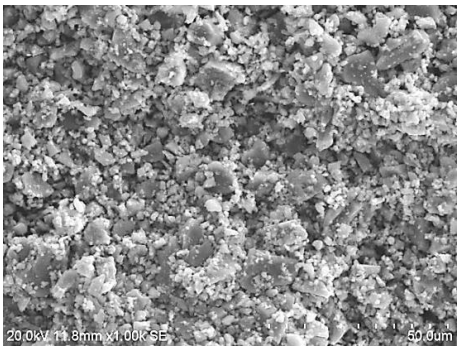

(b) LP1

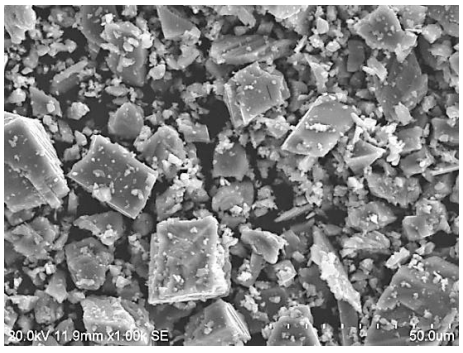

(c) LP2

Figure 6.1 Particle shapes of cement and limestone powder by SEM

6.3.2 Chemical properties

6.3.2.1 Elemental composition by Scanning Electron Microscope equipped with Energy Dispersive X-Ray Spectroscopy (SEM-EDS) and Mapping analysis

This technique was used to measure the spectrum of elements such as Ca, Al, or Si in materials. Moreover, the relationship of the elements such as Ca and Si was investigated. The Ca/Si ratio by weight was used in order to identify some particles that they may be limestone powder particle. The results were shown in Figure 6.2.

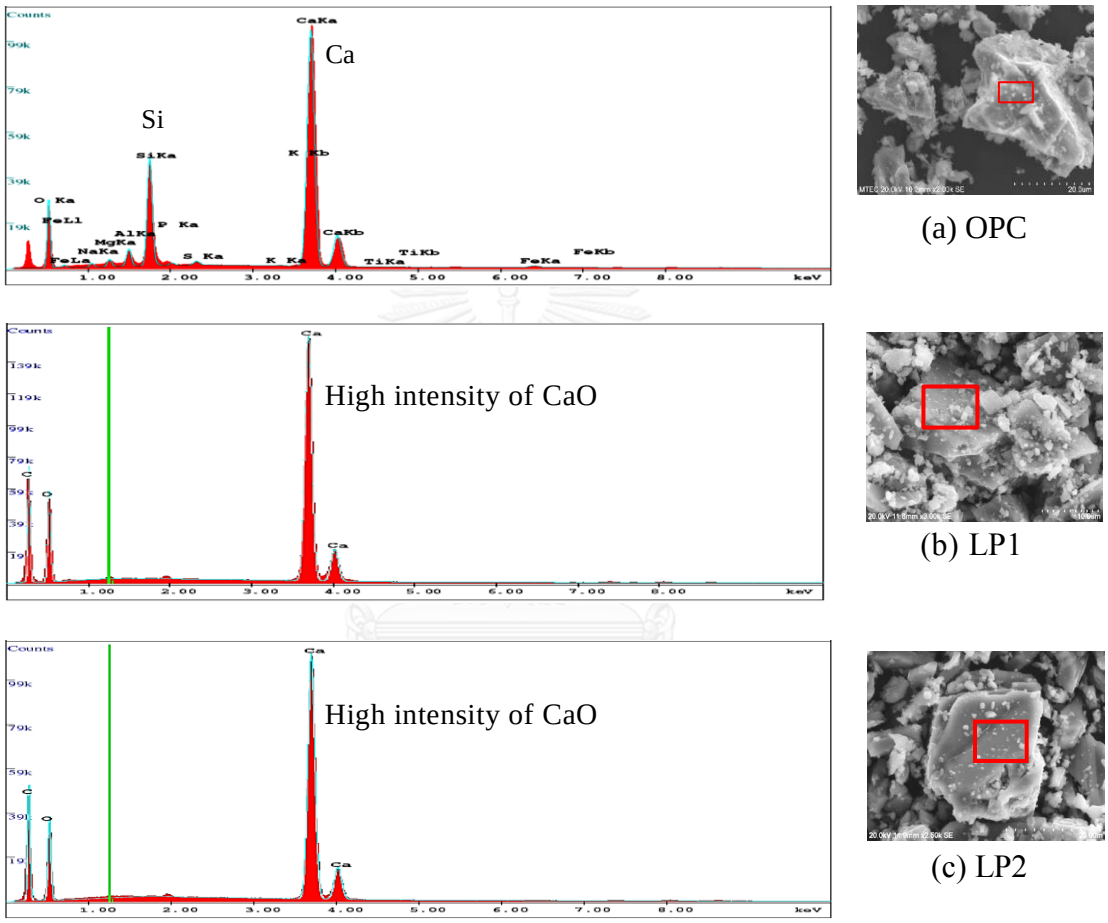

Figure 6.2 Elemental compositions of cement and limestone powder by SEM-EDS

Generally, the mainly chemical composition of cement is CaO and SiO_2, and; the mainly chemical composition of limestone powder is CaO. From the experimental results, the elemental in cement is Ca, Si and other elemental; but almost elemental of both limestone powder is only Ca. The result shown that the elemental of LP1 and LP2 are large CaO, but SiO_2 was not appeared. Hence the amount of Ca/Si of both limestone powders, which are unlimited value, is higher than Ca/Si of cement as shown in Table 6.2.

Table 6.2 Ca/Si ratio by weight of elemental composition of limestone powder

Elemental	Cement	LP1	LP2
Ca (%)	39.79	33.06	41.72
Si (%)	13.38	-	-
Ca/Si Ratio	2.974	n/a	n/a

6.3.2.1 Loss on ignition (LOI)

Loss on ignition (LOI) is a test used in analytical chemistry, particularly in the analysis of materials. It consists of strongly heating a sample at a specified temperature. The volatile materials lost usually consist of "combined water" (hydrates and labile hydroxy-compounds) and "carbon dioxide" from carbonates. Hence, the loss is assumed to represent the total moisture and CO_2 of substance and hydrated product in the sample matrix in this method as followed ASTM C114, the sample was ignited in a muffle furnace at a controlled temperature of 950 ± 50˚C.

Generally, it is known that almost of chemical composition of limestone powder is CaO in form of $CaCO_3$ phase. From Table 3.1, it shown that the main chemical compositions of Portland cement and limestone powder were same CaO, but CaO in cement was main compound as C_2S, C_3S, C_3A, C_4AF. Then, the LOI percentage of LP was higher than cement due to loss of CO_2 from $CaCO_3$. On the other hand, the main chemical composition of sand was SiO_2. This experimental result was used for determining mix proportion of hardened concrete procedure.

6.3.2.3 Selective Dissolution

The Selective dissolution analysis was used to quantify the residues left of each material. The component of limestone powder is mostly CaO, so it is completely dissolved by HCl. So, the residue of limestone powder is zero. The residues left from being dissolved were sand-B and a little amount of cement as shown in Table 6.3. This investigation was utilized for determining mix proportion.

Table 6.3 Residual weight of materials

Samples	Cement-B	LP1	LP2	Sand-B
Residual weight %	0.417	0	0	96.671

6.4 Procedure for investigation of limestone powder existence in hardened concrete

In this procedure is aim to investigate limestone powder existence in hardened concrete. The physical and chemical analytical methods were adopted as SEM-BSE technique, Mapping and SEM-EDS technique. In addition, the concrete samples, which were used for investigation, were mixed in laboratory. LP concrete samples W45LP110-C and W45LP210-C were investigated limestone powder existence in hardened concrete. In this study, limestone powder was use as filler in cement for improves the hydration rate and increases the strength of cement compounds at early age (Ingram and Daugherty 1992). Limestone filler does not have pozzolanic properties, hence only sample at 91 days was used for this process.

6.4.1 Methodology

In order to determine the limestone powder existence in sample, the procedure for determining limestone powder existence in sample is shown in Figure 6.3. The proposed procedure for investigation of limestone powder existence in hardened concrete can divide to 2 main parts as physical and chemical analytical. The physical analytical was investigated particle shape by SEM-BSE and Mapping techniques and then if they can found some particle that may be limestone powder, SEM-EDS technique was used to investigate its elemental composition.

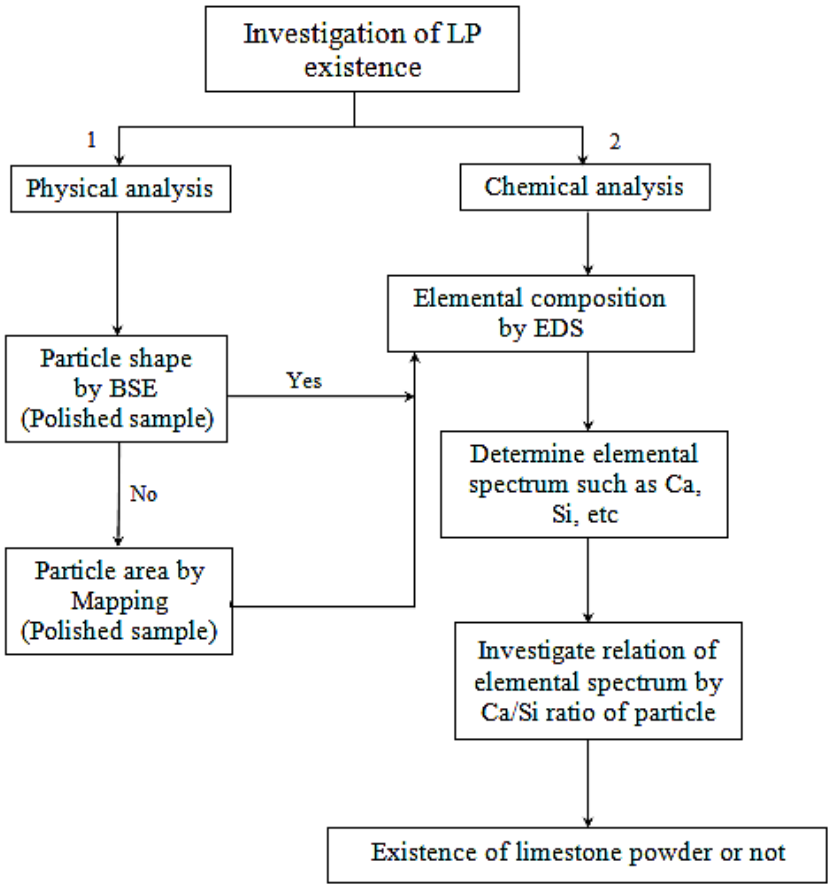

Figure 6.3 Procedure of investigation of limestone powder existence

6.4.1.1 Brightness in sample by Scanning Electron Microscope (SEM) on Back-Scattered Electrons (BSE) technique

The BSE produce image on the surface of polish sample. BSE was used to detect contrast between areas with different chemical compositions, since heavy elements (high atomic number) backscatter electrons more strongly than light elements (low atomic number), and thus appear different brighter in the image. This technique was used to distinguish the different phases such as cement, limestone powder and hydrated product in sample by different brightness. Within the grey-scale from dark to light is the pore, C-S-H gel, CH, limestone powder and some phase of anhydrous cement. In addition, limestone powder fill in the interfacial transition zone between the matrix and aggregate, and make it become much denser, which is the

reason why the porosity of concrete containing limestone powder is lower than that of normal concrete.

Further limestone powder particle will be hardly investigated when long age of sample that it is very dense. Thus, Mapping technique was additional investigating limestone powder particle.

6.4.1.2 EDS-Mapping technique

Mapping technique was investigated adjunct information of determining limestone powder particle. This technique was used to measure the spectrum of elements such as Ca, Al, or Si in materials. It was used EDS system to produce an elemental map into image. The image is produced by progressively rastering the electron beam point by point over an area of interest that suspected area exist particle of limestone powder. Thus, this technique was used to identify particle that it may be limestone powder. Map of different elements over the same area can help to determine what phases are present. For this technique, the same sample with BSE technique was used investigation.

When high dense sample was investigated as mentioned above, consequently the SEM and Mapping techniques were approved by testing mortar sample. The limestone powder-cement mortar was investigated. The cement was replaced 10 percentages by limestone powder. The mortar sample was curing by warm water at 50 ^{o}C for 28 days for accelerating degree reaction. This verifies is purpose for evaluating efficient method. In addition, mix of mortar was designed by s/b ratio that it will be same mix design of concrete, LP2 was used to prepare mortar sample by replaced 10 percentage of cement as W45LP210. And then, the SEM technique was evaluated on concrete sample

After, the limestone powder particle was determined by BSE and Mapping; the suspect particle should be evaluated for confirming as limestone powder particle. Therefore the sample needs more evaluating on their particle with other technique, an additional EDS technique was adopted.

6.4.1.3 Elemental composition by Scanning Electron Microscope equipped with Energy Dispersive X-Ray Spectroscopy (SEM-EDS) technique

This technique was used to measure the spectrum of elements such as Ca, Al, or Si in materials. After, the concrete sample was analyzed by the BSE or Mapping; the EDS was used to identify the particles in sample that it was suspected to be limestone powder particles. The relationship of the spectrum of elements such as Ca, Al or Si of the particles in sample was determined. Normally, the Ca/Si ratio of the cement and hydrated product is higher than 1. In contrast, the Ca/Si ratio of the sand is very low due to very high SiO_2 content and very low CaO. Thus, if the Ca/Si ratio of the suspect particle is very high as shown in Figure 6.2 and Table 6.2, it was been limestone powder particle.

6.4.2 Result and Discussion

6.4.2.1 Brightness in sample by Scanning Electron Microscope (SEM) on Back-Scattered Electrons (BSE) technique

For verifying the BSE method, the mortar samples were evaluated by the BSE as mentioned earlier. From the experimental result, they were found some particle that

it may be limestone powder as shown result in Figure 6.4. All particles were suspect as limestone powder that they can observe whole particle is homogeneous phase and equal brightness. In addition, cement or hydrated products are compounded by many components that they are different brightness.

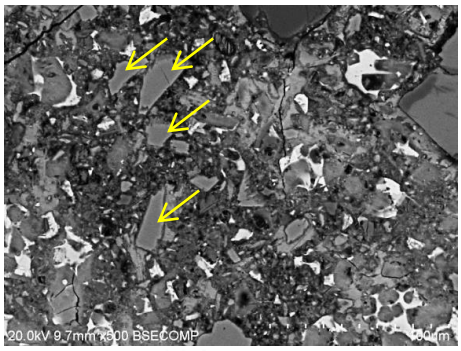

Figure 6.4 Investigation limestone powder existences in W45LP210 mortar

Normally, the particle size of limestone powder is smaller than sand, and sand is high SiO_2 phase that it is darken than CaO phase. Hence, this technique is capably observing some limestone powder particle in sample.

Then, the BSE technique was applied on concrete sample for observing limestone powder existence, the LP concrete expect W45LP220-B were used. The experimental results of LP concrete are shown in Figure 6.5 (a) and (b); it can be observed the some particles that it may be limestone powder particle exist in BSE pictures.

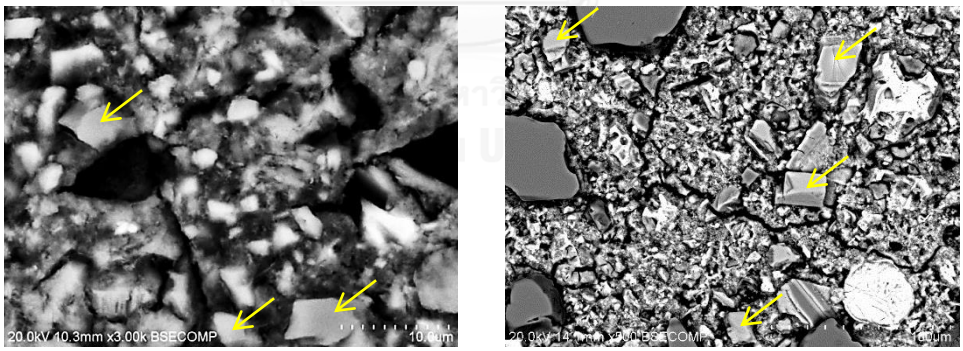

(a) W45LP110-A (b) W45LP210-A

Figure 6.5 Investigation limestone powder existences in hardened concrete

However, if the limestone powder particle is hard distinguished, the Mapping technique will be adopted for observing. And then their particles are needed other technique for confirming limestone powder particle.

6.4.2.2 EDS-Mapping technique

As mentioned above, the Mapping technique was used adjunct information for determining limestone powder particle. For verifying the Mapping method, the mortar samples were evaluated by the Mapping as mentioned earlier. Map of different

elements over the same area was determined what phases are present, and then the limestone powder were identify. From the experimental result in Figure 6.6, they can be observed that suspected area is high intensity of Ca, but low intensity of both Si and Al. For some area is high intensity of Si but low intensity of both Ca and Al which should be sand; and either area should be cement and hydrated product.

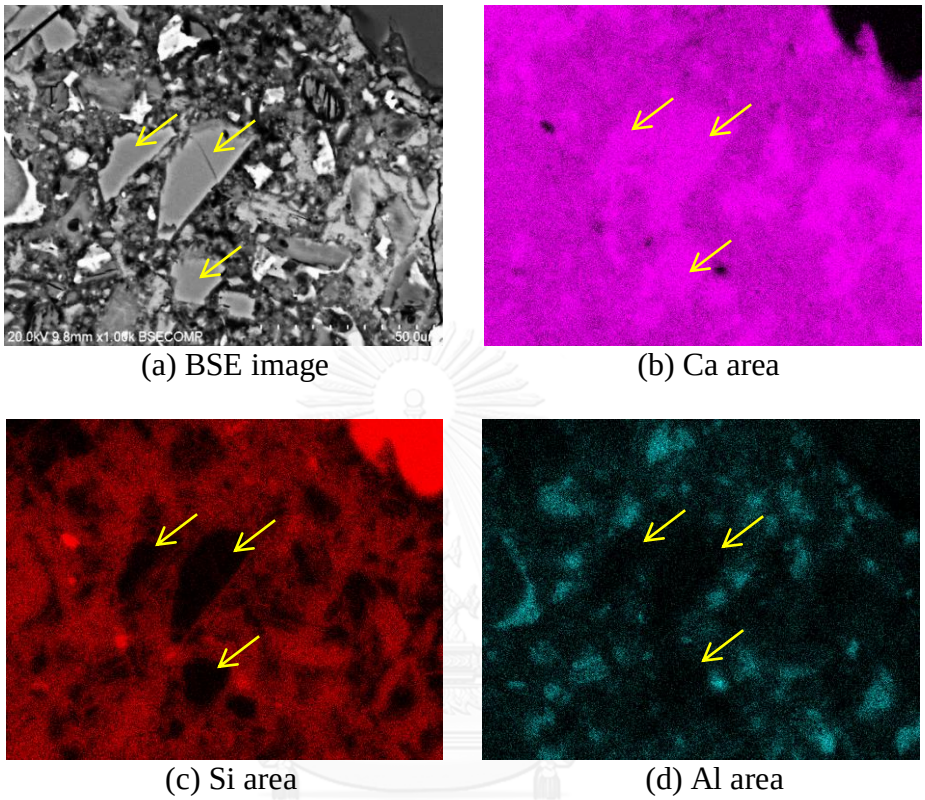

(a) BSE image (b) Ca area

(c) Si area (d) Al area

Figure 6.6 Map of each element over the same area of W45LP210 mortar

Then, the Mapping technique was applied on concrete sample for observing limestone powder existence, the LP concrete expect W45LP220 were used. The experimental results of LP concrete are shown in Figure 6.7 and Figure 6.8, they can be observed the some particles that it may be limestone powder particle exist in BSE pictures.

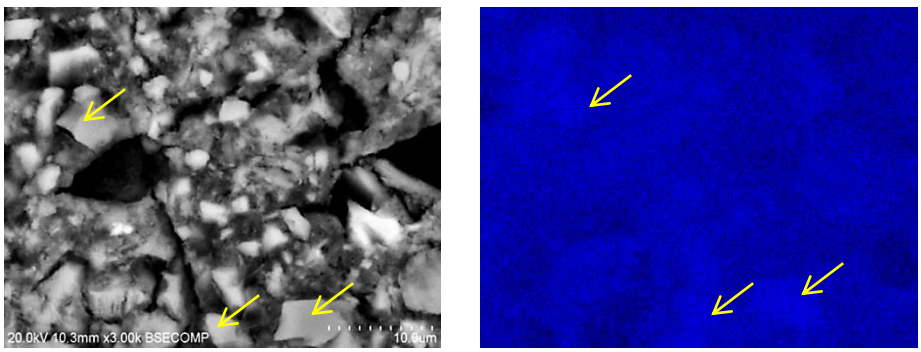

(a) BSE image (b) Ca area

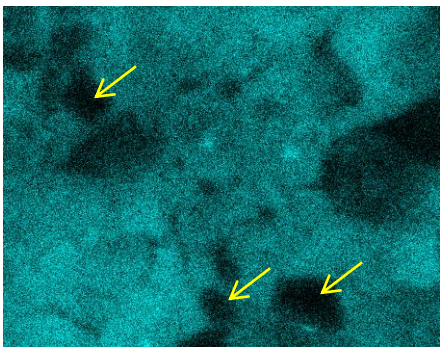

(c) Si area

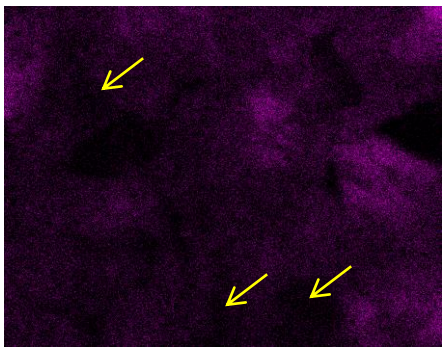

(d) Al area

Figure 6.7 Map of each element over the same area of W45LP110-B concrete

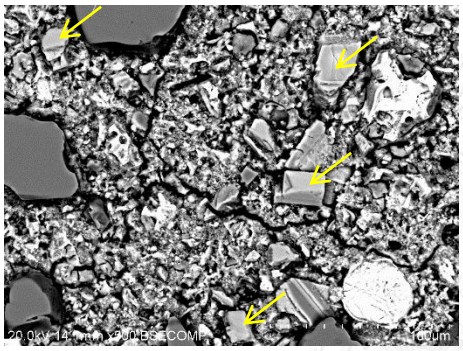

(a) BSE image

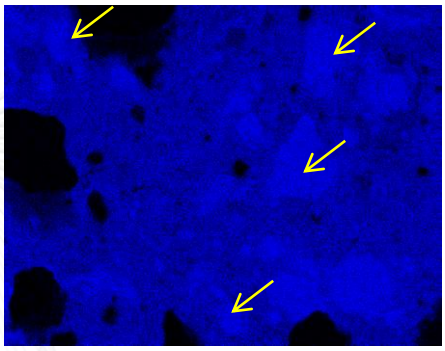

(b) Ca area

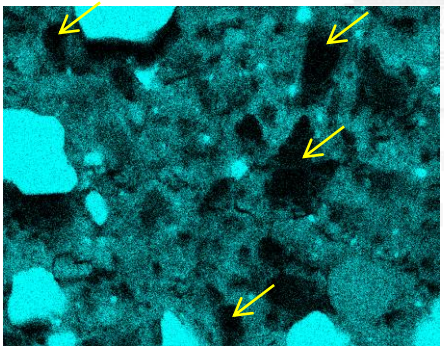

(c) Si area

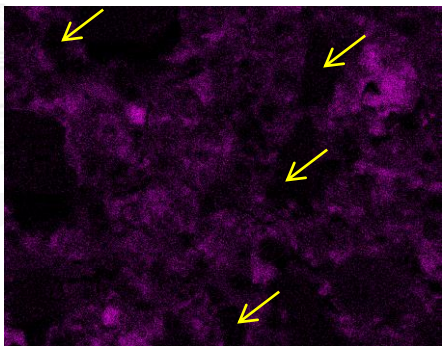

(d) Al area

Figure 6.8 Map of each element over the same area of W45LP210-B concrete

It can be observed that Figure 6.7 is hard observing particle of LP1 owing to its particle is very small. In contrast, the LP2 particle in Figure 6.8 is easier observed. Hence, this technique is increasing capable observing some limestone powder particle in sample. However, the sample needs more evaluating on their particle with other technique, an additional EDS was adopted as mentioned earlier.

6.4.2.3 Elemental composition by Scanning Electron Microscope equipped with Energy Dispersive X-Ray Spectroscopy (SEM-EDS) and Mapping analysis

This result was used to identify some particles that it suspected as limestone powder. From the experimental results of BSE and Mapping testing on sample, the

limestone powder existence in samples was observed. Then, the SEM-EDS technique was applied to investigate its elemental composition on the particles. The SEM-EDS result in Figure 6.9 was investigated suspected particle in the sample.

The SEM-EDS result in Figure 6.9, it can be found that the Ca/Si ratio of the observed. The intensity peak of Ca is very high but without Si, so the amount of Ca/Si ratios is very high. The intensity peak of Ca is high same Figure 6.2 (b) and (c). And the amount of Ca/Si ratio of cement or hydrated product are quite high (normally higher than1), but they are combined another element such as Si and Al as shown in Figure 6.2 (a).

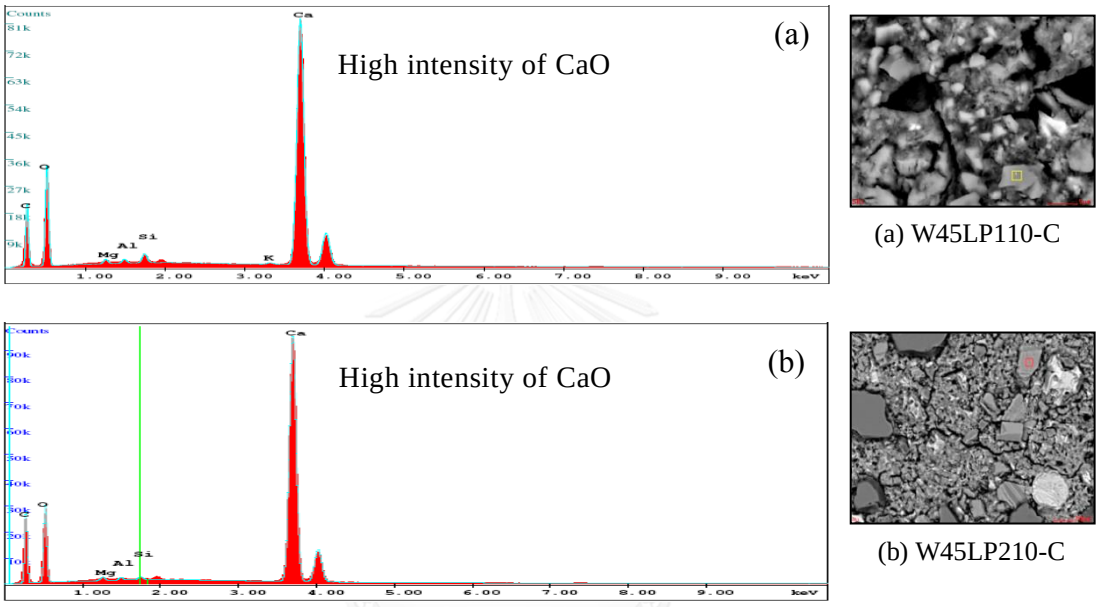

Figure 6.9 Elemental compositions of LP particles of samples by SEM-EDS

These result, it can be concluded that both W45LP110-B and W45LP210-B contain limestone powder; but it cannot be conclude that type of LP due to similarly chemical properties. Thus, BSE, Mapping and EDS procedure was verified, W45LP110-B and W45LP210-B was found LP existence in sample.

6.4.3 Summary

The method for determining limestone powder existence in hardened cement concrete has been proposed in this study. The proposed method was verified by sample prepared in laboratory with known mix design. From the analytical result of SEM technique can be concluded that it can found some particle of limestone powder. For the SEM-EDS technique was adopted for evaluating theirs particle after the SEM testing. The analytical result of EDS technique can be concluded that it is efficiently identifying limestone powder particle also. Hence, the developed method can be used to find both fine-particle and coarse-particle of LP. Although, the sample contained LP1 or LP2, it can found limestone powder existence in sample. However, this method was not determined particle size of limestone powder.

6.5 Procedure for estimation of mix proportion of hardened concrete containing limestone powder

After the limestone powder existence procedure was evaluated, the mix proportion was determined. In order to estimate the mix proportion of hardened concrete, several testing techniques were adopted as Universal testing machine (UTM), Selective dissolution method, Loss on ignition (LOI) technique, and Image processing. In addition, the concrete samples, which were used for determining mix proportion, were mixed in laboratory. Thus, mix design of sample was known, and then this procedure can be verified. Three LP concrete were determined mix proportion of hardened concrete as shown in Table 6.1.

6.5.1 Methodology

In the order of determination of mix proportion of hardened LP concrete, the experimental for estimating mix proportion of hardened concrete has been proposed. In the analysis, three main parts for determining mix proportion were implemented as shown in Figure 6.10. This method is similarly method for estimating mix proportion of cement concrete.

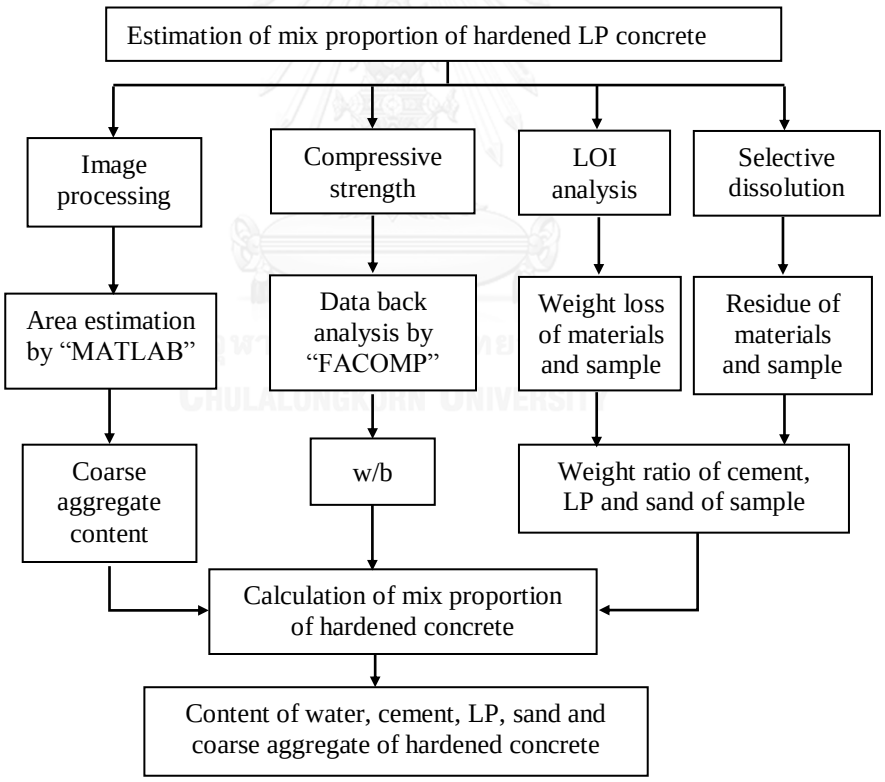

Figure 6.10 Method for determination of mix proportion of hardened LP concrete

The limestone powder content was added determining mix proportion; therefore, the LOI result was added to analyze procedure for determining weight ratio of cement, limestone powder, and sand. The developed method was applied to estimate mix proportions of concrete prepared in laboratory with known mix design in

order to verify its efficiency. Detail of the procedure for determination of mix proportion of hardened concrete is described below.

6.5.1.1 Determination of coarse aggregate by image processing

The image analysis method was used to determine coarse aggregate content of hardened concrete. The analytical procedure is same method as mentioned in Chapter 4.

6.5.1.2 Determination of water to binder ratio

The compressive strength of concrete samples was obtained by using the universal testing machine. Then, the water to binder ratio could be calculated from data back analysis of the compressive strength by using the computer software, "FACOMP". The procedure for determining water to binder ratio is same method as mentioned in Chapter 4.

It is noted that the computer software FACOMP was developed based on the experimental data of compressive strength of OPC concrete and fly ash concrete. The use of this method for determination of water to binder ratio from data back analysis of the compressive strength of LP concrete may result in an inaccurate estimation.

6.5.1.3 Determination of weight ratio of cement, limestone powder and sand by residual weight and LOI content

In order to determine contents of cement, limestone powder and sand in sample, since three unknowns (w_{cs} , w_{LPs} and w_{ss}) could be solved by three equation, three primarily equation were need to solve the weight ratio of cement, limestone powder and sand. Eq. (6.1) to (6.3) were formed based on the mass balance of sample without coarse aggregate at oven-dried state. The equations were used to determine the weight ratio of cement, limestone powder and sand in sample.

First, Eq. (6.1) was formed based on mass balance condition of sample without coarse aggregate (mortar in the concrete), which was cement, limestone powder, sand and water, equal 1. Equation (6.3) was formed by balance of residue weight between sample and total of each material, which was cement, limestone powder and sand, after dissolved by the selective dissolution testing as followed. The residues left from being dissolved were sand, and a little amount of cement. Last, the additional equation was formed by balance of LOI content between sample and total of each material, which was cement, limestone powder and sand, as followed Eq. (6.4).

$$w_{ts} = w_{cs} + w_{LPS} + w_{ss} + w_{ns} \tag{6.1}$$

$$w_{ns} = 0.23(\alpha_{hy} w_{cs}) \tag{6.2}$$

$$r_{ts} w_{ts} = r_c w_{cs} + r_{LP} w_{LPS} + r_s w_{ss} \tag{6.3}$$

$$LOI_{ts} w_{ts} = (1-\alpha_{hy}) LOI_c w_{cs} + \alpha_{hy} LOI_{hp} w_{cs} + LOI_{LP} w_{LP} + LOI_s w_{ss} \tag{6.4}$$

Where r_{ts} is residual weights of sample (g/g of sample), r_c is residual weights of the cement (g/g of cement). r_s is residual weights of sand (g/g) of sand. r_{LP} is residual weights of limestone powder (g/g of limestone powder). w_{ts}, w_{cs}, w_{LPs}, w_{ss} and w_{ns} are oven-dried weight ratio of sample, cement, limestone powder, sand, and combined water of the sample to oven-dried weight ratio of sample without coarse aggregate (mortar in concrete) , respectively. w_{ts} is equal 1. α_{hy} is degree of cement hydration. In this study, the degree of hydration reaction was obtained by FACOMP. 0.23 is assumed the combined water value of hydration of cement for full degree reaction (Taylor 1997). $LOI_{ts}, LOI_c, LOI_{hp}, LOI_{LP}$ and LOI_s are percentage of loss on ignition of the sample, cement, hydrated product, limestone powder and sand, respectively.

Limestone filler does not have pozzolanic properties, but it reacts with the alamina phases of cement to form an Afm phase (calcium monocarboaluminate hydrate) with no significant changes on the strength of blended cement (Soroka and Setter 1977). But the research of only degree reaction of limestone powder reacts with alumina is rarely studies. Then, this study is assumed that limestone powder is filler which are chemically inert. And LOI_{hp} is assumed as LOI of hydrated cement product equal 25.59 % which was obtained by average test result of sample with known mix design various w/c as 0.25, 0.45, 0.55 and 0.65 at age 3, 7 and 14 days.

6.5.1.4 Calculation of mix proportion of hardened concrete

After the coarse aggregate content and weight ratio of cement, limestone powder and sand in sample were previously obtained, they were modified to weight ratio of concrete. The oven-dried weight ratio of coarse aggregate can be obtained by Eq. (4.28). Then, the oven-dried weight ratio of cement, limestone powder, sand of concrete can be modified as Eq. (6.5).

$$w_{tc} = w_{cc} + w_{LPC} + w_{sc} + w_{nc} + w_G \tag{6.5}$$

Where $w_{tc}, w_{cc}, w_{LPC}, w_{sc}, w_{nc}$ and w_G are ratio of oven-dried weight of concrete sample cement, limestone powder, sand, combined water, and coarse aggregate to oven-dried weight of concrete, respectively. w_{tc} is equal 1.

Then, the oven-dried weight ratios of concrete compositions are converted to mass of cement, limestone powder, sand and water at SSD state as shown in Eq. (6.6).

$$\left.\begin{aligned} W_{cc} &= w_{cc} \times UW_d \\ W_{LPc} &= w_{LPc} \times UW_d \\ W_{sc} &= w_{sc} \times UW_d \times (1 + a_s) \\ W_{wc} &= (W_{cc} + W_{LPc}) \times (w/b) \end{aligned}\right\} \tag{6.6}$$

Where W_{cc}, W_{LPc}, W_{sc} and W_{wc} are mass of cement, limestone powder, sand and water of concrete at SSD state, respectively (kg). a_s is absorption of sand. w/b is water to binder ratio.

Generally, the mix design of concrete is estimated for 1 m^3 of volume based on SSD state of the aggregates. Hence, volume of each concrete ingredient per 1000 liters of concrete is shown in Eq. (6.7). The volume of each concrete ingredient can be obtained by dividing its mass (Eq. (6.6)) by the specific gravity. Then, the content of cement, limestone powder, sand, and water of the mix proportion were obtained by Eq. (6.8).

$$V_t = 1000 = V_c + V_{LP} + V_s + V_w + V_G + V_{air} \tag{6.7}$$

$$\left.\begin{aligned} W_c &= V_c \times SG_c \\ W_{LP} &= V_c \times SG_{LP} \\ W_s &= V_s \times SG_s \\ W_w &= (W_c + W_{LP}) \times (w/b) \end{aligned}\right\} \tag{6.8}$$

Where $V_t, V_c, V_{LP}, V_s, V_w, V_G$ and V_{air} are total volume of concrete, cement, limestone powder, sand, water, coarse aggregate and air of concrete for 1000 liters at SSD state, respectively (liters/m^3). SG_c, SG_{LP}, SG_s and SG_G are specific gravity of cement, limestone powder, sand and coarse aggregate, respectively. W_c, W_{LP}, W_s and W_w are mass of cement, limestone powder, sand, and water, respectively (kg/m^3).

6.5.2 Result and Discussion

6.5.2.1 Determination of coarse aggregate by image processing

The analytical procedure for determining coarse aggregate content is same method as mentioned in Chapter 4. Hence, the concrete sample in this study, the reasonable Z-score between -1 to 1 (-1 < Z < 1) was applied to analyze the results of the coarse aggregate content.

Table 6.4 Analytical result of coarse aggregate content of LP concrete by image analysis

Sample	Design content (kg/m^3)	-1.0 < Z < 1.0	
		kg/m^3	% Err.
W45LP110-B	1072	1090	+1.67
W45LP210-B	1072	1104	+2.92
W45LP220-B	1072	1115	+3.98

Note: - and + is underestimate and overestimate respectively.

For the LP concrete, the content of coarse aggregate estimated by image processing technique is shown in Table 6.4. From the analytical results, the error percentages are between 1.67% (or 18 kg/m^3) to 3.98% (or 43 kg/m^3). The maximum error is 3.98 % which is acceptable. This result was used to determine mix proportion analysis.

6.5.2.2 Determination of water to binder ratio

The compressive strength of concrete sample is shown in Table 6.5. The water to cement ratio obtained from the data back analysis of the compressive strength by using FACOMP is shown in Table 6.6.

From Table 6.6, it can be seen that the water to binder ratio obtained from data back analysis of the compressive strength by using FACOMP is close to the designed water to binder ratio for some sample and age; in contrast, some sample is more be different with the designed w/b. However, the mean error of analytical w/b result of LP concrete not exceed 10% by designed w/b, the mean error of w/b of LP concrete at 28 and 91 days are -0.74 % and +4.44 %, respectively. In addition, the analytical result of water to binder ratio was depended on the compressive strength test, so more error of w/b involves between tested compressive strength with data back analysis of compressive strength from analytical mix proportion by using the computer software "FACOMP".

Table 6.5 Tested compressive strength results of hardened LP concrete by UTM

Sample	Compressive strength (MPa)	
	28 days	91 days
W45LP110-B	43.72	45.39
W45LP210-B	39.90	51.35
W45LP220-B	31.20	35.88

Table 6.6 Analytical result of w/b ratio of LP concrete by FACOMP

Sample	Design	w/b			
		28 days		91 days	
		Trial	Error (%)	Trial	Error (%)
W45LP110-B	0.45	0.41	-8.89	0.46	+2.22
W45LP210-B	0.45	0.43	-4.44	0.42	-6.67
W45LP220-B	0.45	0.50	+11.11	0.53	+17.78
Mean error (%)		**-0.74**		**+4.44**	
		+1.85			

Note: - and + is underestimate and overestimate, respectively.

6.5.2.3 Calculation of mix proportion of hardened concrete

6.5.2.3.1 Calculation of mix proportion with designed value of w/b and coarse aggregate content

In this order, the proposed method for calculation of mix proportion of LP concrete was verified by using design w/b and coarse aggregate content with calculating procedure. This verification was also analyzing efficiently developed

method of determination of content of cement, limestone powder and sand by residue weight and LOI content.

Residual weights and LOI content of concrete sample are shown in Table 6.7. They were subsequently used to calculate weight ratio of cement, limestone powder and sand by Eq. (6.1) to (6.4), and then the mix proportion was calculated by Eq. (6.5) to (6.8) as mentioned above. The analytical result and percentage error of mix proportion by proposed method are obtained as shown in Table 6.8 and 6.9, respectively.

Table 6.7 Residual weight and LOI content of LP concrete sample

Sample	Residue (%)		LOI (%)	
	28 days	91 days	28 days	91 days
W45LP110-B	59.92	59.40	8.70	9.10
W45LP210-B	59.85	58.93	8.74	10.76
W45LP220-B	60.67	60.73	9.46	10.08

Table 6.8 The analytical results of mix proportion of LP concrete with designed w/b and coarse aggregate content

Sample	w/b	Cement (kg/m^3)	LP		Water (kg/m^3)	Sand (kg/m^3)	Coarse aggregate (kg/m^3)
			% rep.	(kg/m^3)			
W45LP110-B	**Design**	**364**	**10**	**40**	**182**	**740**	**Design**
28 days	*0.45*	340	13.2	52	176	765	*1072*
91 days	*0.45*	336	15.0	59	178	756	*1072*
W45LP210-B	**Design**	**364**	**10**	**40**	**182**	**740**	**Design**
28 days	*0.45*	358	8.4	33	176	767	*1072*
91 days	*0.45*	283	29.7	119	181	733	*1072*
W45LP220-B	**Design**	**321**	**20**	**80**	**181**	**740**	**Design**
28 days	*0.45*	307	20.4	79	174	770	*1072*
91 days	*0.45*	282	27.0	104	174	766	*1072*

Table 6.9 Percentage error of mix proportion of LP concrete with designed w/b and coarse aggregate content

Sample	Age (days)	% Error			
		Cement	LP	Water	Sand
W45LP110-B	28	-6.70	+27.48	-3.28	+3.38
	91	-7.73	+46.21	-2.34	+2.22
W45LP210-B	28	-1.60	-18.99	-3.34	+3.78
	91	-22.33	+195.07	-0.59	-0.91
W45LP220-B	28	-4.29	-1.70	-3.77	+4.10
	91	-12.14	+29.68	-3.78	+3.61
Mean error (%)		**-9.13**	**+46.29**	**-2.85**	**+2.70**

Note: - and + is underestimate and overestimate respectively.

From the analytical results, it can be seen that the calculating procedure can be obtained cement, limestone powder, water and sand content of each hardened concrete sample; but the many result are more error than 10 percentages especially limestone powder content that almost it is highest error percentage. The maximum errors of the determination of content of cement, limestone powder, water, and sand are -22.33 %, +195.07 %, -3.78 %, and +4.10 %, respectively. The mean errors of analytical result of content of cement, limestone powder, water and sand are -9.13 %, +46.29 %, -2.85 %, and +2.70 %, respectively. The mean errors of concrete materials do not exceed 10% to except limestone powder. High errors percentage of limestone powder may be occur from low content of mix design as a result of different small error content as result in more error percentage. Moreover, the percentage replacement cement by limestone powder is close to designing except W45LP210-B at 91 days. These errors especially W45LP210-B at 91 days may occur owing to some assume parameter of analytical procedure such as degree of hydration from FACOMP. Hence, the analysis of LP concrete will be evaluated and developed further.

6.5.2.3.2 Calculation of mix proportion with analytical result of coarse aggregate content and trial w/b

Mix proportion of concrete estimated by the proposed method and its percentage error are shown in Tables 6.10 and 6.11, respectively.

Table 6.10 The analytical results of mix proportion of LP concrete

Sample	w/b	Cement (kg/m^3)	LP		Water (kg/m^3)	Sand (kg/m^3)	Coarse aggregate (kg/m^3)
			% rep.	(kg/m^3)			
W45LP110-B	**0.45**	**364**	**10**	**40**	**182**	**740**	**1072**
28 days	0.41	345	13.2	52	163	776	1090
91 days	0.46	330	15.0	58	179	743	1090
W45LP210-B	**0.45**	**364**	**10**	**40**	**182**	**740**	**1072**
28 days	0.43	356	8.38	33	167	762	1103
91 days	0.42	283	29.7	119	169	734	1103
W45LP220-B	**0.45**	**321**	**20**	**80**	**181**	**740**	**1072**
28 days	0.50	290	20.4	75	182	726	1115
91 days	0.53	261	27.0	96	190	709	1115

From the analytical result was obtained cement, limestone powder, sand, water and coarse aggregate content of hardened concrete. The maximum errors of the determination of content of cement, limestone powder, water, sand, and coarse aggregate are -22.25 %, +195.37 %, -10.50 %, +5.00 %, and +3.98 %, respectively. The mean errors of the determination ofcontent of cement, limestone powder, water, sand, and coarse aggregate are +10.50 %, +43.63 %, -3.66 %, +0.31 %, and +2.85 %, respectively. Since, the error of each procedure as coarse aggregate content from image analysis and w/b from data back analysis of compressive strength; the mean error of cement and water is changed. The analytical results show that the proposed method can be used to estimate mix proportion of hardened concrete with different

percentage replacement of limestone powder and type of limestone powder. Both early and later age of sample is unrelated to tendency of the error of analytical result; because of the age of concrete is concerned to analyze procedure. Hence, the proposed method can be applied to determine mix proportion although the different age of concrete.

Table 6.11 Percentage error of mix proportion of LP concrete

Sample	Age	% Error					
		w/b	Cement	LP	Water	Sand	Coarse aggregate
W45LP110-B	28	-8.89	-5.24	+29.47	-10.50	+5.00	+1.67
	91	+2.22	-9.35	+43.65	-1.91	+0.43	+1.67
W45LP210-B	28	-4.44	2.21	-19.50	-8.20	+3.14	+2.92
	91	-6.67	-22.25	+195.37	-7.12	-0.81	+2.92
W45LP220-B	28	+11.11	-9.72	-7.29	+0.85	-1.81	+3.98
	91	+17.78	-18.66	+20.06	+4.92	-4.07	+3.98
Mean error (%)		**+1.85**	**-10.50**	**+43.63**	**-3.66**	**+0.31**	**+2.85**

Note: - and + is underestimate and overestimate respectively.

6.5.3 Summary

The method for estimating mix proportion of hardened LP concrete has been proposed in this study. The proposed method was applied to estimate mix proportions of concrete prepared in laboratory with known mix design in order to verify its efficiency. In addition, the determination of mix proportion of hardened concrete was analyzed by many procedures as shown in Figure 6.10. The error of coarse aggregate content by image processing and w/c ration was effected analytical result as shown in Figure 6.11 (a) and (b). It was found that some results increase error but some results reduce error owing to the analytical procedure of w/b, and the coarse aggregate content from image analysis. However, the determination of mix proportion of hardened LP concrete will be evaluated and developed further.

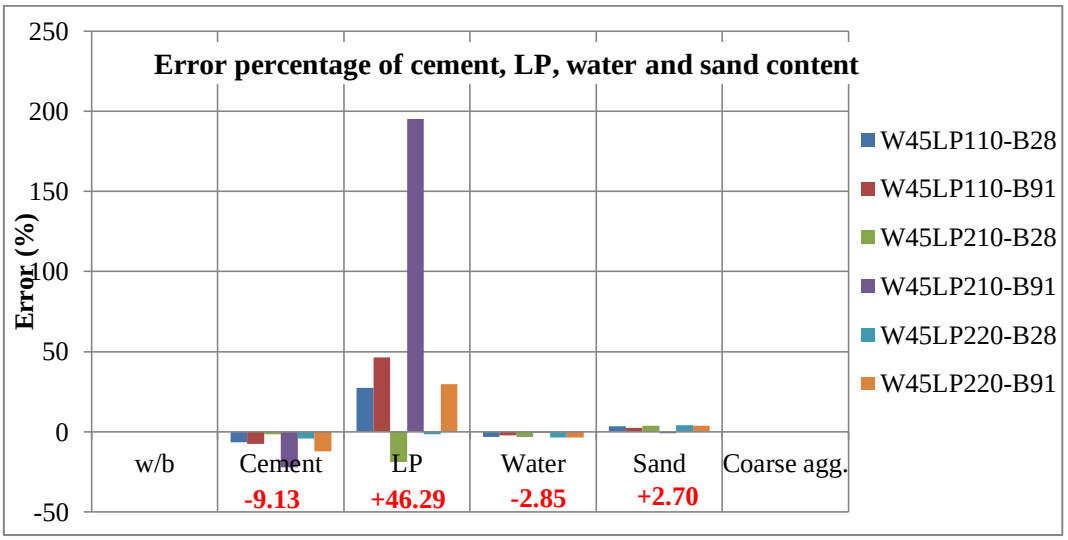

(a) Determining mix proportion with designed w/b and coarse aggregate

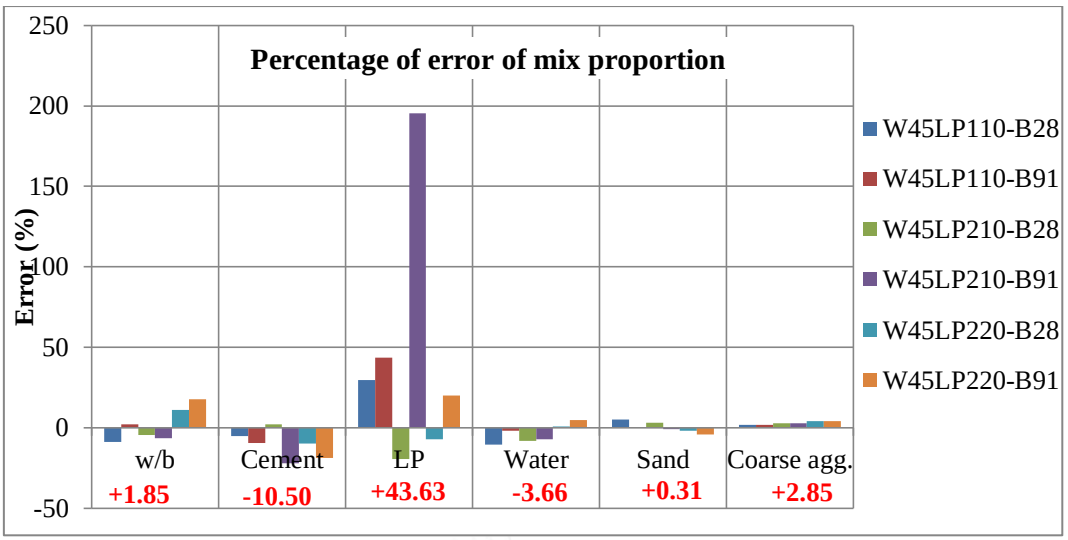

(b) Determining mix proportion with analytical result of w/b and coarse aggregate content

Figure 6.11 The error percentages of analytical result of each materials of LP concrete

CHAPTER 7
DETERMINATION OF MIX PROPORTION OF HARDENED CONCRETE EXPOSED TO REAL ENVIRONMENT

7.1 General

Later, the developed method for estimating mix proportion of normal hardened concrete cured water at laboratory was verified its accuracy; it was applied existing hardened concrete. Then this chapter is applying developed method to hardened concrete with exposing real environment or existing structure that they were divided as two cases. First the mixed concrete in the laboratory with known mix design had been exposed marine environment. Other the concrete sample with unknown mix design was cored from existing structure. Hence analytical result of mix proportion and its efficiency of developed method with hardened concrete expose to real environment were presented in this chapter.

7.2 Mixed concrete in laboratory with exposed in marine environment: Case I

This case study is applicable developed method for estimating mix proportion of hardened concrete which was deteriorated from marine environment. The concrete sample, which was prepared in laboratory, had been exposed marine environment for long time. Thus the analytical result of determination of mix proportion of concrete can be verified that the concrete samples already known mixed design.

7.2.1 Material and Mix proportion

Concrete was prepared by different brand and type of cement. Portland cement type I and type V were prepared. The brands of cement were used as Siam Cement Group type I (SCG1) and type V (SCG5), Siam City Cement public company limited type I (SCC1), TPI polene public company limited type I (TPI1). Their chemical compositions are shown in Table 7.1. Concrete samples were prepared with water to cement ratio (w/c) of 0.40 and 0.50, and 0.60. Specific gravity of sand was 2.60. Specific gravity of coarse aggregates (Crushed limestone) was 2.70. The ratio by volume of sand to total aggregate (s/a) was 0.44 that its void ratio was 0.23. Six mix designs of concrete specimens are shown in Table 7.2.

In order to specimen preparation, the concrete samples were mixed and filled into mold, which is cube with dimension of 30x30 cm in length. After, they were demolded, they had been immersed at tidal zone of sea in Chonburi, Thailand for 4 years. The concrete samples at specified age were cored for 3 cylindrical concrete which is dimension of 5 cm in diameter and 10 cm in length. Three specimens were prepared for compressive strength test, and then the broken specimens from the

compressive strength test were subsequently used for selective dissolution testing that its preparation and testing method were mentioned in Chapter 3.

Table 7.1 Chemical composition of cement

Chemical compositions	SCC1	TPI1	SCG1	SCG5
SiO_2 (%)	20.94	20.08	19.51	21.87
Al_2O_3 (%)	4.58	5.17	4.97	3.87
Fe_2O_3 (%)	3.49	3.58	3.78	4.34
CaO (%)	64.53	64.17	65.38	64.56
MgO (%)	1.38	1.28	1.08	1.11
SO_3 (%)	2.92	2.47	2.16	2.08
Na_2O (%)	0.01	0.01	0.01	0.01
K_2O (%)	0.47	0.27	0.47	0.24
TiO_2 (%)	0.21	0.27	0.25	0.21
P_2O_5 (%)	0.07	0.06	0.07	0.05
LOI (%)	1.20	2.61	2.27	1.59

Table 7.2 Mix proportion of hardened concrete sample exposed sea water environment

Sample	w/c	Cement		Water	Sand	Coarse aggregate
		Type	(kg/m^3)	(kg/m^3)	(kg/m^3)	(kg/m^3)
SCC1W40	0.40	SCC1	435	174	776	1025
SCC1W50	0.50	SCC1	382	191	776	1025
TPI1W50	0.50	TPI1	382	191	776	1025
SCG1W50	0.50	SCG1	382	191	776	1025
SCG5W50	0.50	SCG5	382	191	776	1025
SCC1W60	0.60	SCC1	340	204	776	1025

7.2.2 Estimation of mix proportion of hardened cement concrete

In the analysis for determining mix proportion of hardened cement concrete, three major investigation techniques are implemented as mentioned in Chapter 4. Image processing technique is used for determination of coarse aggregate content. Water to cement ratio was calculated from data back analysis of the compressive strength by using the computer software. Cement and sand contents are obtained based on the residues after selective dissolution of the sample. Contents of all concrete compositions in 1 m^3 of concrete can be derived from a set of mass balance equations. These method were developed with sample cured water at laboratory, and it was verified its efficiency. Hence analytical result of mix proportion and its efficiency of developed method with hardened concrete expose to marine environment were presented below.

In addition, the existing fly ash and limestone powder was not investigated owing to concrete samples already known that fly ash and limestone powder were not mixed in concrete sample. Moreover, the purpose of investigation of this case study is examined the proposed method for calculating mix proportion that it can be adopted to analyze hardened concrete unless sample had cured in water at laboratory. The proposed method will be observed its efficiency for applying exposed concrete with a marine environment.

7.2.2.1 Determination of coarse aggregate content (W_G) by image analysis

The image analysis method was used to determine coarse aggregate content of hardened concrete. The ratios between the area of the coarse aggregate and the total cross-sectional area of the concrete slices were then converted to volumetric ratios of the coarse aggregate to the concrete. The content of coarse aggregate could be obtained by multiplying its volume by the specific gravity. It is noted that gradation of coarse aggregate could not be evaluated by this method. The chemical attack of chloride is not affect to the image analysis method because of it is no effect to coarse aggregate particle. Hence, the determination of coarse aggregate content of this sample set is not presented. Moreover the sample was not enough for investigating

7.2.2.2 Determination of water to cement ratio

The compressive strength of concrete samples was obtained by using the universal testing machine at 180 days, 365 days and 4 years. The water to cement ratio could be calculated from data back analysis of the compressive strength by using the computer software, "FACOMP". Models for predicting compressive strength of concrete constructed based on experimental data were implemented in the FACOMP. It has been proven that the prediction models could be used to accurately predict the compressive strength of concrete age up to 365 days within acceptable limits. In addition, compressive strength of concrete is exposed real environment then they may be defected when compared with compressive strength of unexposed concrete. And the predicted compressive strength of FACOMP is being suitable with concrete which is cured by normal water with standard condition. But the concrete sample in this study had been immersed in seawater for long time.

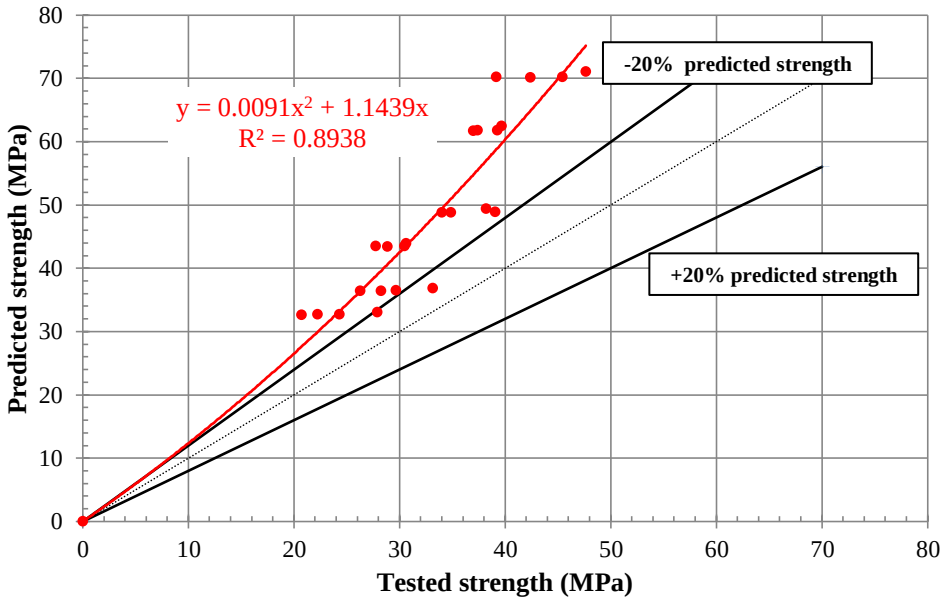

Figure 7.1 Relationship between strength of normal concrete in laboratory with concrete exposed marine environment

$$y = 0.0091x^2 + 1.1439x \quad (7.1)$$

Where x and y are tested result and adjusted result of compressive strength.

Thus the tested compressive strength was modified by compressive strength of unexposed concrete. The relationship of strength between exposed concrete and unexposed concrete is shown in Figure 7.1. It shown that compressive strength of concrete exposed to marine environment is decrease when compare with result of unexposed concrete which cured by normal water with standard condition. Hence, the compressive strength at 180 and 365 days were used for determining water to cement ratio, after they were modified by Eq. (7.1). The tested result and modified result of compressive strength as shown in Table 7.3.

Table 7.3 Compressive strength results by UTM

Sample	Tested strength (MPa)		Modified strength (MPa)	
	180 days	365 days	180 days	365 days
SCC1W40	39.26	45.43	58.93	70.74
SCC1W50	30.46	39.07	43.29	58.58
TPI1W50	28.87	34.87	40.60	50.95
SCG1W50	30.60	38.21	43.52	57.00
SCG5W50	27.72	34.02	38.70	49.45
SCC1W60	22.25	29.64	29.96	41.90

Then, the determination of water to cement ratio were obtained from the data back analysis of both modified compressive strength at 180 and 365 days by using FACOMP is shown in Table 7.4, It can be seen that the analytical results of water to cement ratio is close to the designed water to cement ratio for all mixtures. The maximum error percentages is ±6.00% and the mean error percentages is -2.22 %. This can be presented that the proposed method can be adopted to determine water to cement ratio of hardened concrete exposed marine environment, but the compressive strength have to modify to normal concrete condition. Consequently the compressive strength of concrete need evaluated, before it was used to determine water to cement ratio.

Table 7.4 Result of w/c ratio by FACOMP

Sample	Design	w/c	
		Trial	Error (%)
SCC1W40	0.40	0.40	0
SCC1W50	0.50	0.47	-6.00
SCG1W50	0.50	0.50	0
SCG5W50	0.50	0.47	-6.00
TPI1W50	0.50	0.51	+2.00
SCC1W60	0.60	0.58	-3.33
Mean err. (%)		**-2.22**	

Note: - and + is underestimate and overestimate, respectively.

7.7.2.3 Determination of weight ratio of cement and sand by selective dissolution

Residual weight of cement, sand and sample by selective dissolution testing are shown in Table 7.5 and Table 7.6, respectively. They are subsequently used to calculate weight ratio of cement and sand first as mentioned earlier. The proposed method for determining cement, water and sand, which was followed in Chapter 4, was calculated by using design w/c and coarse aggregate content for evaluating efficient developed method with sample exposed to marine environment. Because of the selective dissolution result may be affected from marine environment such as contaminations into sample by chloride ion exist either in physical absorption and chemical reaction in sample (Yuan, Shi et al. 2009, Florea and Brouwers 2012).

Table 7.5 Residual weight of concrete materials by selective dissolution method

Materials	Residue (%)			
	SCC1	TPI1	SCG1	SCG5
Cement	2.500	2.233	2.820	3.840
Sand*	96.671			

Note: * is assumed by tested result of sand C (the same source was used to prepare sample).

Table 7.6 Residual weight of concrete sample by selective dissolution method

Sample	Residue (%)
SCC1W40	52.858
SCC1W50	59.395
TPI1W50	60.301
SCG1W50	57.329
SCG5W50	57.386
SCC1W60	61.351

The ratio of cement and sand in sample were obtained. The results of cement, water and sand content and percentage error are shown in Table 7.7 and 7.8, respectively. In addition, this procedure was evaluated capability of the proposed method for calculation of mix proportion with deteriorated hardened concrete sample. Where, the degree of hydration of cement was assumed to equal 0.95. Because of, the concrete samples had been exposed seawater at tidal zone for 4 years after hardening; they are affected of degree reaction to full hydration due to hindrance of both chemically bound to the unhydrated products and physically held to the surface of the hydrated products by chloride ion.

From the analytical results, it can be seen that the proposed equation can be adopted to estimate cement and sand content of hardened concrete with good accuracy for all tested mixtures, although the concrete sample was 4 years exposed in marine environment. The maximum errors of the determination of content of cement and sand are +10.80% and -11.36%, respectively. The mean errors of the determination of content of cement and sand are +6.19% and -6.57%, respectively. It can be observed that the sample exposed seawater is higher mean errors than sample cured in laboratory, as the result of the concrete sample are deteriorate that they may be occur to chemical attack and contaminate some matter from environment for long time.

Table 7.7 The analytical results of mix proportion of concrete with designed w/c and coarse aggregate content

Sample	w/c	Cement (kg/m^3)	Water (kg/m^3)	Sand (kg/m^3)	Coarse aggregate (kg/m^3)
SCC1W40	**Design**	**435**	**174**	**776**	**Design**
	0.40	482	193	688	*1025*
SCC1W50	**Design**	**382**	**191**	**776**	**Design**
	0.50	395	197	748	*1025*
TPI1W50	**Design**	**382**	**191**	**776**	**Design**
	0.50	388	193	765	*1025*
SCG1W50	**Design**	**382**	**191**	**776**	**Design**
	0.50	413	206	710	*1025*
SCG5W50	**Design**	**382**	**191**	**776**	**Design**
	0.50	416	208	703	*1025*
SCC1W60	**Design**	**340**	**204**	**776**	**Design**
	0.60	357	214	737	*1025*

Table 7.8 Percentage error of mix proportion of concrete with designed w/c and coarse aggregate content

Sample	% Error		
	Cement	Water	Sand
SCC1W40	+10.80	+10.80	-11.36
SCC1W50	+3.38	+3.38	-3.66
TPI1W50	+1.23	+1.23	-1.41
SCG1W50	+8.01	+8.01	-8.50
SCG5W50	+8.87	+8.87	-9.40
SCC1W60	+4.85	+4.85	-5.08
Mean err. (%)	**+6.19**	**+6.19**	**-6.57**

Note: - and + is underestimate and overestimate respectively.

7.2.2.4 Determination of mix proportion of hardened concrete

Mix proportion of concrete estimated by the developed method and its percentage error are shown in Tables 7.9 and 7.10, respectively.

From the analytical results, it can be seen that the developed method can be adopted to estimate mix proportion of deteriorated hardened concrete with capability for all tested mixtures. The maximum errors of the determination of content of water, cement, and sand are +10.80 %, +10.80 %, and -11.36 %, respectively. The mean errors of the determination of content of cement, water, and sand are +6.99 %, +4.60 %, and -5.58 %, respectively. Hence, the results show that the proposed method can be applied to estimate mix proportion of deteriorated hardened concrete exposed marine environment for long time. Hence, it can conclude that the proposed method is effectively applied to calculate mix proportion of hardened concrete exposed in

marine environment although they were deteriorated by seawater, and prepared by different cement brand and type.

Table 7.9 Mix proportion of concrete sample (Case I)

Sample	w/c	Cement (kg/m^3)	Water (kg/m^3)	Sand (kg/m^3)	Coarse aggregate (kg/m^3)
SCC1W40	**0.40**	**435**	**174**	**776**	**Design**
	0.40	482	193	688	1025
SCC1W50	**0.50**	**382**	**191**	**776**	**Design**
	0.47	403	189	762	1025
TPI1W50	**0.50**	**382**	**191**	**776**	**Design**
	0.50	388	193	765	1025
SCG1W50	**0.50**	**382**	**191**	**776**	**Design**
	0.47	421	198	724	1025
SCG5W50	**0.50**	**382**	**191**	**776**	**Design**
	0.51	413	211	698	1025
SCC1W60	**0.60**	**340**	**204**	**776**	**Design**
	0.58	361	209	745	1025

Table 7.10 Percentage error of mix proportion of concrete sample (Case I)

Sample	% Error				
	w/c	Cement	Water	Sand	Coarse aggregate
SCC1W40	0	+10.80	+10.80	-11.36	0
SCC1W50	-6.00	+5.42	-0.90	-1.75	0
TPI1W50	0	+1.23	+1.23	-1.41	0
SCG1W50	-6.00	+10.24	+3.63	-6.61	0
SCG5W50	+2.00	+8.13	+10.29	-10.01	0
SCC1W60	-3.33	+6.09	+2.55	-3.96	0
Meam err. (%)	**-2.22**	**+6.99**	**+4.60**	**-5.85**	**0**

Note: - and + is underestimate and overestimate respectively.

7.3 Cored concrete from existing structure: Case II

In this case, the existent mass concrete structure, which was constructed in 1998, had been damaged. Crack in the concrete were observed in many locations. The cracks were repaired but they were continuously extended and new cracks were formed. Then, the cause of deterioration of concrete structure need evaluated to arrange proper repair and maintenance planning of the concrete structure. The mix proportion need determined to analyze cause of crack such as thermal effect and shrinkage that they can occur on mass concrete structure.

Base on the visual examination, damage of the concrete structures can be divided into 4 levels accordingly to amount of cracks and crack width of the concrete structure that is Very severe (A), Severe (B), Moderate (C), and None (D).

In addition, this concrete structure had been constructed since 1998 that its age is about 15 years. Since, the existing structure in this case was constructed for long time ago; the document of mix designed was unavailable examined. In the past, fly ash of Thailand was not used widespread due to limit amount researching for supported many properties and characteristic of using fly ash of Thailand into concrete. At that time most construction project of government was required only cement concrete, therefore the procedure for investigating fly ash or limestone powder existence in sample of this case study was disregarded.

7.3.1 Sample preparation

The concrete sample in this study was cored from structure. Four concrete sample as A, B, C and D were investigated. The cored concrete with dimension of 7 cm in diameter as shown in Figure 7.2 was cut with a diamond saw to separate each test method for estimating mix proportion procedure. And then, the cored samples were prepared as followed in Chapter 3.

Figure 7.2 Cored concrete samples

7.3.2 Estimation of mix proportion of hardened cement concrete

In the analysis for determining mix proportion of hardened cement concrete, three major investigation techniques are implemented as mentioned before. The efficiency of developed method was presented previous. Hence analytical result of mix proportion and its efficiency of developed method with hardened concrete from existing structure were presented below.

7.3.2.1 Determination of coarse aggregate by image processing

The analytical procedure for determining coarse aggregate content is same method as mentioned in Chapter 4. Eight cut faces of concrete sample were bought to produce image analysis. And the reasonable Z-score between -1 to 1 ($-1 < Z < 1$) was applied to analyze the results of the coarse aggregate content. The content of coarse aggregate results were estimated by image processing technique as shown in Table 7.11

Table 7.11 Result of coarse aggregate content by image analysis (Case II)

Sample	Volume ratio of Coarse Aggregate (SSD)	Coarse aggregate content (kg/m^3)
A	0.315	849.5
B	0.325	876.6
C	0.360	973.1
D	0.352	949.8

Note: Coarse aggregate content is calculated based on 2.7 of specific gravity. And, its content was average from 8 faces of sample

7.3.2.2 Determination of water to cement ratio

Since, the existing structure was constructed in 1998 that it is age around 14 years but the FACOMP can predict the compressive strength of concrete within 365 days. Consequently, the tested compressive strength results were adjusted, the compressive strength was regarded to data back analysis for determining the water to cement ration as tested result at 365 days. Some researchers studied to develop concrete strength in long-term. They presented results of development of concrete in long-term that compressive strength at 15 years have increased around 15-25% after 1 year (Mohamed 2008). So, the strength result was decrease 20% of testing that they would be used for determination of water to cement ratio by FACOMP.

The compressive strength of concrete sample and the water to cement ratio obtained from the data back analysis of the adjusted compressive strength by using FACOMP is shown in Table 7.12.

Table 7.12 Compressive strength results by UTM and result of w/c (Case II)

Sample	Compressive strength (MPa)		w/c
	14 years	1 year	
A	57.01	45.61	0.54
B	53.52	42.81	0.56
C	59.04	47.24	0.53
D	59.56	47.65	0.52

7.3.2.3 Calculation of mix proportion of hardened concrete

Residual weight of cement and sand was assumed as 0.42% and 89.03%, respectively. Residual weights of sample by selective dissolution method are shown in Table 7.13. They are subsequently used to calculate weight ratio of cement and sand. The proposed calculation method by selective dissolution and the calculation of mix proportion of cement concrete, which was followed in Chapter 4. In addition, the degree of hydration of cement was assumed as 95% of full hydration and the specific gravity of cement, sand and coarse aggregate is 3.15, 2.6 and 2.7, respectively. Mix proportion of concrete estimated by the developed method and its percentage error are shown in Tables 7.14.

Table 7.13 Residual weight of concrete sample by selective dissolution method (Case II)

Sample	Residue (%)
A	61.494
B	60.213
C	59.228
D	59.056

Table 7.14 Mix proportion of concrete sample of cored sample (Case II)

Sample	w/c	Cement (kg/m^3)	Water (kg/m^3)	Sand (kg/m^3)	Coarse aggregate (kg/m^3)
A	0.54	354	191	968	850
B	0.56	357	200	915	877
C	0.53	353	187	859	973
D	0.52	362	188	872	950

CHAPTER 8

CONCLUSIONS AND RECOMMENDATIONS

8.1 Conclusions

From the analytical results, the procedures for investigating fly ash or limestone powder existence and determining mix proportion of hardened concrete can be concluded and be summarized as followed

1. The investigation of fly ash existence procedure has been proposed in this study. The proposed method was verified by sample prepared in laboratory with known type of admixture. It can be concluded from the analytical result of the SEM analysis that this SEM technique is efficient to find some spherical particles of fly ash although only 5% of fly ash was replaced in sample. Then the SEM-EDS technique was adopted for evaluating theirs particle after the SEM testing. The analytical result of EDS technique can be concluded that it is efficiently identifying type of fly ash particle. And, XRD technique was adopted investigating fly ash existence for ensuring.

2. The investigation of limestone powder existence procedure has been proposed in this study. The proposed method was verified by sample prepared in laboratory with known type of admixture. It can be concluded from the analytical result that some particles of limestone powder can be found by SEM technique. Then the SEM-EDS technique was adopted to confirm theirs particle after the SEM testing. The analytical result of EDS technique can be concluded that it is efficiently identifying limestone powder particle in concrete regardless of particle size of the limestone powder.

3. The coarse aggregate content is determined by image processing. It can be observed that the appropriate standard score of this method is in a range of ±1.00 of Z-score. The maximum error of the analytical result with Z-score between -1 to 1 ($-1 < Z < 1$) is 5.28% (or 54 kg/m^3), which is within acceptable limits. This can be confirmed that the image processing technique can be efficiently used to determine coarse aggregate content of hardened concrete regardless source and s/a of aggregate. Consequently, this method can be even applied to different type of coarse aggregate of this study as the result of the chemical composition of coarse aggregate is disregarded in analysis procedure of this method. However this method cannot determine grading of coarse aggregate.

4. The water to binder ratio is obtained from data back analysis of the compressive strength by using FACOMP. It can be seen that almost analytical result is close to the designed water to binder ratio for all mixtures and test ages. This can also be confirmed that the proposed method can be efficiently used to determine water to binder ratio of hardened concrete. However, the predicted compressive strength of

FACOMP is suitable for concrete cured in water with normal condition. Moreover the prediction models could be used to accurately predict the compressive strength of concrete age up to 365 days within acceptable limits. Hence, age of concrete and curing condition are needed to be known for evaluating compressive strength result, before it was used to determine water to binder ratio.

5. A method for estimating mix proportion of hardened cement concrete was developed in this study. From the analytical results, it was found that the developed method could be used to estimate mix proportion of hardened concrete with different water to cement ratios and different sources and s/a of aggregate at any age of concrete. The maximum error of the determination of w/c was -8.89 %. The maximum errors of the determination of content of cement, water, sand, and coarse aggregate are -10.28 %, -7.57 %, +5.02 %, and +5.28 %, respectively. The mean errors of the determination of content of cement, water, sand, and coarse aggregate are -4.69 %, -4.52 %, +2.58 %, and +1.79%, respectively. The accuracy was acceptable. Moreover, it was found that the proposed calculation method can be used to determine mix proportion of hardened concrete with good accuracy even though different age of concrete sample, since the effect of age of concrete is covered by taking into account the degree of hydration of sample in the analysis.

6. A method for estimating mix proportion of hardened fly ash concrete was developed in this study. From the analytical results, it was found that the developed method could be used to estimate mix proportion of hardened fly ash concrete with different water to binder ratios, different type and percent replacement of fly ash at different age of concrete. The maximum errors of the determination of content of cement, fly ash, water, and sand are +6.27 %, -8.83 %, +5.89 %, and -6.71 %, respectively. It shows that the maximum errors of each material are lower than 10 %. The mean errors of analytical result of content of cement, fly ash, water and sand are +1.25 %, -0.85 %, +0.59 %, and -0.60 %, respectively. The accuracy was acceptable. Moreover, it was found that the proposed calculation method can be used to determine mix proportion of hardened concrete with good accuracy even though different age of concrete sample, since the effect of age of concrete is covered by taking into account the degree of hydration and the degree of pozzolanic reaction of sample in the analysis.

7. A method for estimating mix proportion of hardened limestone powder concrete was developed in this study. From the analytical results, it was found that the developed method could be used to estimate mix proportion of hardened limestone powder concrete with different water to binder ratios, different type and percent replacement of limestone powder at different age of concrete. The maximum errors of the determination of content of cement, limestone powder, water, and sand are -22.33 %, +195.07 %, -3.78 %, and +4.10 %, respectively. The mean errors of analytical result of content of cement, limestone powder, water and sand are -9.13 %, +46.29 %, -2.85 %, and +2.70 %, respectively. The mean errors of concrete materials except limestone powder do not exceed 10%. High error percentages of limestone powder may be occurred from human error on experimental procedure, and may be because of low content of limestone powder in the designed mix proportion. However, more

accuracy of the analytical method for limestone powder concrete will be developed in the future work.

8.2 Limitations

A method for determination of mix proportion of hardened concrete has been proposed in this study. However, there are some limitations of the proposed expressions and application.

This method was developed based on normal concrete sample cured in the laboratory conditions which is different from the real condition at field, where the environment affects the properties of hardened concrete, such as mechanical and chemical properties. Since some properties, such as compressive strength was used in the analysis. When concrete is subjected to some chemical attacks from environment causing a reduction in compressive strength and change in the chemical composition of the concrete, the developed method may inappropriate to be applied for those concretes.

Moreover, properties of materials are needed to be assumed in some cases of concrete sample from existing concrete structures such as specific gravity of material especially coarse aggregate. This will cause error of the determination of the mix proportion of hardened concrete. However, the error is insignificant as 1% of change of specific gravity of coarse aggregate results in 1% of error of the determination of coarse aggregate content.

8.3 Recommendations for future study

1. The investigation of fly ash or limestone powder existence procedure, more data base of basic properties of materials should be collected in order to be able to correctly identify their type.

2. Since many binder types are used to produce concrete in nowadays. The method for determining other admixtures in addition to fly ash and limestone powder should be further studied.

3. Many brands and types of cement are used widespread today. Thus the determination of mix proportion of hardened cement concrete should be studied further for concrete made with various types of cement.

4. Since many binder types are used to produce concrete in nowadays. The estimation of mix proportion of concrete containing other types of binder should be developed in the future such as concrete containing silica flume or slag and concrete with ternary binder (3 binders).

5. The determination of coarse aggregate content by image processing should be further studied with different size, grading, and type of coarse aggregate.

6. More convenient and precise method for determination of coarse aggregate content by image processing technique should be further developed.

7. The determination of mix proportion of hardened concrete with different size and shape of concrete sample should be further studied.

REFERENCES

Abbas, A., G. Fathifazl, B. Fournier, O. B. Isgor, R. Zavadil, A. G. Razaqpur and S. Foo (2009). "Quantification of the residual mortar content in recycled concrete aggregates by image analysis." Materials Characterization **60**(7): 716-728.

Antiohos, S. and S. Tsimas (2005). "Investigating the role of reactive silica in the hydration mechanisms of high-calcium fly ash/cement systems." Cement and Concrete Composites **27**(2): 171-181.

ASTM (1996). C 1356-96. Standard Test Method for Determiantion of Phases in Portland Cement Clinker by Microscopical Point-Count Procedure. United States, ASTM International.

ASTM (1997). C 642-97. Standard Test Method for Density, Absorption, and Voids in Hardened Concrete. United States, ASTM International.

ASTM (2002). C 1084–02. Standard Test Method for Portland-Cement Content of Hardened Hydraulic-Cement Concrete. United States, ASTM International.

ASTM (2003). C 39/C 39M-03. Standard Test Method for Compressive Strength of Cylindical Concrete Specimens. United States, ASTM International.

ASTM (2003). C 42/C 42M-03. Standard Test Method for Obtaining and Testing Drilled Cores and Sawed Beams of Concrete. United States, ASTM International.

ASTM (2003). C 568-03. Standard Specification for Limestone Dimension Stone. United States, ASTM International.

ASTM (2003). C 615-03. Standard Specification for Granite Dimension Stone. United States, ASTM International.

ASTM (2004). C 114-04. Standard Test Methods for Chemical Analysis of Hydraulic Cement. United States, ASTM International.

Banta, L., K. Cheng and J. Zaniewski (2003). "Estimation of limestone particle mass from 2D images." Powder Technology **132**(2-3): 184-189.

Barzin, M., B. Aboozar and A. Sudheen (2007). Modeling of sulfate resistance of fly ash blended cement concrete material. World of Coal Ash (WOCA). Covington, Kentucky, USA**:** 1-12.

Bonavetti, V. L., V. F. Rahhal and E. F. Irassar (2001). "Studies on the carboaluminate formation in limestone filler-blended cements." Cement and Concrete Research **31**(6): 853-859.

Booher, H. B., D. V. Martello, J. P. Tamilia and G. A. Irdi (1994). "Microscopic study of spheres and microspheres in fly ash." Fuel **73**(2): 205-213.

Chindaprasirt, P., C. Jaturapitakkul and T. Sinsiri (2007). "Effect of fly ash fineness on microstructure of blended cement paste." Construction and Building Materials **21**(7): 1534-1541.

Choktaweekarn, P. (2008). Thermal properties and model for predicting temperature and thermal cracking in mass concrete. PhD.Thesis, SIIT- Thammasat University.

Clemeiia, G. G. (1972). Determination of the cement content of hardened concrete by selective dissolution Highway Research Analyst. Charlottesville, Virginia, Department of Highways and the University of Virginia**:** 32.

Department of Primary Industries and Mines (2007). คุณลักษณะของแร่ตามมาตรฐานการใช้งานและมาตรฐานการซื้อขายแร่ในตลาดแต่. Thailand, Department of Primary Industries and Mines.

Elsen, J., N. Lens, T. Aarre, D. Quenard and V. Smolej (1995). "Determination of the ratio of hardened cement paste and concrete samples on thin sections using automated image analysis techniques." Cement and Concrete Research **25**(4): 827-834.

FACOMP (2006). FACOMP. The computer software. SIIT, Thammasat University, Thailand.

Feng, X., E. J. Garboczi, D. P. Bentz, P. E. Stutzman and T. O. Mason (2004). "Estimation of the degree of hydration of blended cement pastes by a scanning electron microscope point-counting procedure." Cement and Concrete Research **34**(10): 1787-1793.

Fernlund, J. M. R. (2005). "Image analysis method for determining 3-D shape of coarse aggregate." Cement and Concrete Research **35**(8): 1629-1637.

Florea, M. V. A. and H. J. H. Brouwers (2012). "Chloride binding related to hydration products: Part I: Ordinary Portland Cement." Cement and Concrete Research **42**(2): 282-290.

Haha, M. B., K. De Weerdt and B. Lothenbach (2010). "Quantification of the degree of reaction of fly ash." Cement and Concrete Research **40**(11): 1620-1629.

Heikal, M., H. El-Didamony and M. S. Morsy (2000). "Limestone-filled pozzolanic cement." Cement and Concrete Research **30**(11): 1827-1834.

Ingram, K. and K. Daugherty (1992). Limestone additions portland cement: uptake, chemistry and effects. Proc. 9th International Congress The Chemistry of Cement, New Delhi, India, National Council for Cement and Building Materials.

John, N. and C. B. S. (2003). Advanced Concrete Technology: Constituent Materials. Great Britain, Butterworth-Heinemann.

Julnipitawong, P. (2003). Effect of curing temperature on early-age compressive strength of fly ash concrete. Master Thesis, SIIT-Thammasat University.

Jung, M. S., M. C. Shin and K. Y. Ann (2012). "Fingerprinting of a concrete mix proportion using the acid neutralisation capacity of concrete matrices." Construction and Building Materials **26**(1): 65-71.

Kakali, G., S. Tsivilis, E. Aggeli and M. Bati (2000). "Hydration products of C_3A, C_3S and Portland cement in the presence of $CaCO_3$." Cement and Concrete Research **30**(7): 1073-1077.

Kutchko, B. and A. Kim (2006). "Fly ash characterization by SEM–EDS." Fuel **85**(17-18): 2537-2544.

Lam, L., Y. L. Wong and C. S. Poon (2000). "Degree of hydration and gel/space ratio of high-volume fly ash/cement systems." Cement and Concrete Research **30**(5): 747-756.

Linares, L., M. López-Atalaya and S. Chinchón (2009). "Cement content determination through selective stain in hardened concrete." Cement and Concrete Research **39**(11): 1105-1109.

Lothenbach, B., G. Le Saout, E. Gallucci and K. Scrivener (2008). "Influence of limestone on the hydration of Portland cements." Cement and Concrete Research **38**(6): 848-860.

Mohamed, A. E.-R. (2008). Assessment and Repair of Corrosion, CRC press.

Ohsawa, S., K. Asaga, S. Goto and M. Daimon (1985). "Quantitative determination of fly ash in the hydrated fly ash - $CaSO_4 \cdot 2H_2OCa(OH)_2$ system." Cement and Concrete Research **15**(2): 357-366.

P. Kumar, M. and M. Paulo J.M. (2006). Concrete: Microstructure, Properties, and Materials (3rd Edition). U.S.A., McGraw-Hill Companies.

Presuel-Moreno, F. J. and A. A. Sagüés (2009). "Bulk magnetic susceptibility measurements for determination of fly ash presence in concrete." Cement and Concrete Research **39**(2): 95-101.

R. Doug, H. and R. C. A. (1995). "Determination of slag and fly ash content in hardened concrete." Cement, Concrete and Aggregates **17**(1): 55-60.

Ramezanianpour, A. A., E. Ghiasvand, I. Nickseresht, M. Mahdikhani and F. Moodi (2009). "Influence of various amounts of limestone powder on performance of Portland limestone cement concretes." Cement and Concrete Composites **31**(10): 715-720.

Saengsoy, W. (2002). Simulation of thermal properties and adiabatic temperature rise of fly ash concrete. Master Thesis, SIIT- Thammasat University.

Saengsoy, W., T. Nawa and P. Termkhajornkit (2007). Effect of curing conditions on internal relative humidity and compressive strength of fly ash-cement paste. Concrete Engineering Series 74**:** 31-36.

Sahu, S., S. Badger, N. Thaulow and R. J. Lee (2004). "Determination of water-cement ratio of hardened concrete by scanning electron microscopy." Cement and Concrete Composites **26**(8): 987-992.

Sakai, E., S. Miyahara, S. Ohsawa, S.-H. Lee and M. Daimon (2005). "Hydration of fly ash cement." Cement and Concrete Research **35**(6): 1135-1140.

Shuhua, L. and Y. Peiyu (2010). "Effect of limestone powder on microstructure of concrete." Journal of Wuhan University of Technology-Mater. Sci. Ed. **25**(2): 328-331.

Shunsuke, H., T. Fuminori, K. Makoto and H. KwangRyul (2001). "Effects of water/powder ratio, mixing ratio of fly ash, and curing temperature on pozzolanic reaction of fly ash in cement paste." Cement and Concrete Research **31**: 31-39.

Sidney, M., Y. J. Francis and D. David (2003). Concrete (2nd Edition). U.S.A., Prentice Hall, Pearson Education, Inc. Upper Saddle River, NJ 07458.

Soroka, I. and N. Setter (1977). "The effect of fillers on strength of cement mortars." Cement and Concrete Research **7**(4): 449-456.

Standards, B. (1988). BS 1881 : Part 124. Testing concrete: Methods for analysis of hardened concrete, British Standards Institution.

Tahir, M. A. (1998). Model for predicting strength development of concrete incorporating fly ash of variable chemical composition and fineness. PhD. Thesis, Asian Institute of Technology.

Tangtermsirikul, S., P. Jitvutikrai and T. Kaewkhluab (2004). "A compressive strength model for roller-compacted concrete with fly ash." Magazine of Concrete Research **56**(1): 35-44.

Tangtermsirikul, S. and H. LeViet (2007). "A strength model for no-slump concrete with fly ash." Magazine of Concrete Research **59**(3): 211-221.

Tangtermsirikul, S. and W. Saengsoy (2002). "Simulation of free water content of paste with fly ash." Research and Development Journal of the Engineering Institute of Thailand **13**(4): 1-10.

Taylor, H. F. W. (1997). Cement Chemistry (2nd Edition), Thomas Telford Publishing, Thomas Telford Services Ltd, London.

Vagelis, G. P. (1999). "Effect of fly ash on Portland cement systems Part I. Low-calcium fly ash." Cement and Concrete Research **29**(11): 1727-1736.

Wang, W. (1999). "Image analysis of aggregates." Computers & Geosciences **25**(1): 71-81.

Wong, H. S. and N. R. Buenfeld (2009). "Determining the water–cement ratio, cement content, water content and degree of hydration of hardened cement paste: Method development and validation on paste samples." Cement and Concrete Research **39**(10): 957-965.

Ye, G., X. Liu, G. De Schutter, A. M. Poppe and L. Taerwe (2007). "Influence of limestone powder used as filler in SCC on hydration and microstructure of cement pastes." Cement and Concrete Composites **29**(2): 94-102.

Yuan, Q., C. Shi, G. De Schutter, K. Audenaert and D. Deng (2009). "Chloride binding of cement-based materials subjected to external chloride environment – A review." Construction and Building Materials **23**(1): 1-13.

Zeng, Q., K. Li, T. Fen-chong and P. Dangla (2012). "Determination of cement hydration and pozzolanic reaction extents for fly-ash cement pastes." Construction and Building Materials **27**(1): 560-569.

Zhang, Y. M., W. Sun and H. D. Yan (2000). "Hydration of high-volume fly ash cement pastes." Cement and Concrete Composites **22**(6): 445-452.

APPENDICES

Appendix A

Results of Compressive Strength for Analyzing Water to Binder Ratio

Table A1 Average compressive strength of concrete sample cured water in laboratory

No.	Sample	14 days (MPa)	28 days (MPa)	91 days (MPa)
1	W45C-A	-	43.99	48.95
2	W45C-B	-	41.30	46.81
3	W45C-C	33.96	-	41.87
4	W55C-C	22.61	-	33.04
5	W65C-C	17.66	-	23.23
6	W45FA130-A	-	38.33	46.30
7	W55FA130-A	-	21.24	27.90
8	W45FA230-A	-	32.09	46.05
9	W45FA150-B	-	27.50	33.56
10	W45LP110-B	-	43.72	45.39
11	W45LP210-B	-	39.90	51.35
12	W45LP220-B	-	31.20	35.88

Table A2 Average compressive strength of concrete sample exposed sea water

No.	Sample	Tested strength (MPa)		Modified strength (MPa)	
		180 days	365 days	180 days	365 days
1	W45SCC1	39.26	45.43	58.93	70.74
2	W50SCC1	30.46	39.07	43.29	58.58
3	W50TPI1	28.87	34.87	40.60	50.95
4	W50SCG1	30.60	38.21	43.52	57.00
5	W50SCG5	27.72	34.02	38.70	49.45
6	W60SCC1	22.25	29.64	29.96	41.90

Table A3 Average compressive strength of concrete sample cored existing structure

No.	Sample	Tested strength (MPa)	Modified strength (MPa) at 365 days
1	A	57.01	45.61
2	B	53.51	42.81
3	C	59.04	47.24
4	D	59.56	47.65

Appendix B

Image of cross-sectional area of concrete slices for determining coarse aggregate content by image processing

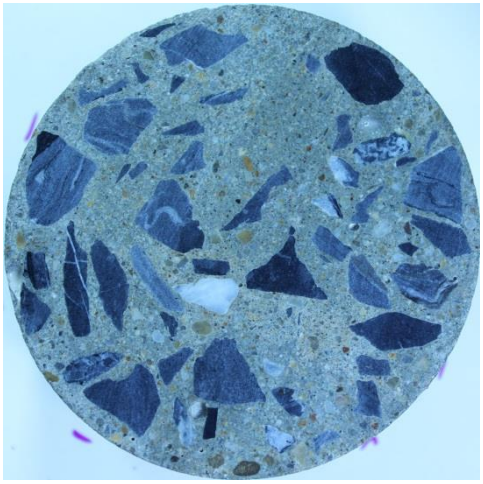

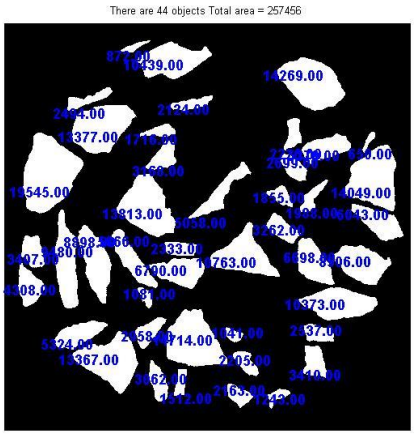
There are 44 objects Total area = 257456

P1-1

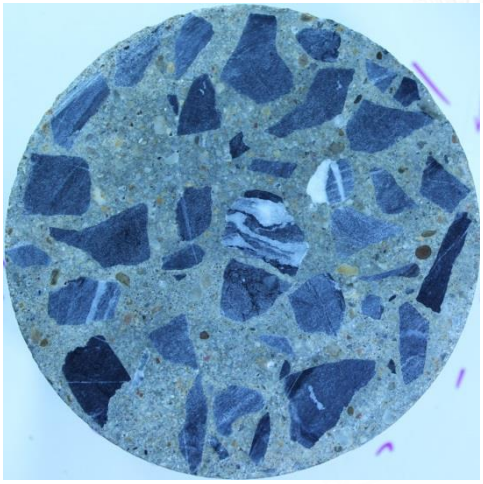

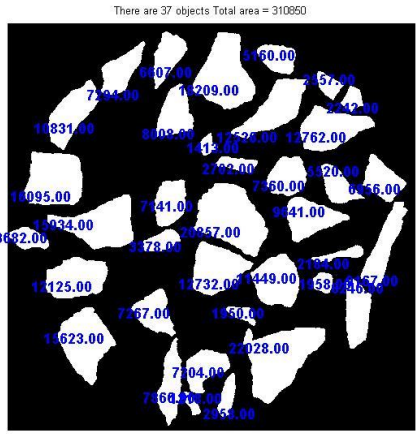
There are 37 objects Total area = 310850

P1-2

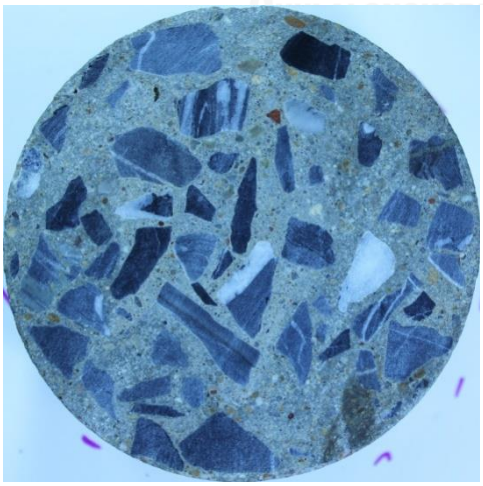

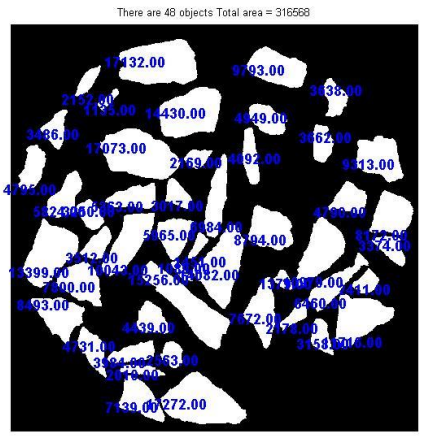
There are 48 objects Total area = 316568

P1-3

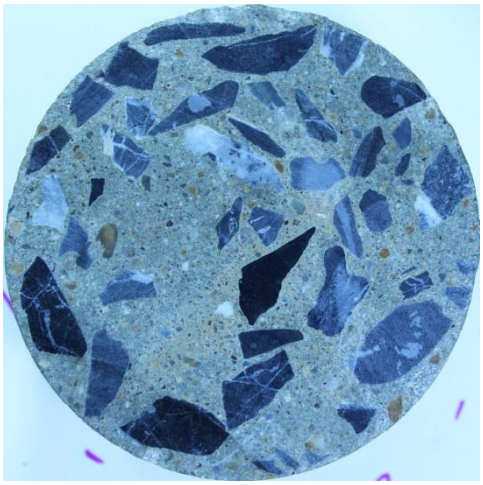

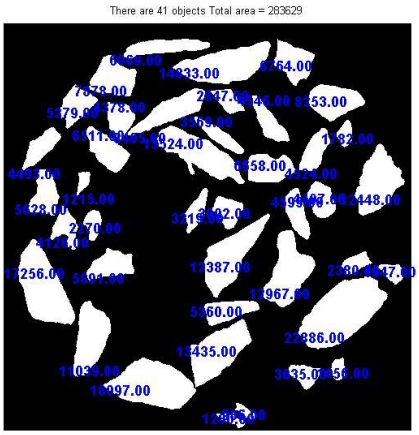

P1-4

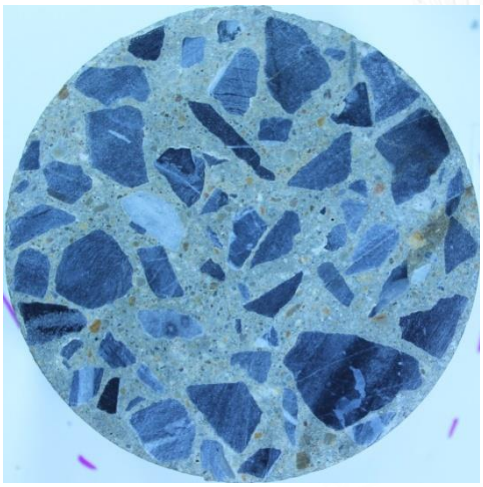

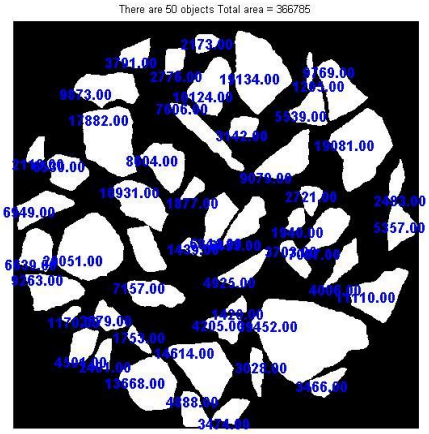

P1-5

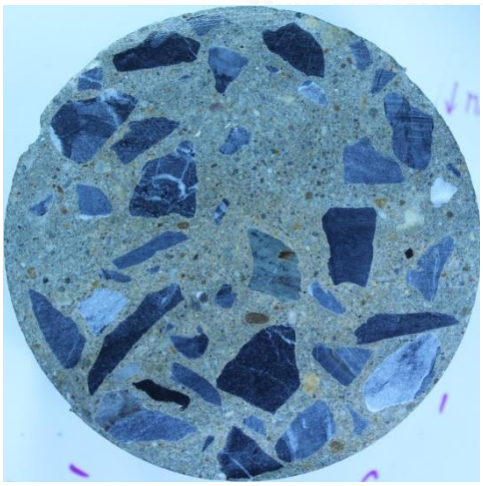

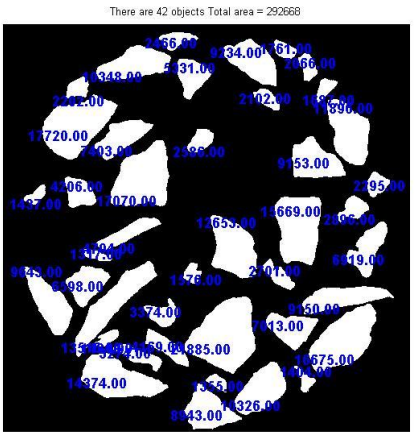

P1-6

(B1-P1) Image of cross-section of sample W45C-A

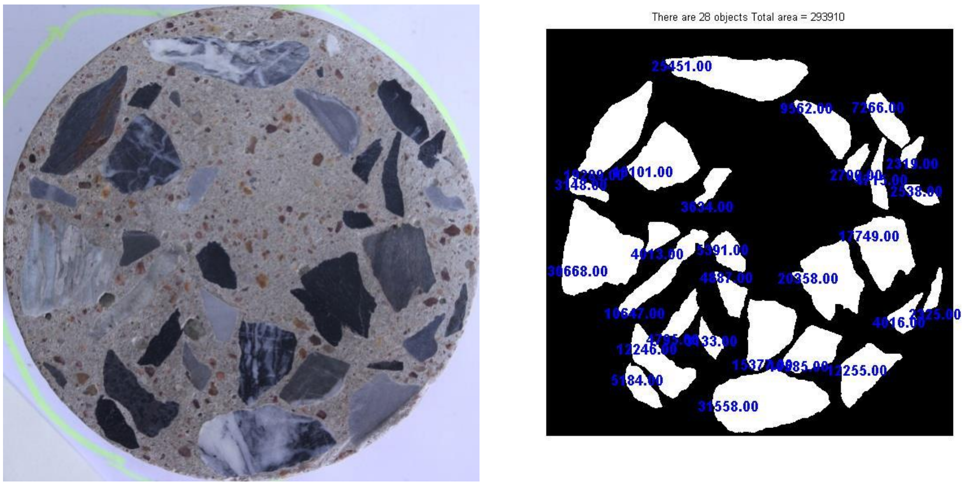
There are 28 objects Total area = 293910

P2-1

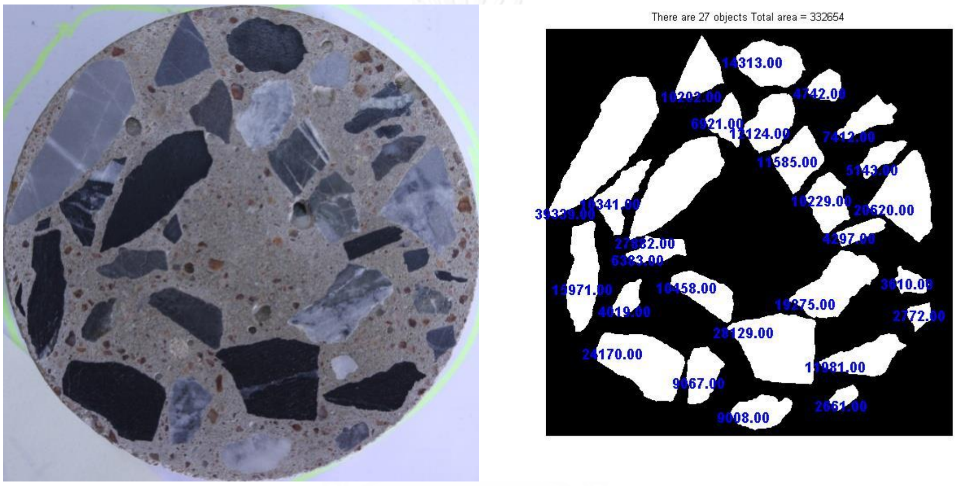
There are 27 objects Total area = 332654

P2-2

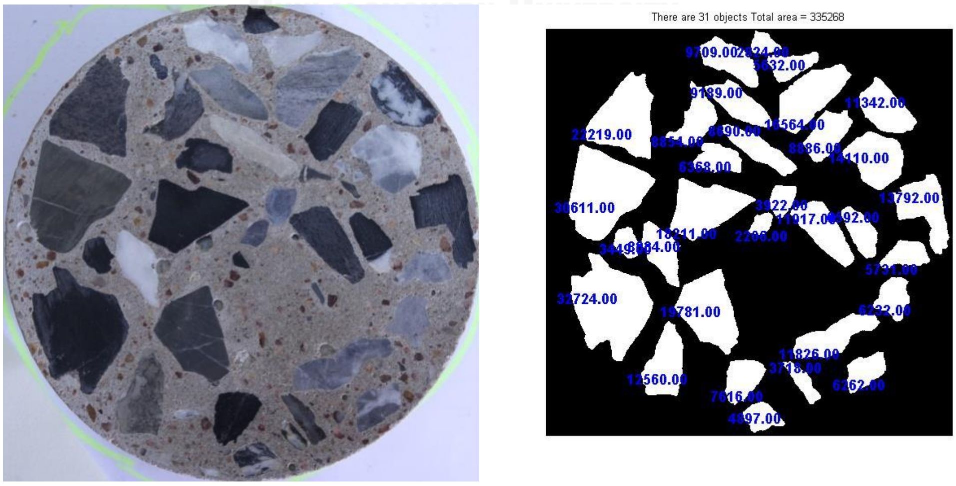
There are 31 objects Total area = 335268

P2-3

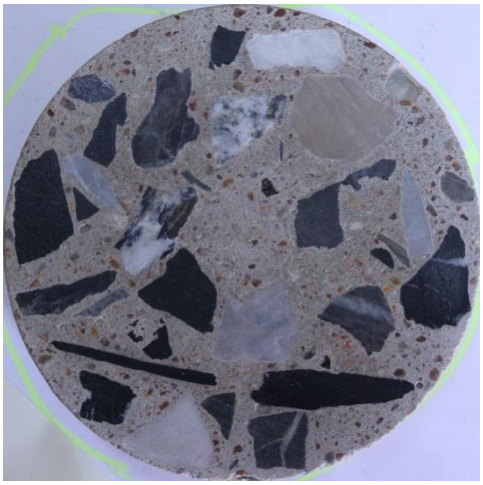

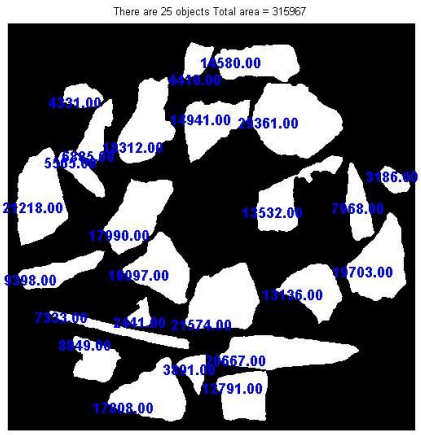

P2-4

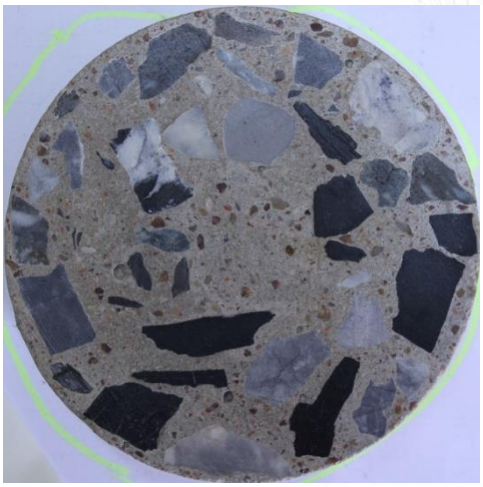

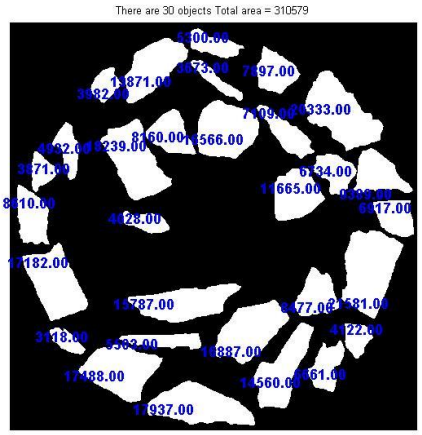

P2-5

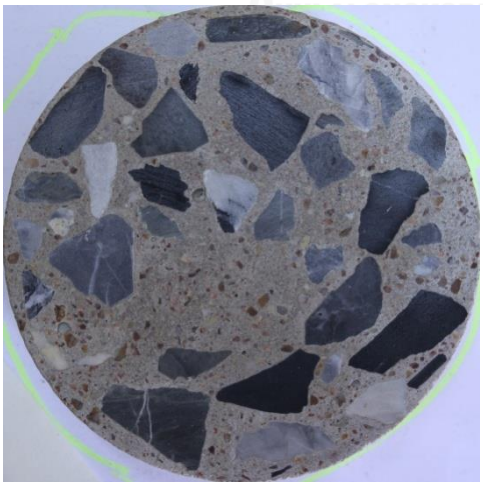

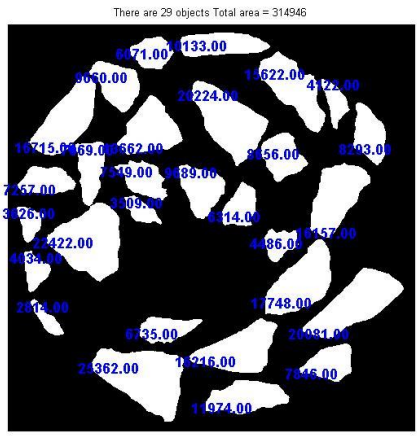

P2-6

(B1-P2) Image of cross-section of sample W45C-B

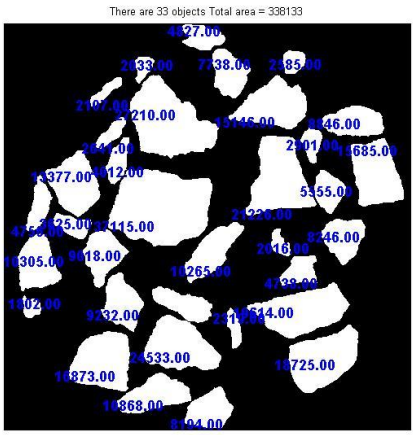
There are 33 objects Total area = 338133
4527.00
2033.00
7738.00
2685.00
2210.00
8346.00
2685.00
5355.00
8346.00
9018.00
9232.00
15725.00
15873.00

P3-1

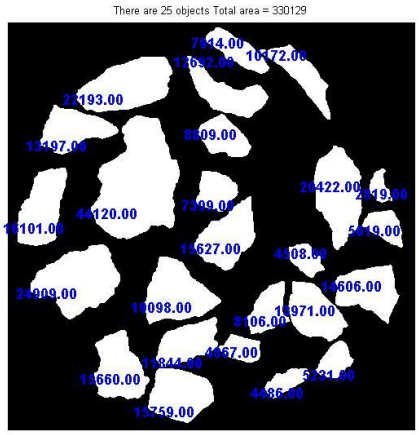
There are 25 objects Total area = 330129
7914.00
10472.00
25193.00
8509.00
13197.00
20422.00
7309.00
44120.00
15627.00
24909.00
18098.00
15971.00
15660.00
15759.00

P3-2

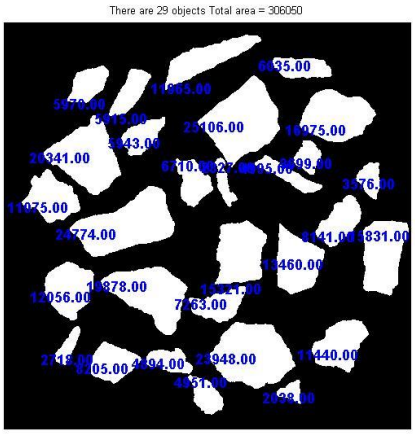
There are 29 objects Total area = 306050
8035.00
25106.00
11075.00
25341.00
11075.00
24774.00
13460.00
18878.00
12056.00
7563.00
23948.00
11440.00

P3-3

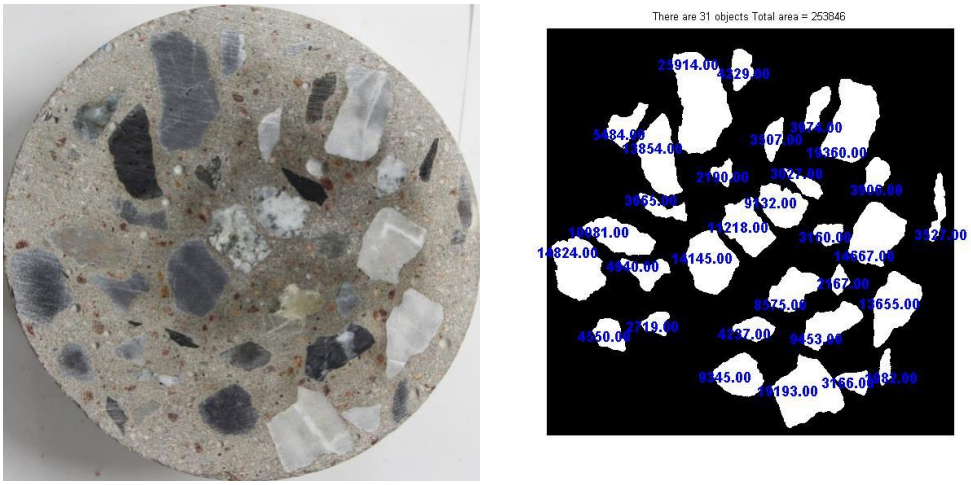

P3-4

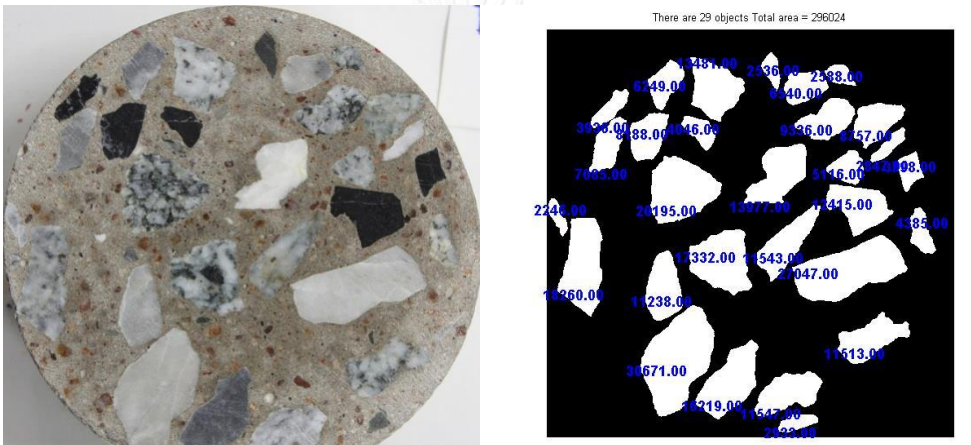

P3-5

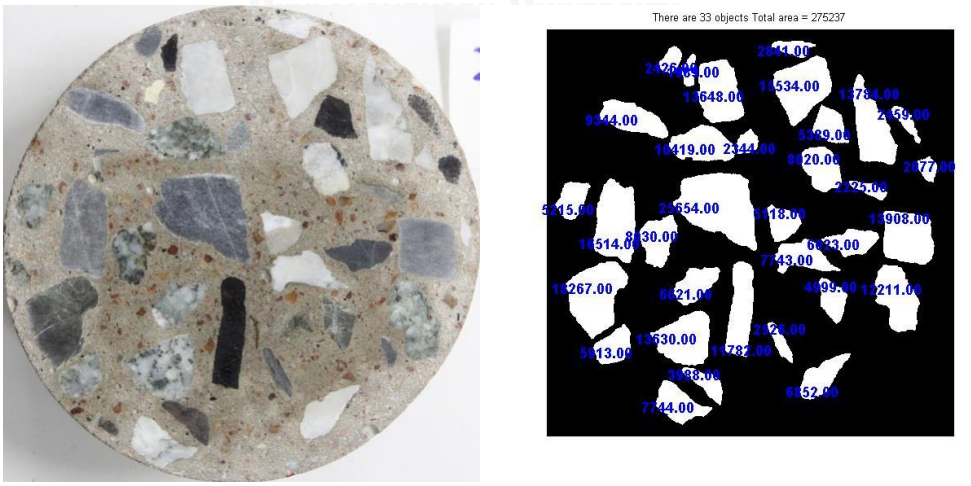

P3-6

(B1-P3) Image of cross-section of sample W45C-C

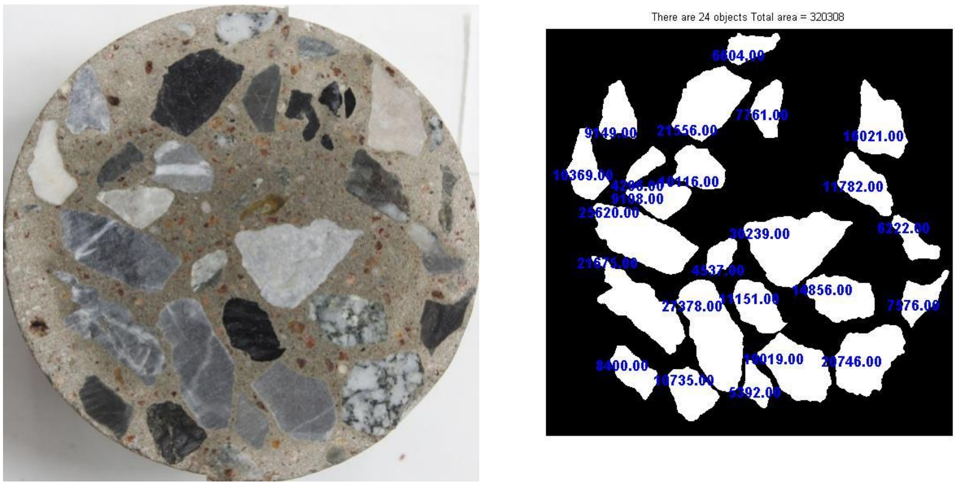
There are 24 objects Total area = 320308

P4-1

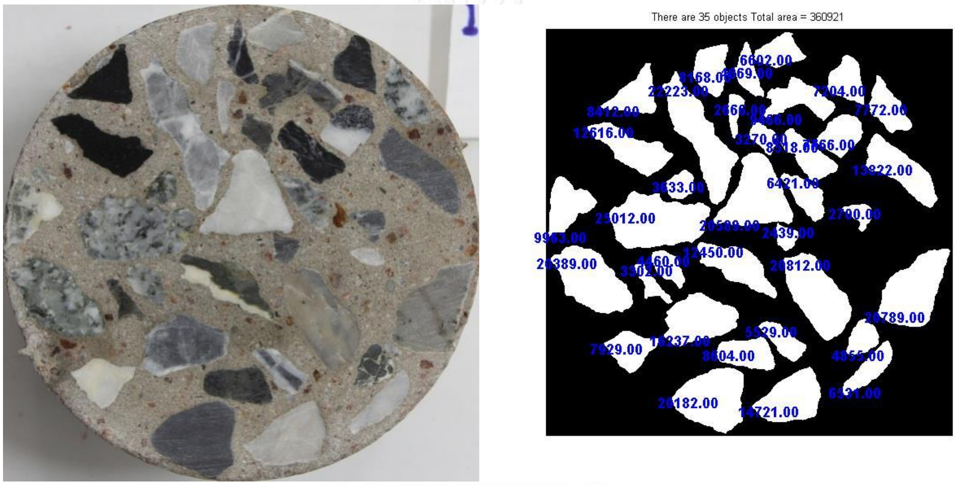
There are 35 objects Total area = 360921

P4-2

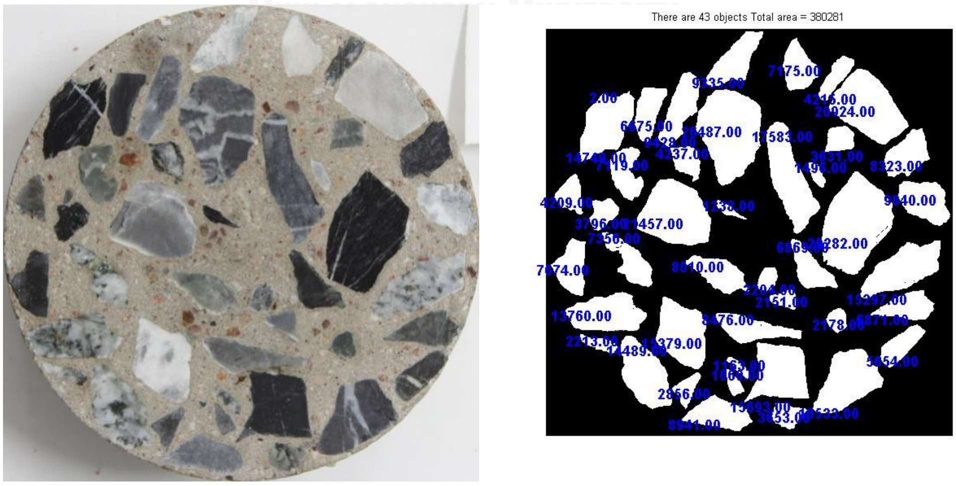
There are 43 objects Total area = 380281

P4-3

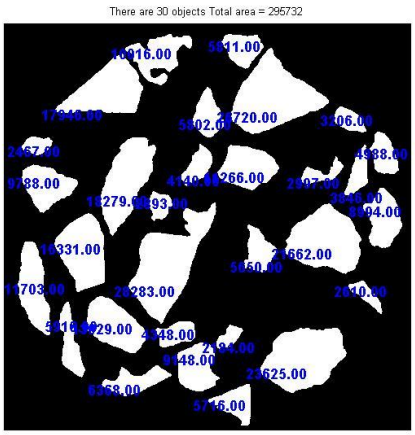

P4-4

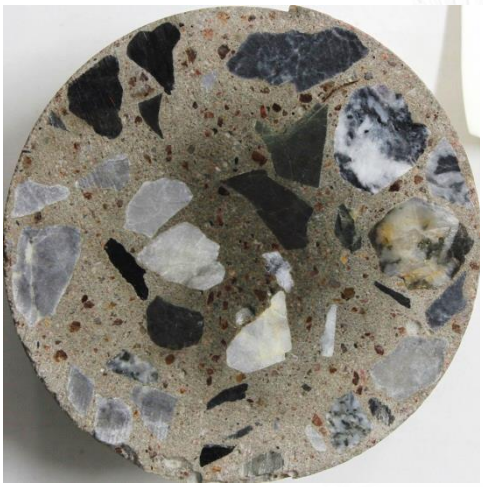

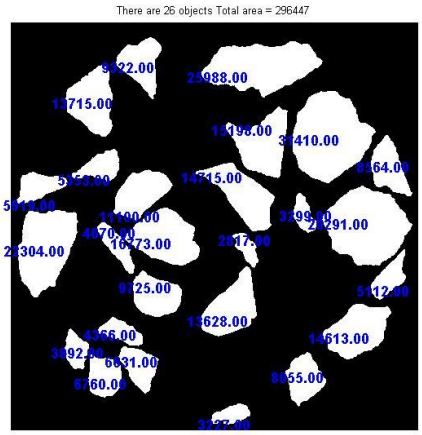

P4-5

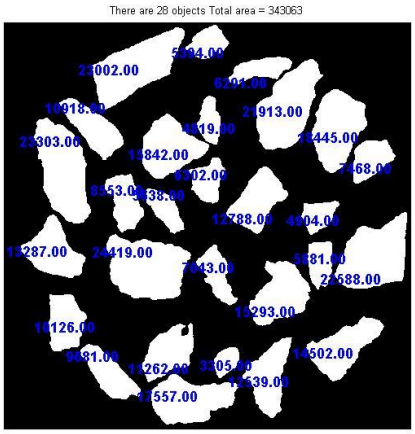

P4-6

(B1-P4) Image of cross-section of sample W55C-C


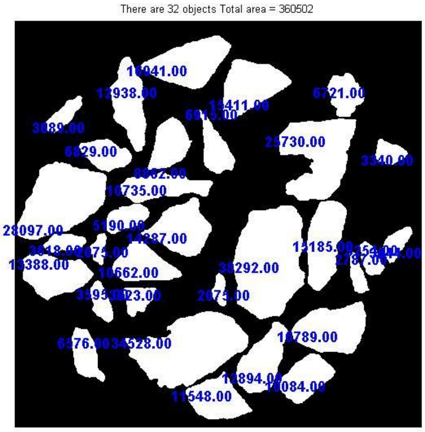

P5-1


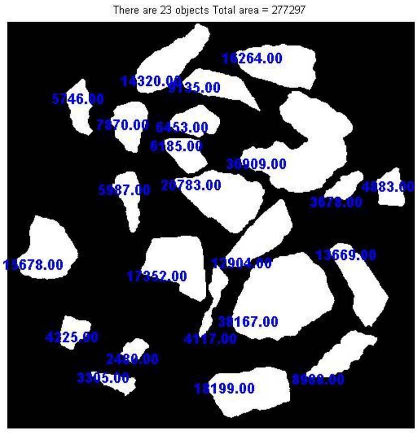

P5-2

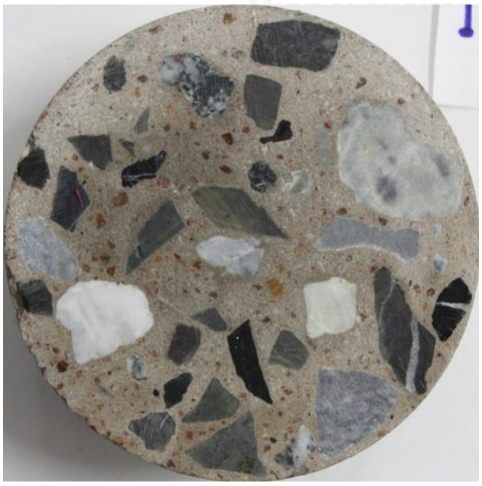
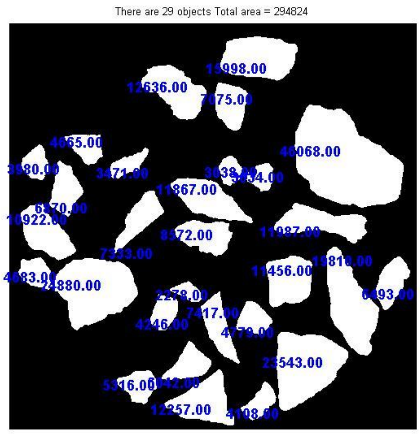

P5-3

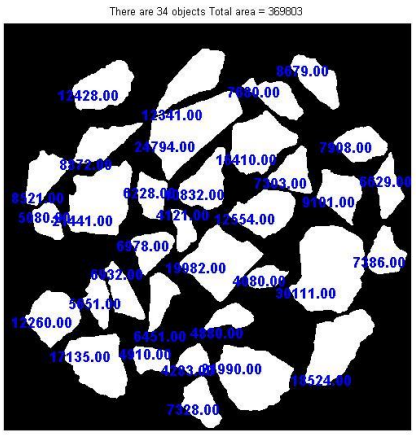

P5-4

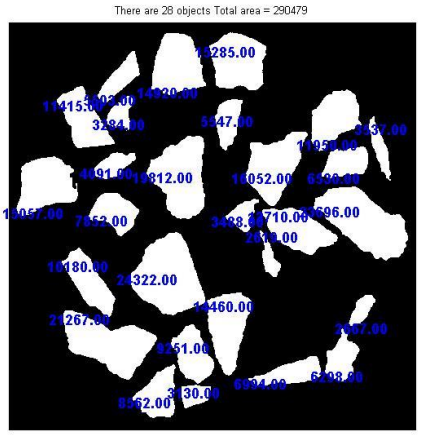

P5-5

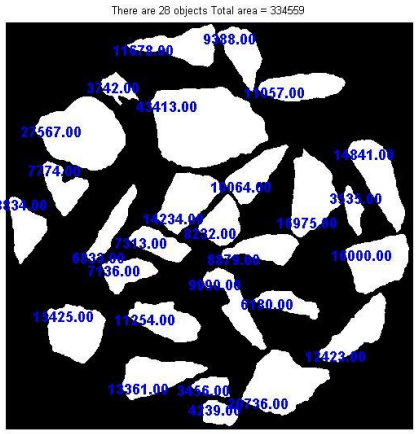

P5-6

(B1-P5) Image of cross-section of sample W65C-C

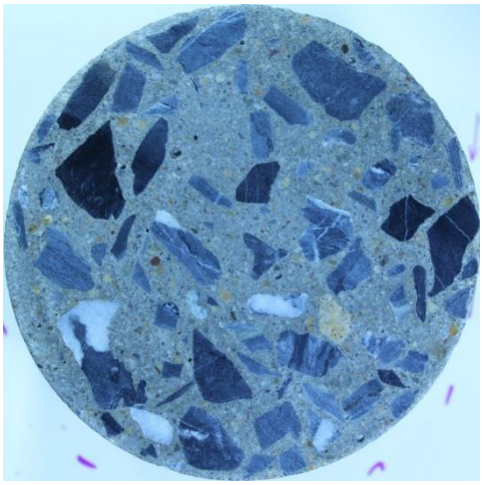

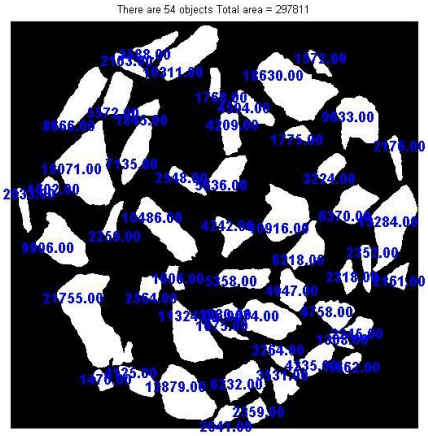
There are 54 objects Total area = 297811

P6-1

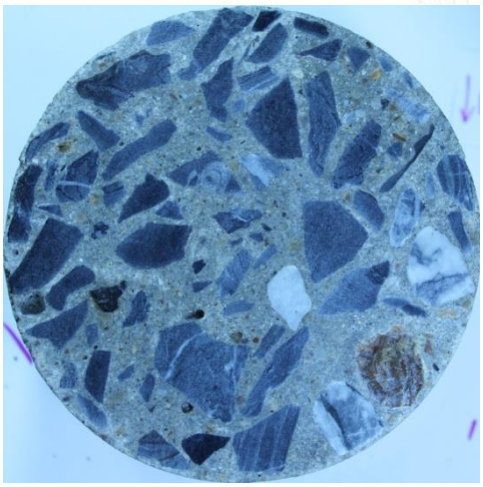

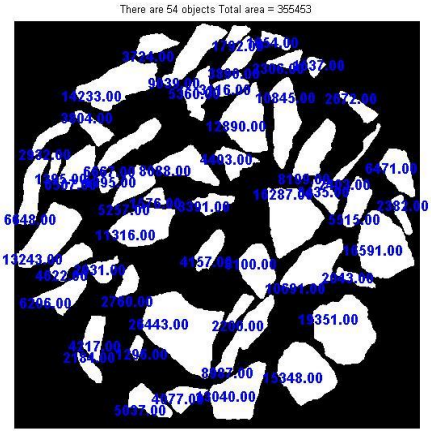
There are 54 objects Total area = 355453

P6-2

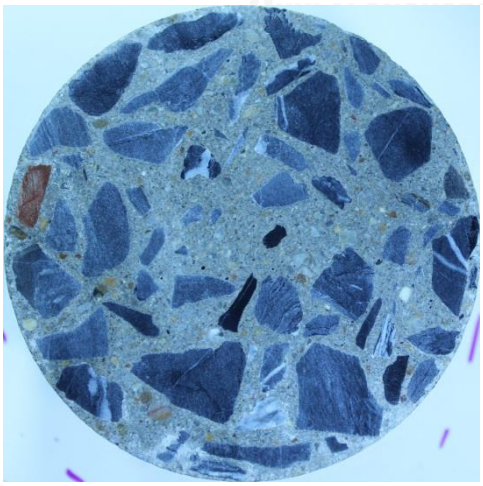

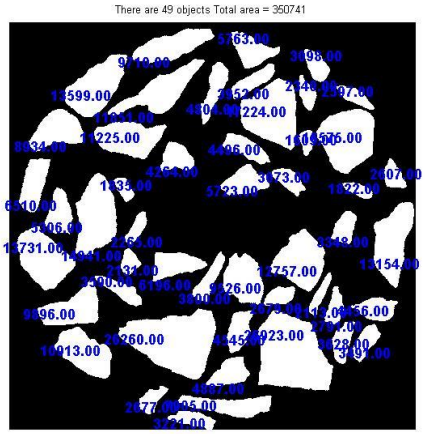
There are 49 objects Total area = 350741

P6-3

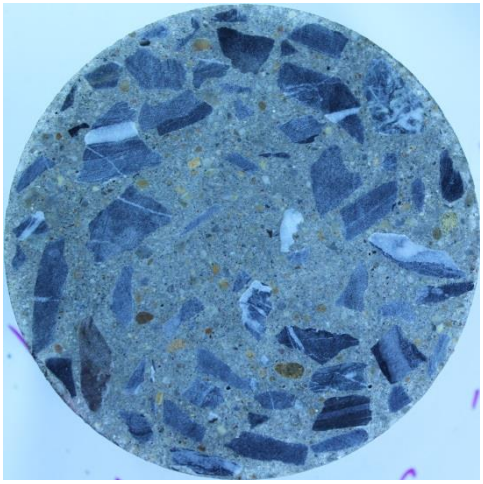

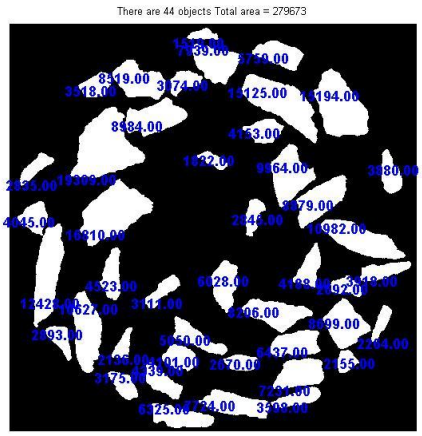

P6-4

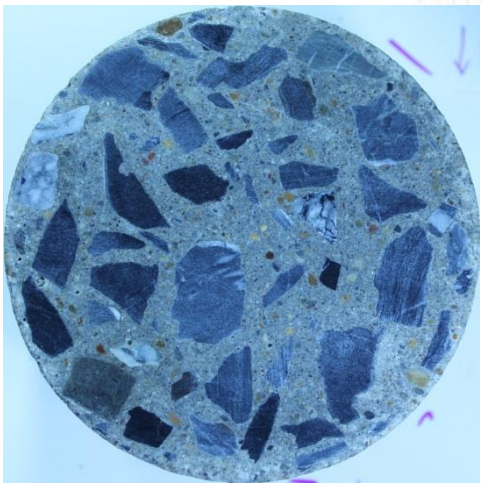

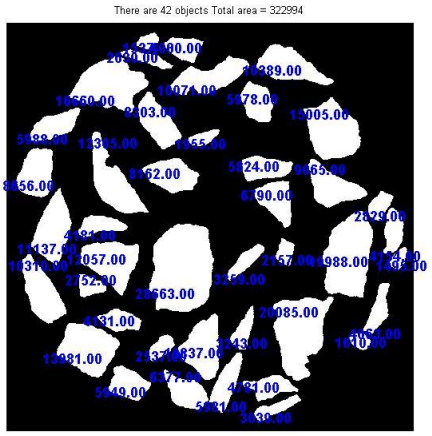

P6-5

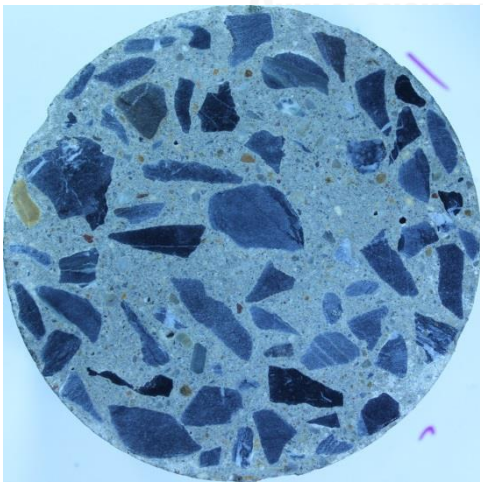

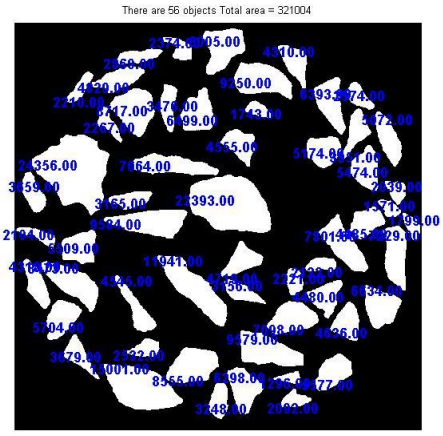

P6-6

(B1-P6) Image of cross-section of sample W45FA130-A

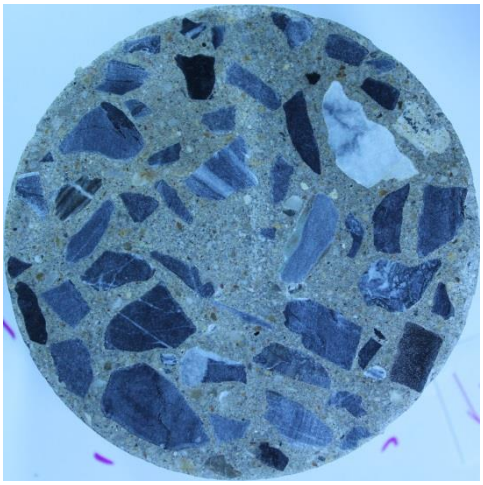

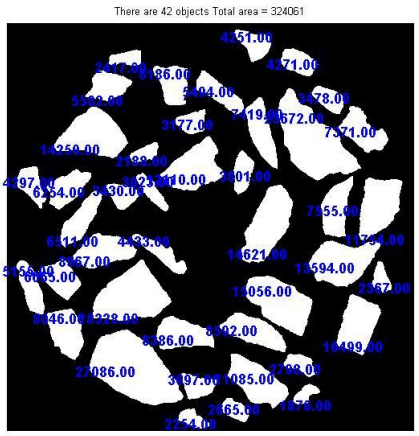
There are 42 objects Total area = 324061
4151.00
4271.00
7555.00
14621.00
13594.00
15056.00
25086.00

P7-1

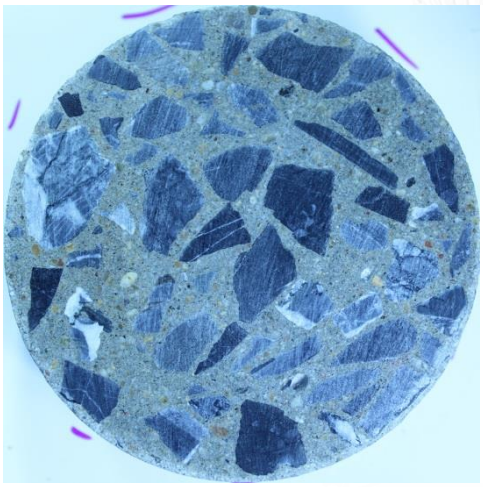

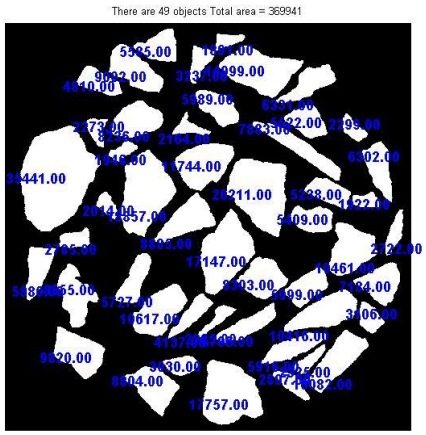
There are 49 objects Total area = 369941
5585.00
9893.00
5839.00
6302.00
25441.00
11744.00
25211.00
5509.00
11147.00
11617.00
9820.00
8504.00
11757.00

P7-2

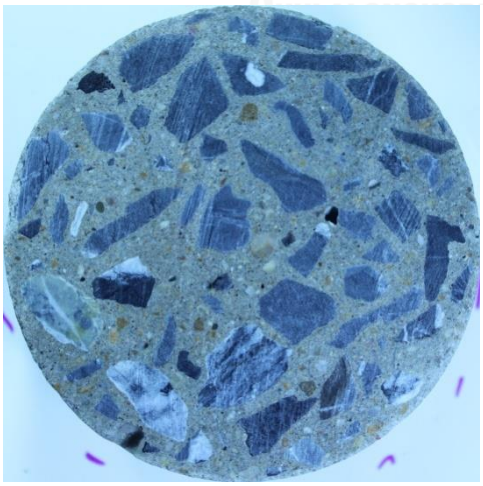

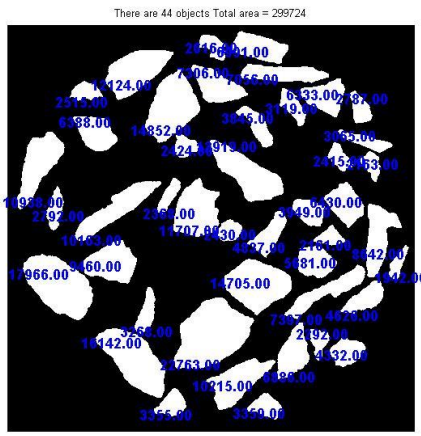
There are 44 objects Total area = 299724
6124.00
6388.00
14852.00
9460.00
11966.00
14705.00
16142.00
10215.00

P7-3

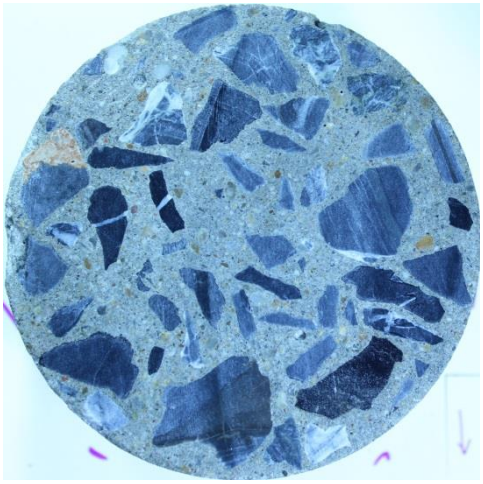

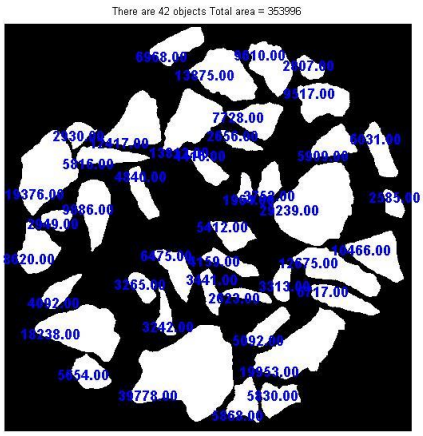

P7-4

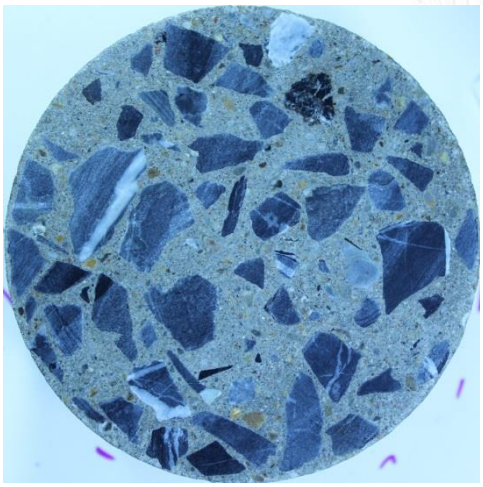

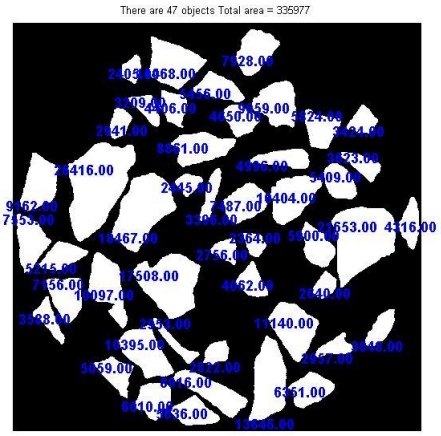

P7-5

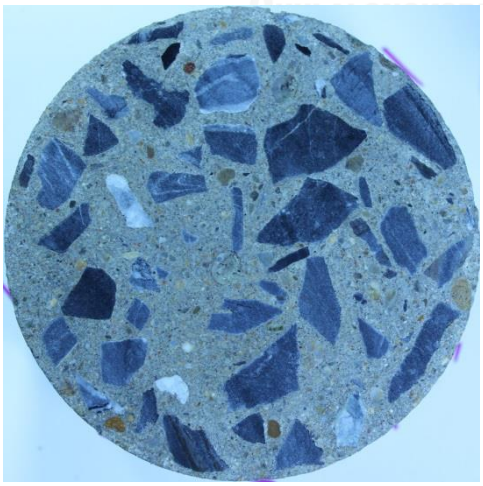

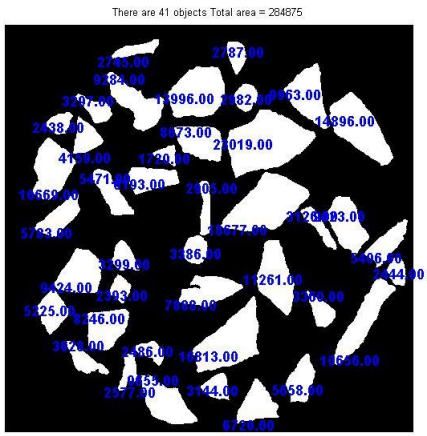

P7-6

(B1-P7) Image of cross-section of sample W55FA130-A

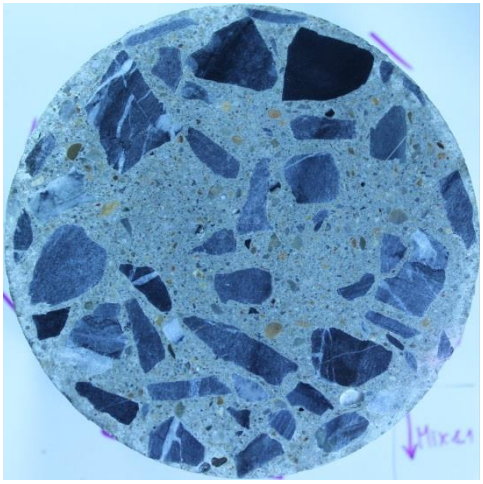

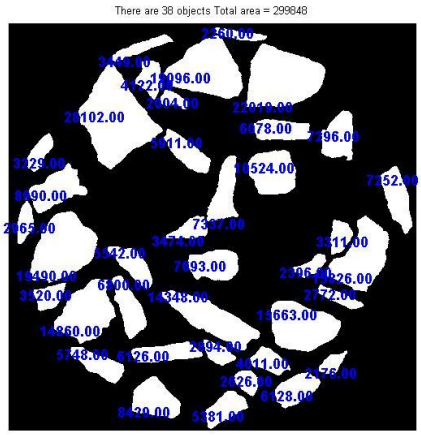
There are 38 objects Total area = 299848

P8-1

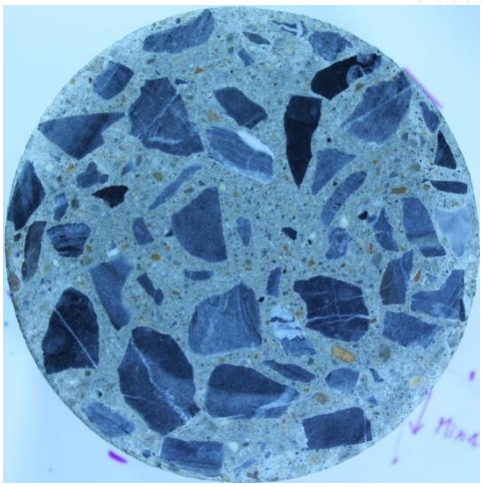

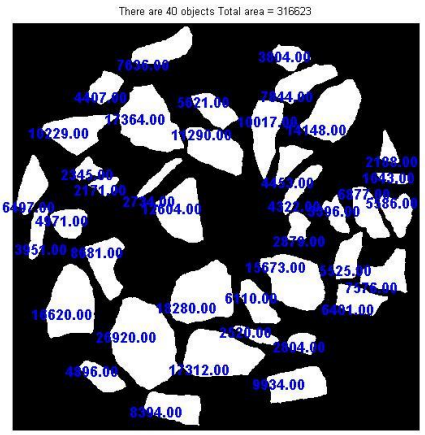
There are 40 objects Total area = 316623

P8-2

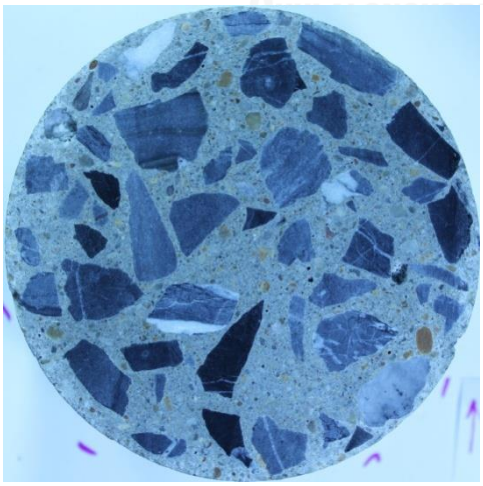

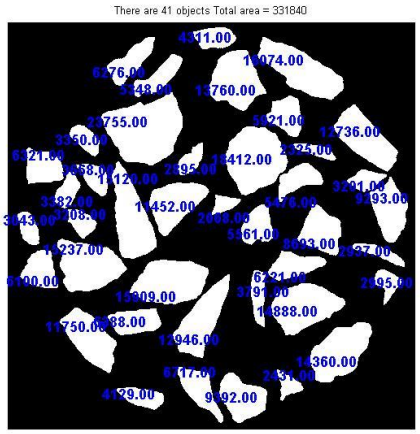
There are 41 objects Total area = 331840

P8-3

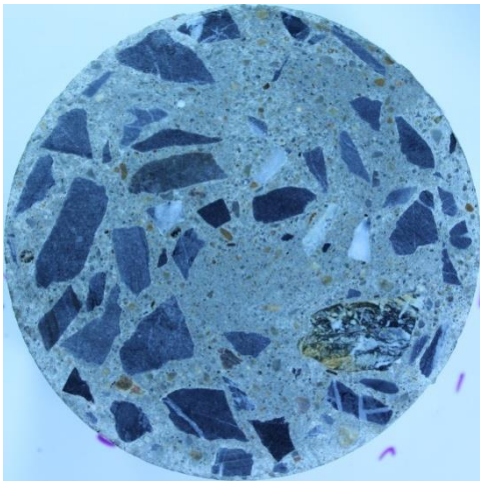

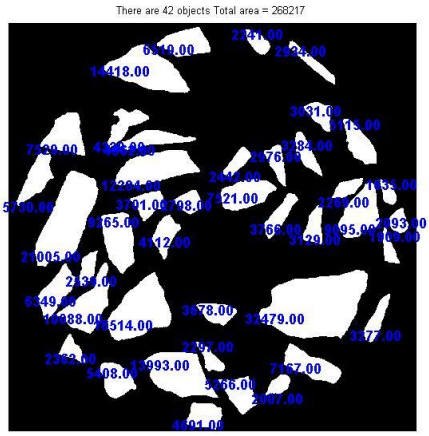

P8-4

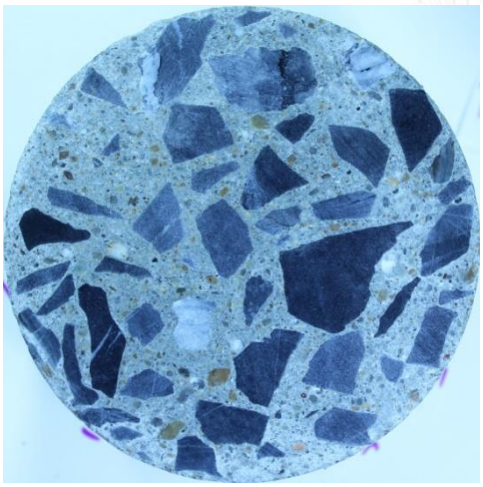

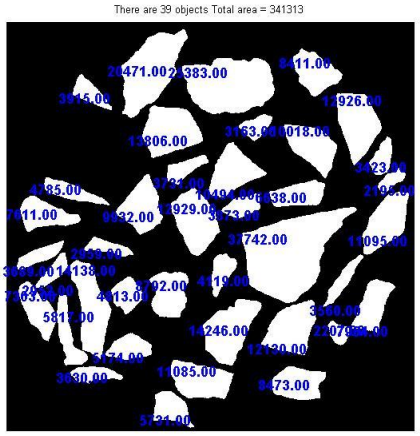

P8-5

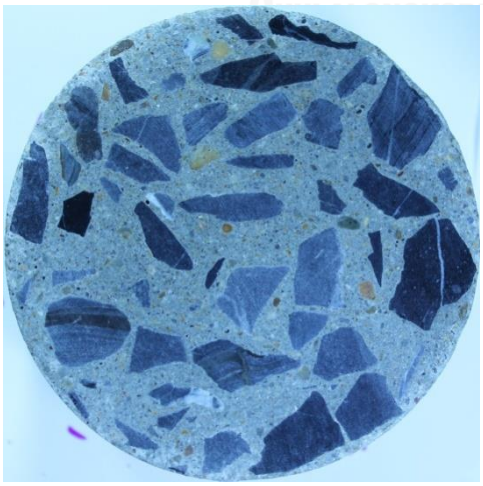

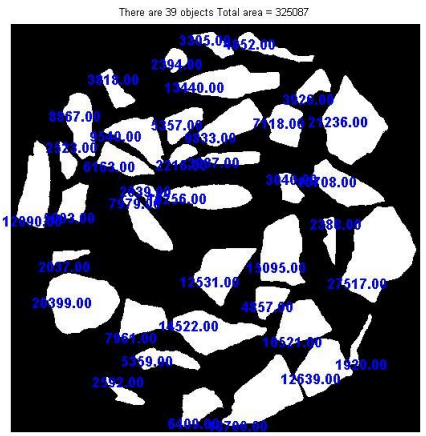

P8-6

(B1-P8) Image of cross-section of sample W45FA230-A

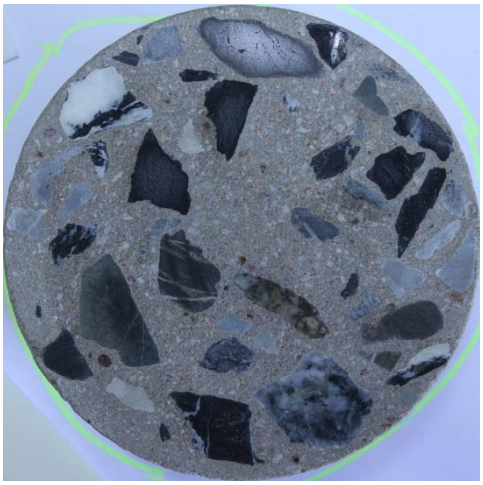

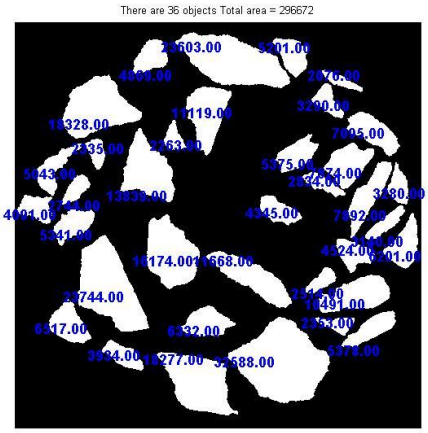
There are 36 objects Total area = 296672

P9-1

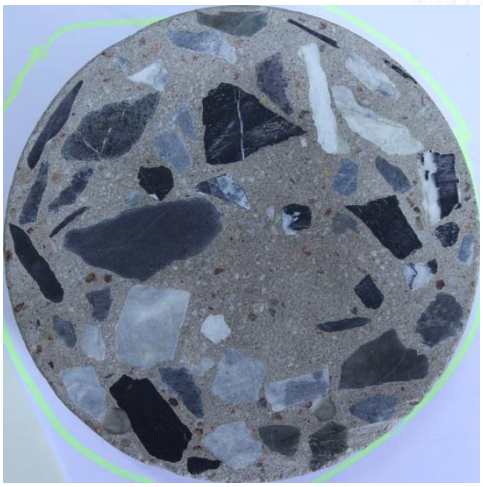

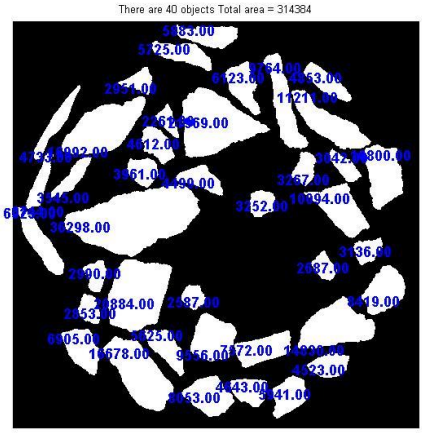
There are 40 objects Total area = 314384

P9-2

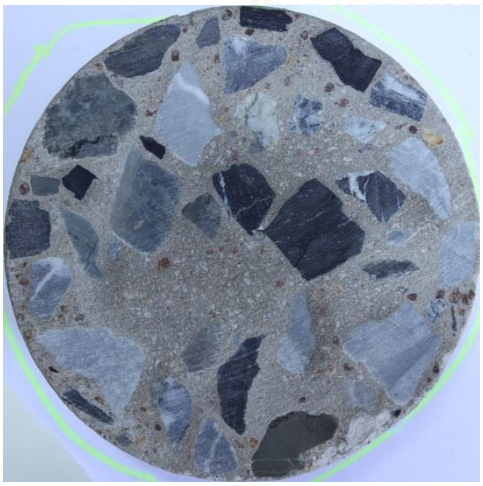

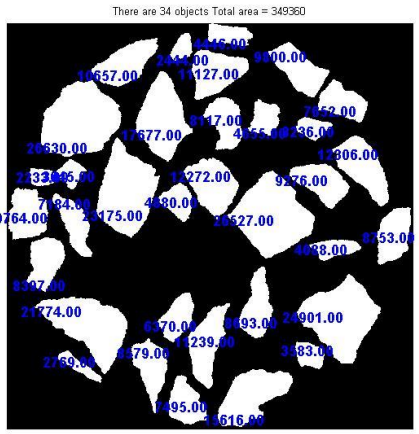
There are 34 objects Total area = 349360

P9-3

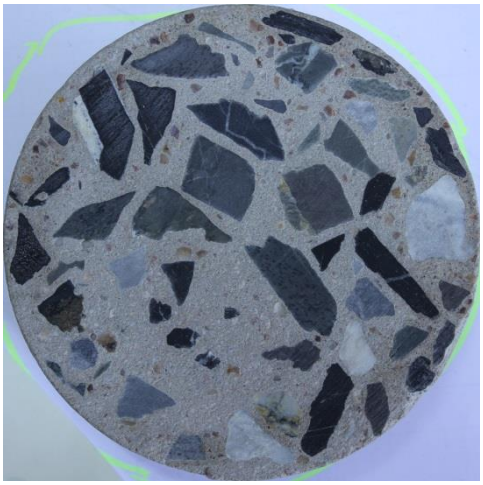

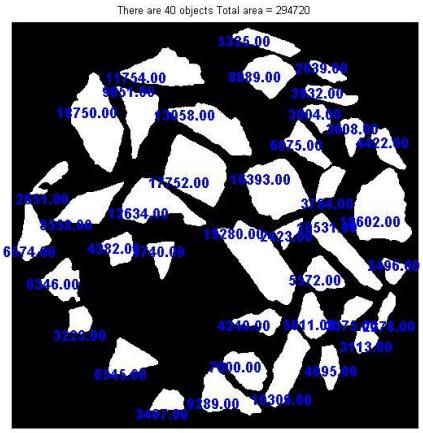

P9-4

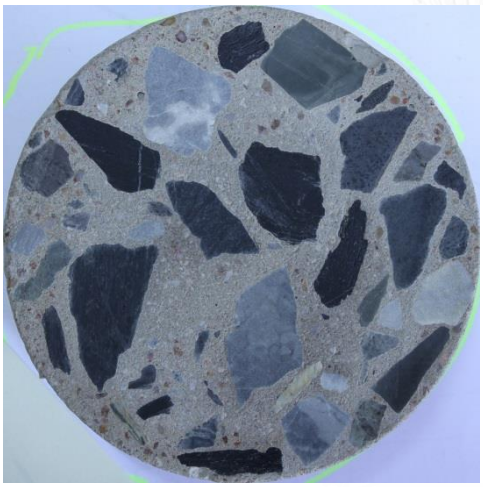

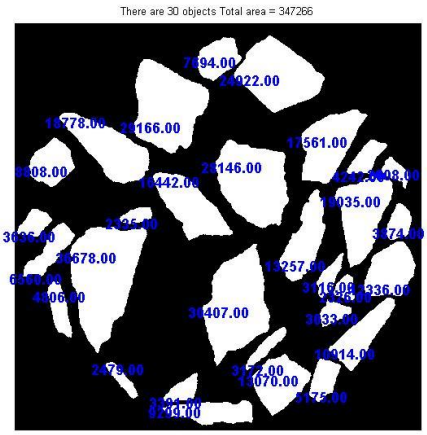

P9-5

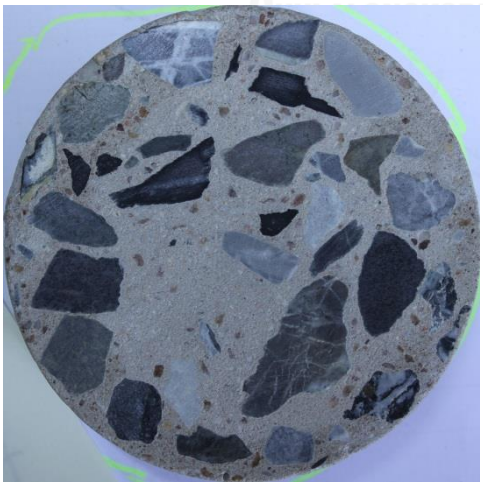

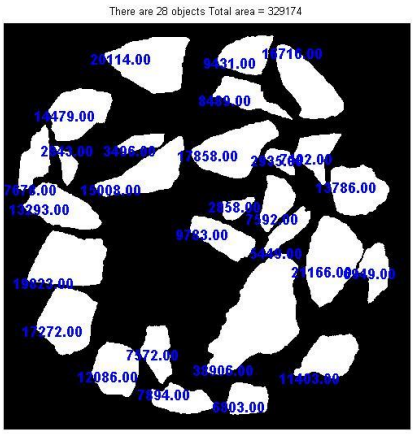

P9-6

(B1-P9) Image of cross-section of sample W45FA150-B

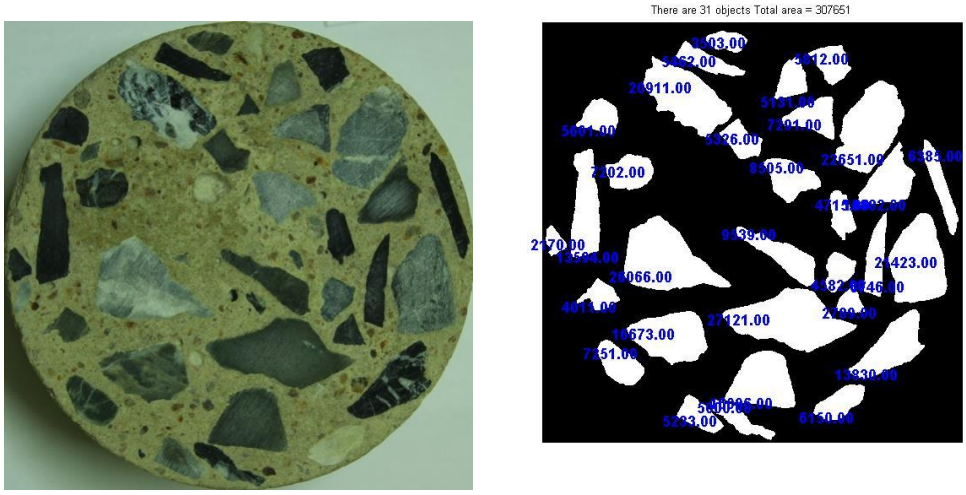

P10-1

P10-2

P10-3

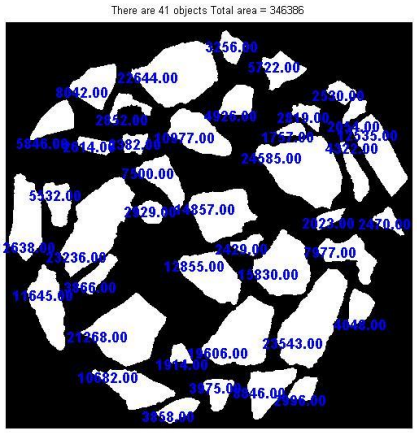

P10-4

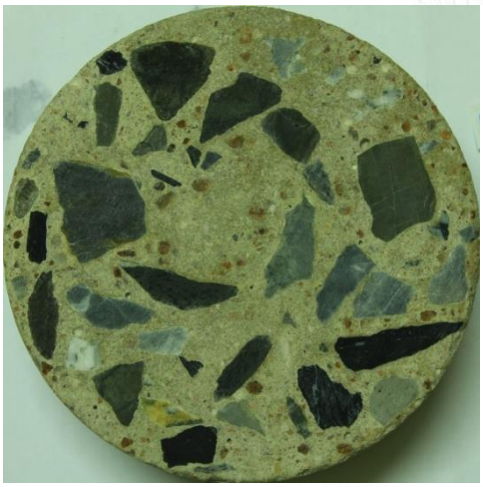

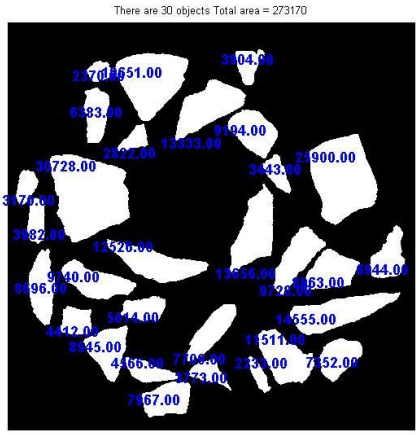

P10-5

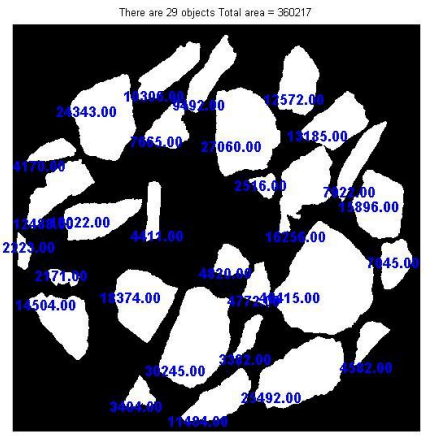

P10-6

(B1-P10) Image of cross-section of sample W45LP110-B

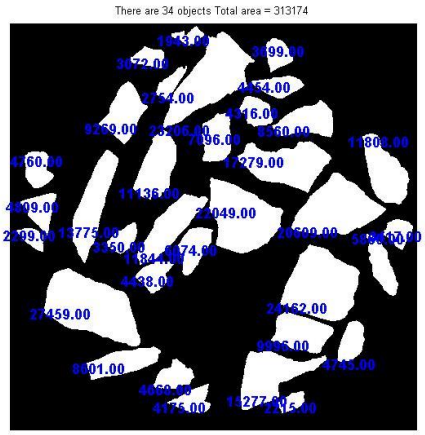

P11-1

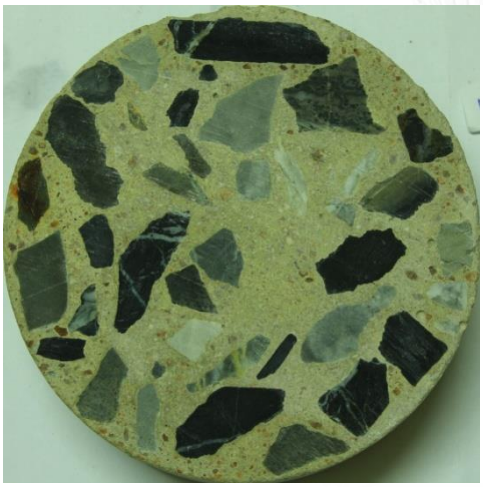

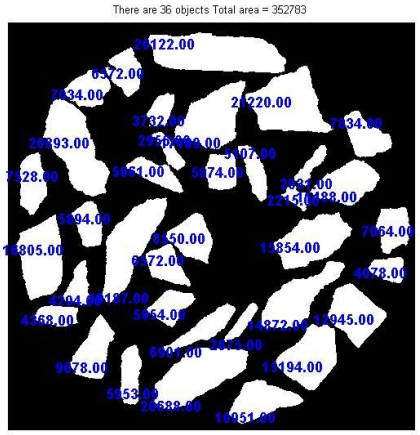

P11-2

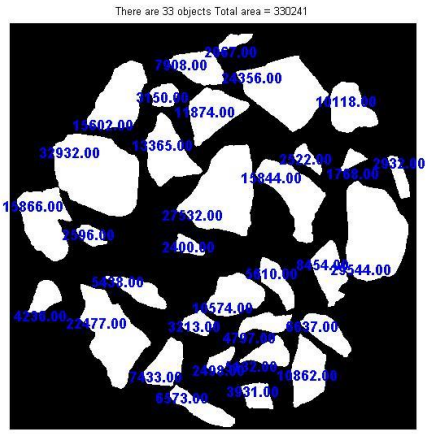

P11-3

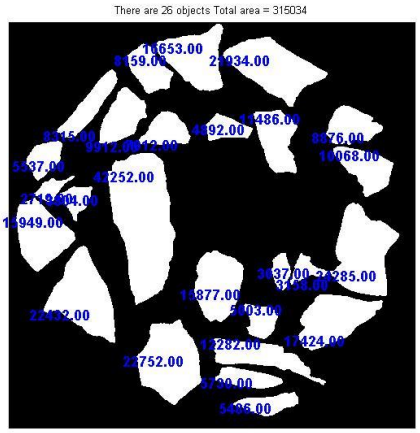

P11-4

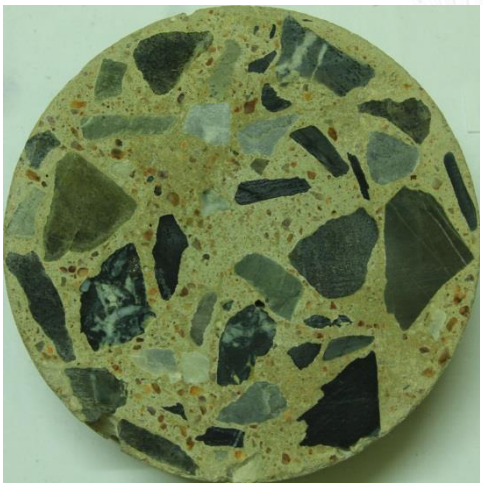

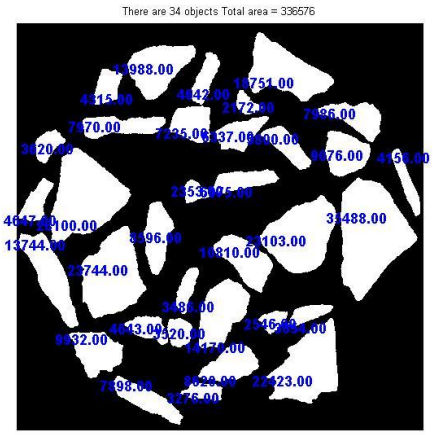

P11-5

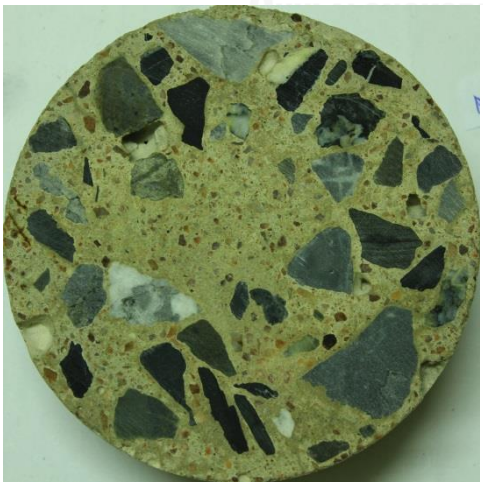

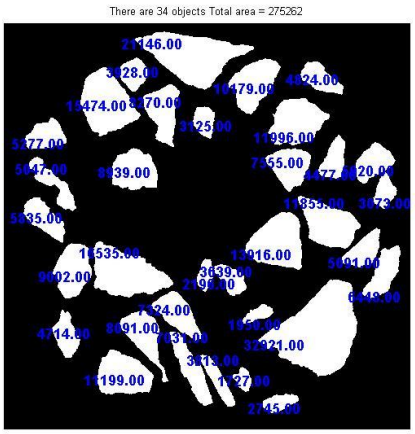

P11-6

(B1-P11) Image of cross-section of sample W45LP210-B

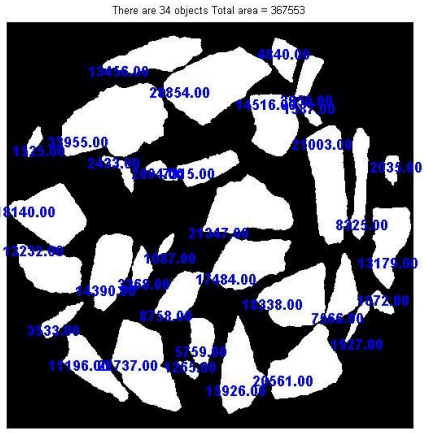

P12-1

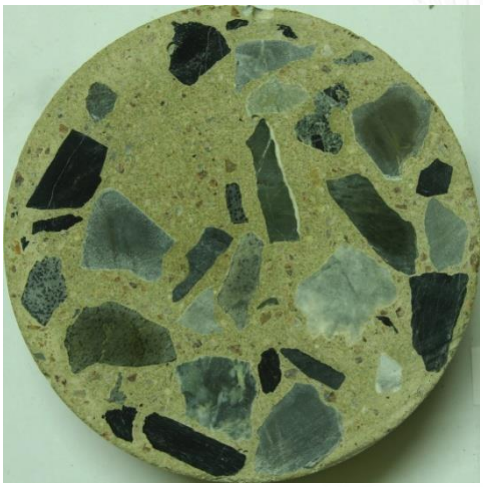

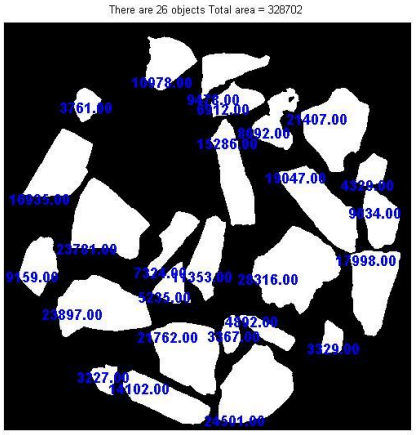

P12-2

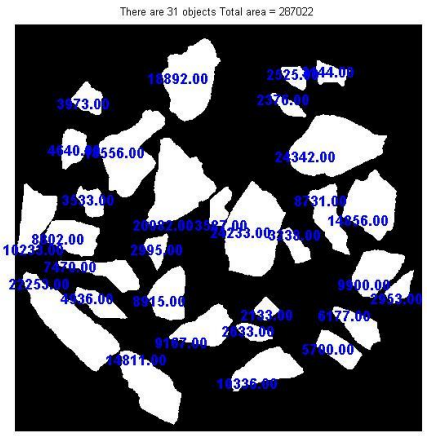

P12-3

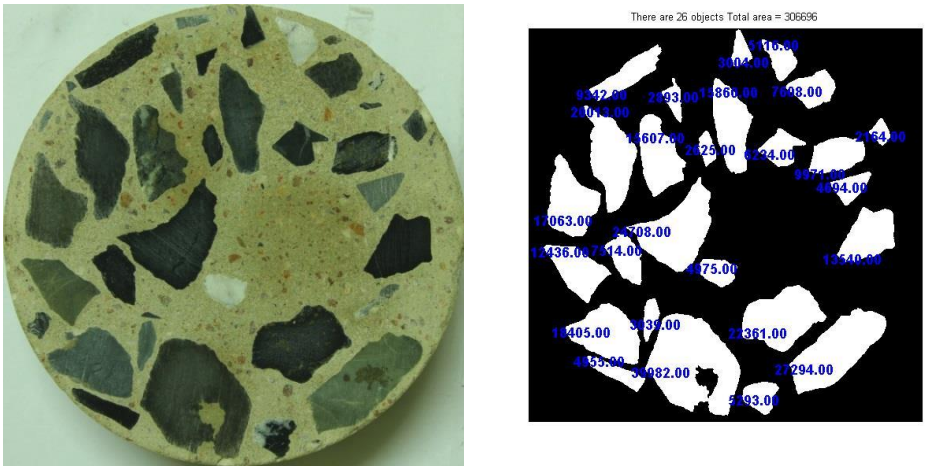

P12-4

P12-5

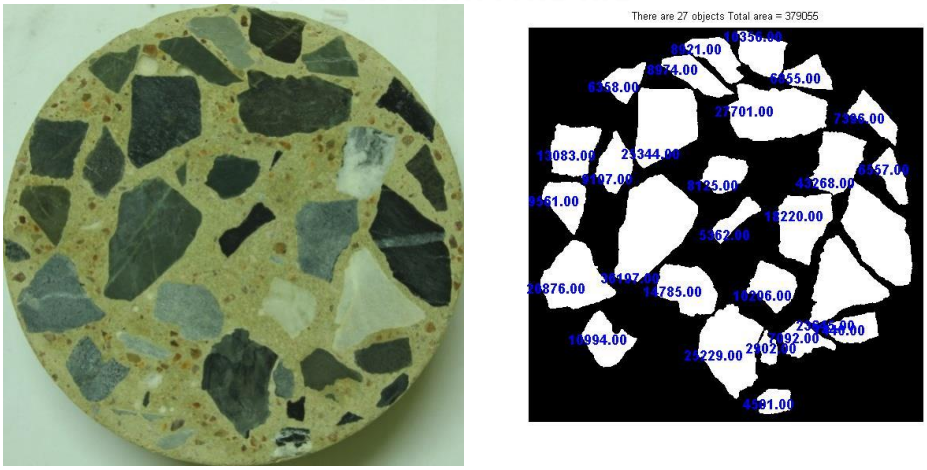

P12-6

(B1-P12) Image of cross-section of sample W45LP220-B

Figure B1 (P1-P12) Image of cross-section of concrete sample cured water in laboratory

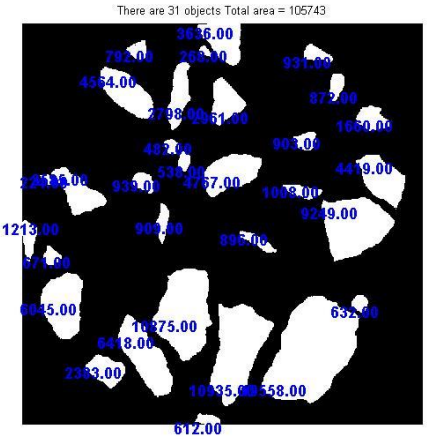

P13-1

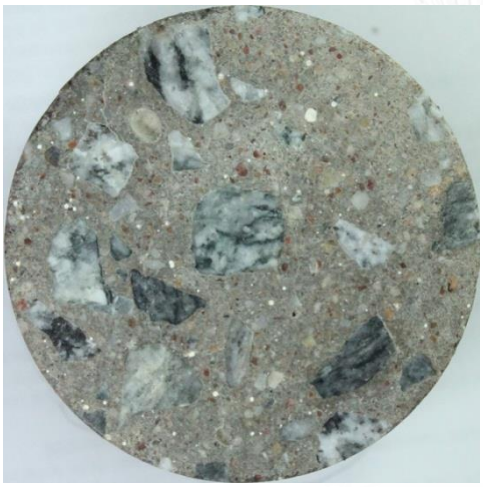

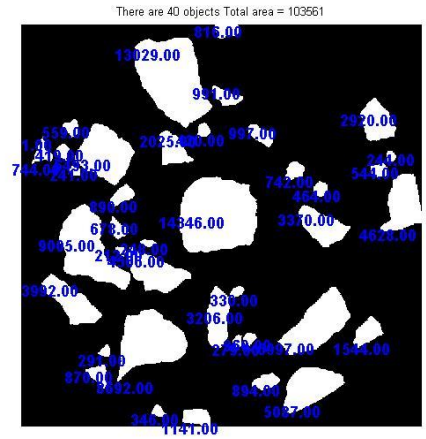

P13-2

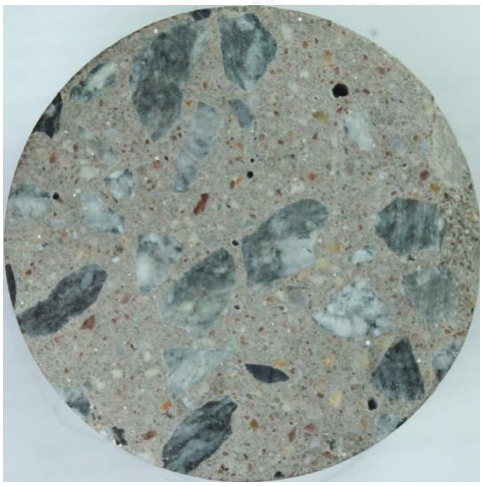

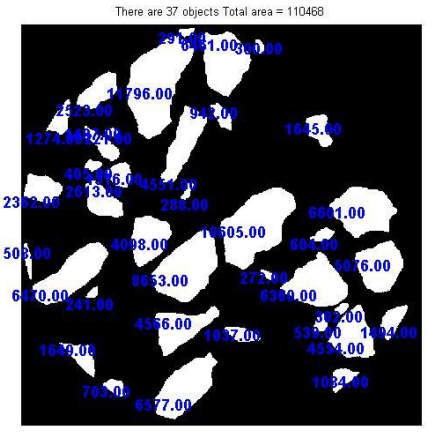

P13-3

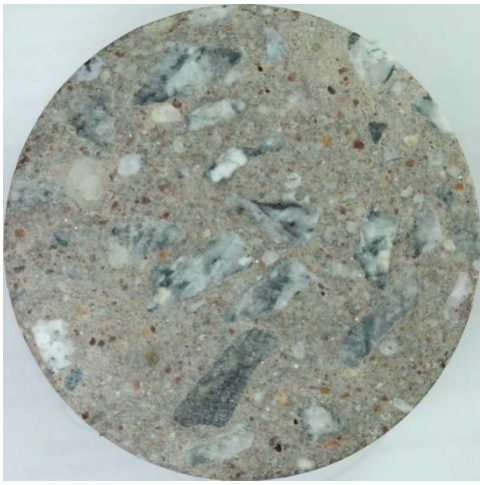

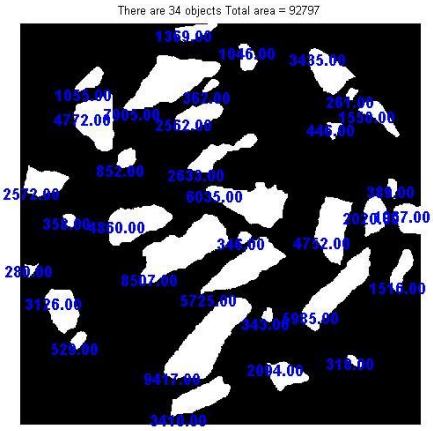

P13-4

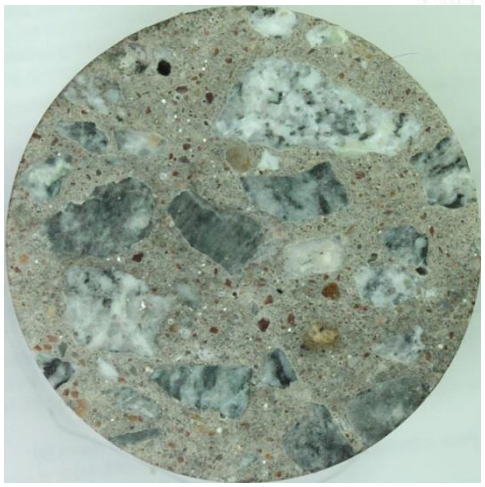

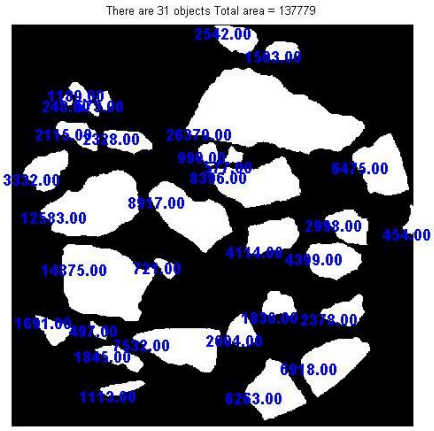

P13-5

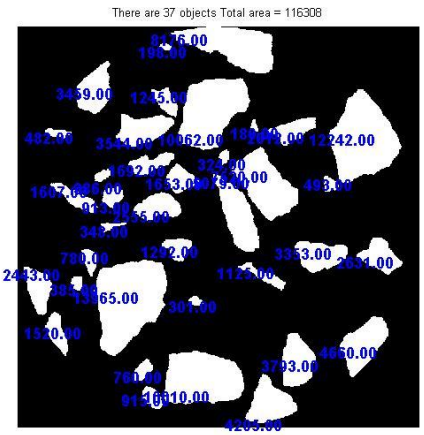

P13-6

(B2-P13) Image of cross-section of sample A

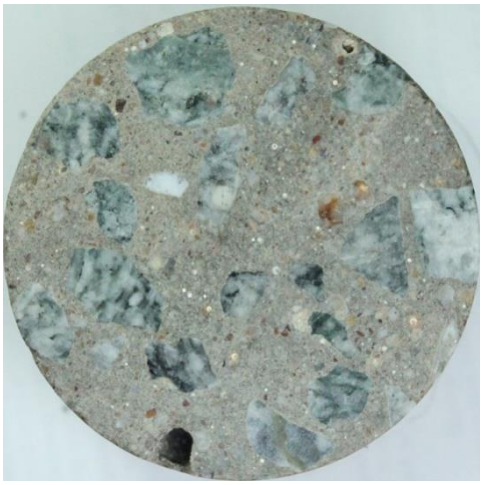

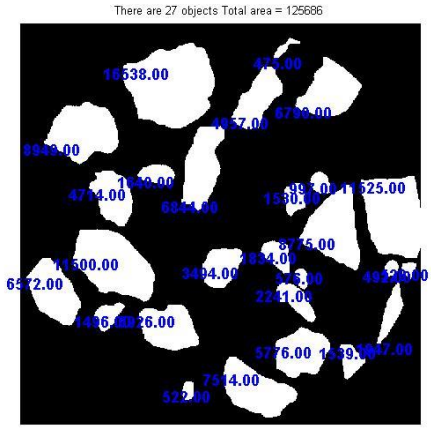

P14-1

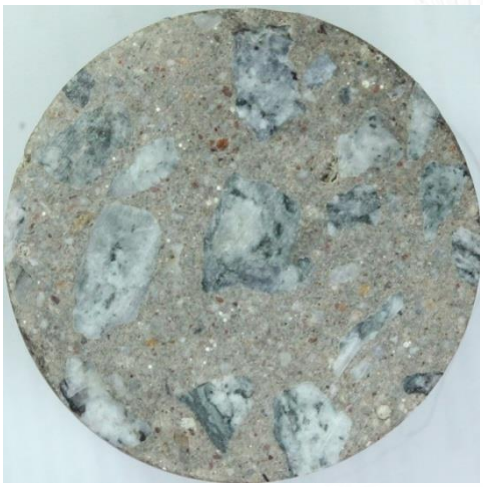

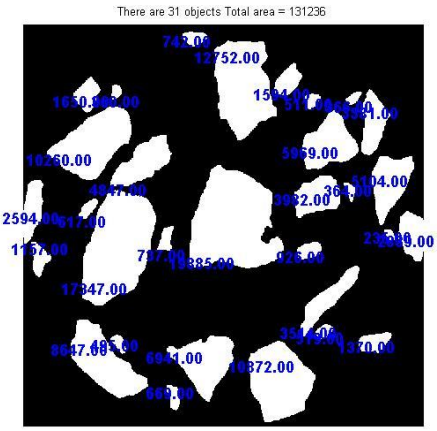

P14-2

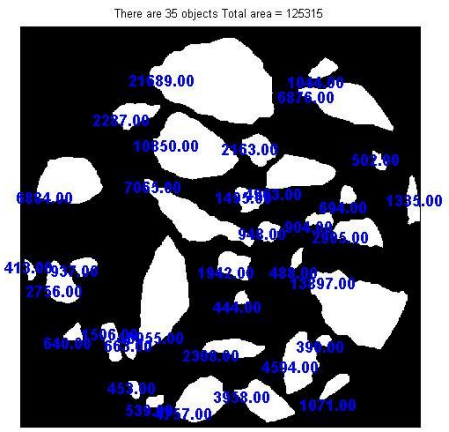

P14-3

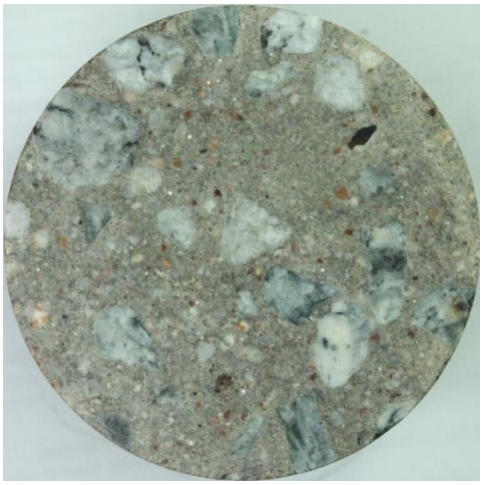

P14-4

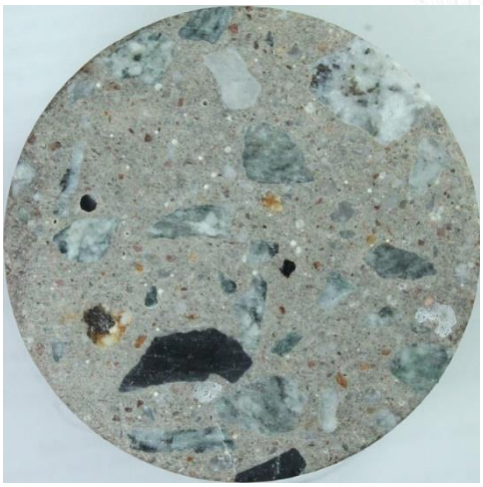

P14-5

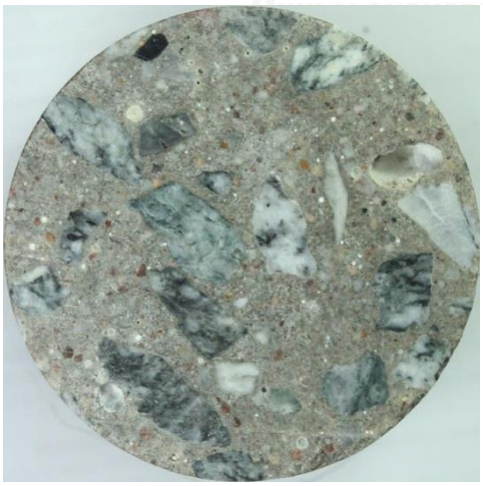

P14-6

(B2-P14) Image of cross-section of sample B

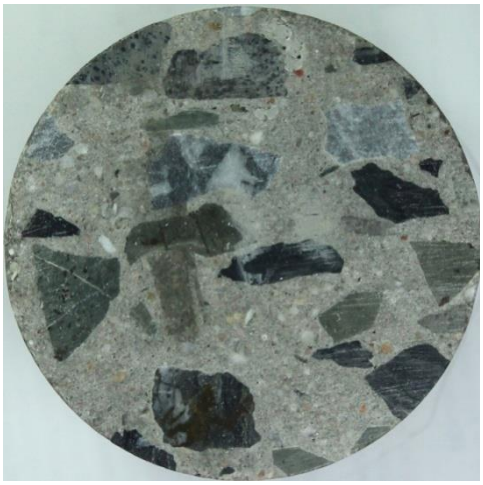

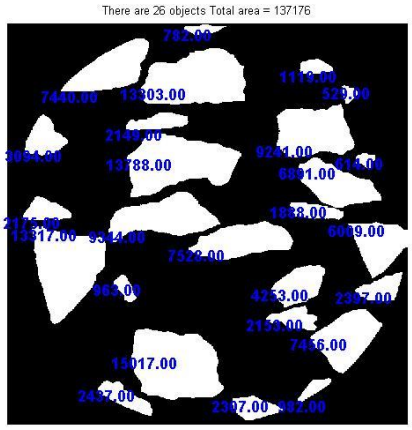

P15-1

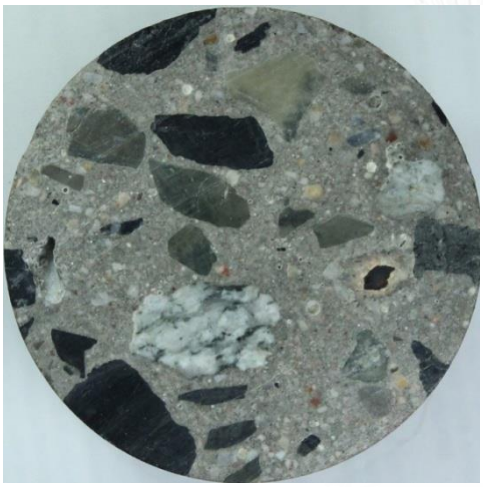

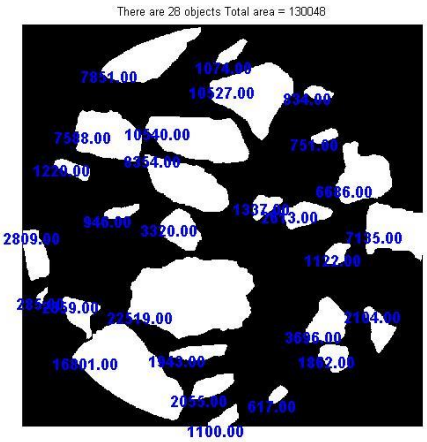

P15-2

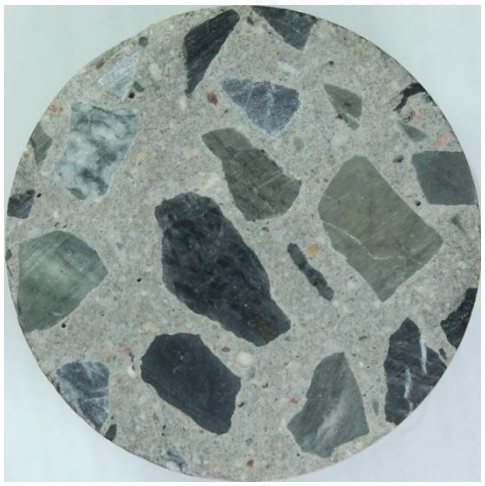

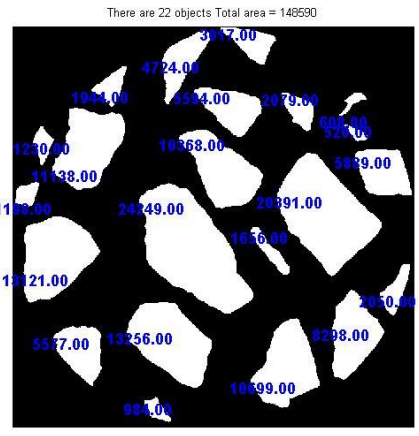

P15-3

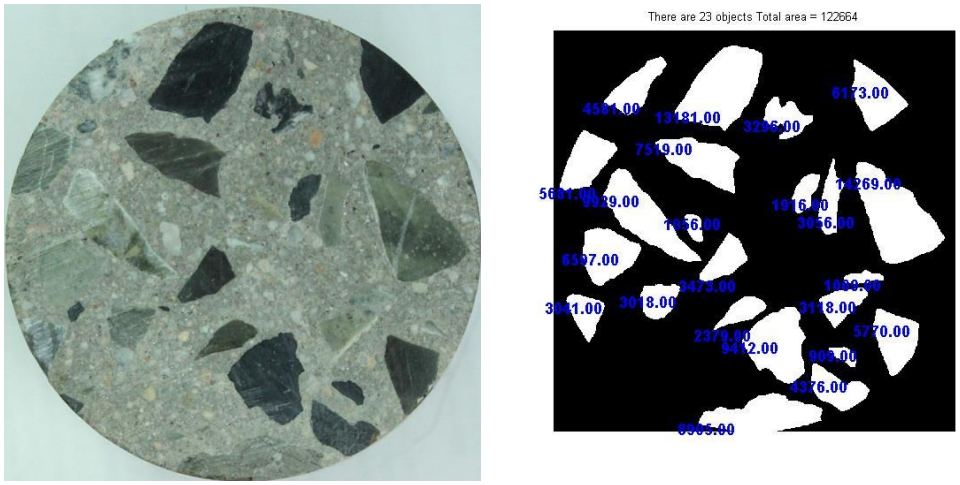

P15-4

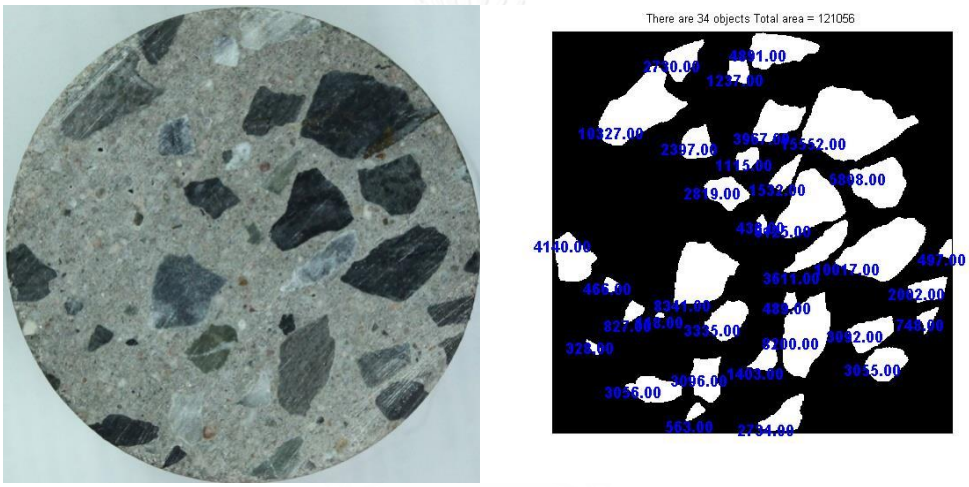

P15-5

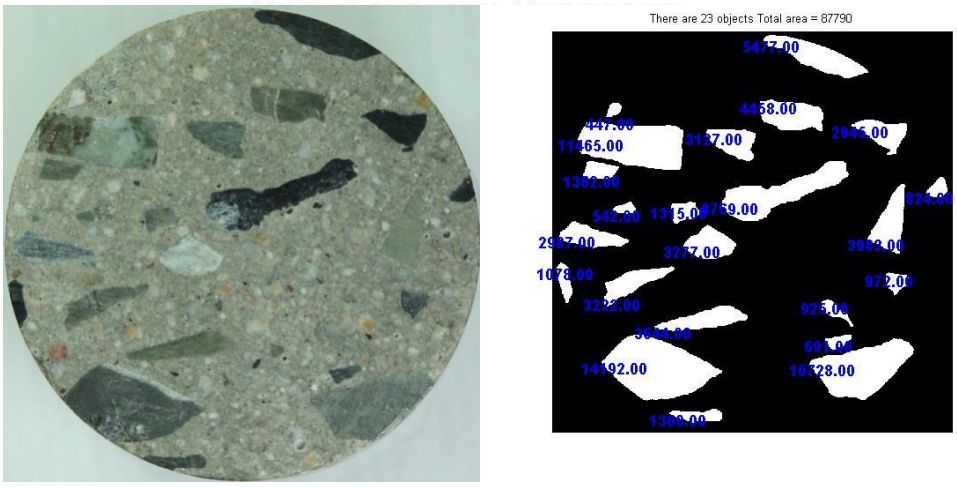

P15-6

(B2-P15) Image of cross-section of sample C

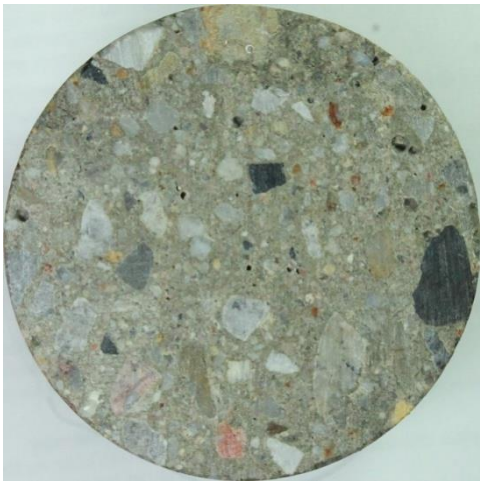

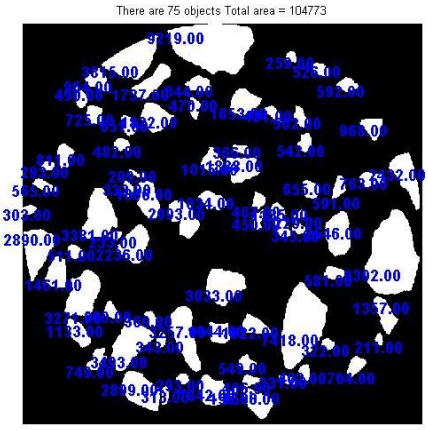

P16-1

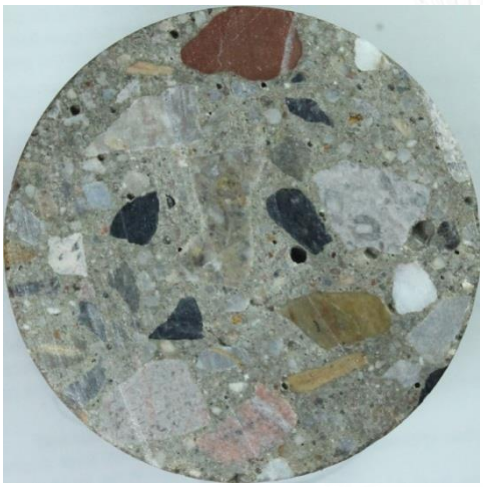

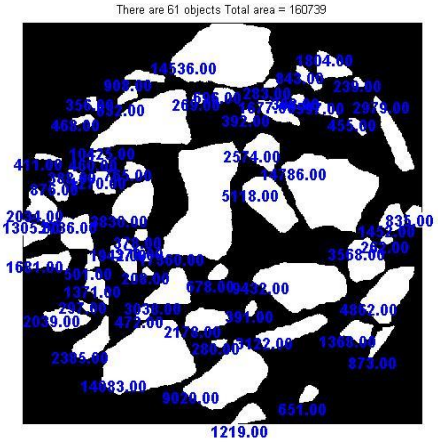

P16-2

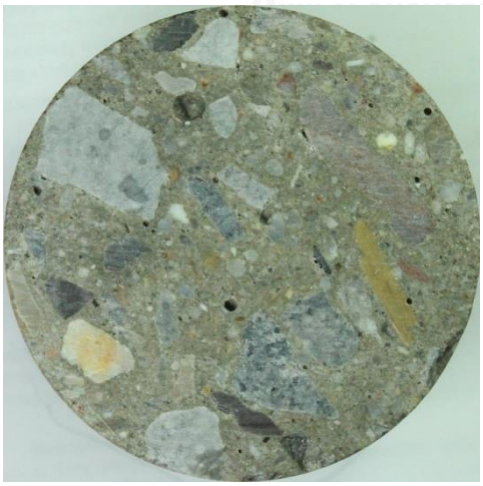

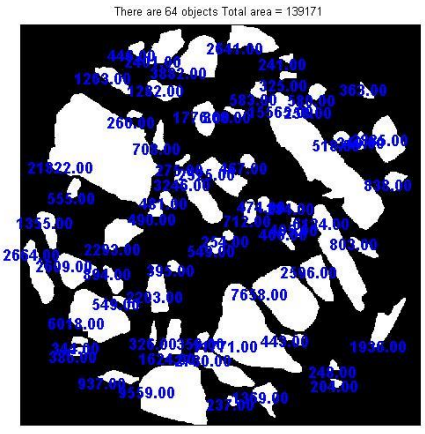

P16-3

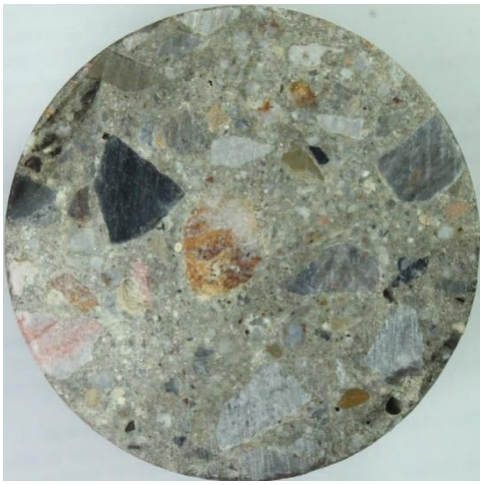

P16-4

P16-5

P16-6

(B2-P16) Image of cross-section of sample D

Figure B2 Image of cross-section of concrete sample cored existing structure

Table B1 Result of Image analysis of concrete sample cured water in laboratory													
Notation	Sample	Z=±0.25			Z=±0.50			Z=±0.75			Z=±1.00		
		CA/C*	kg.**	% errs.	CA/C*	kg.**	% errs.	CA/C*	kg.**	% errs.	CA/C*	kg.**	% errs.
P1	W45C-A	0.391	1057	+0.91	0.389	1050	+0.26	0.383	1033	-1.31	0.383	1033	-1.31
P2	W45C-B	0.395	1065	+0.34	0.398	1075	+1.24	0.393	1062	+0.03	0.397	1071	+0.93
P3	W45C-C	0.383	1035	+0.95	0.383	1035	+0.95	0.383	1035	+0.95	0.384	1037	+1.23
P4	W55C-C	0.408	1101	+7.41	0.408	1101	+7.41	0.422	1140	+11.23	0.400	1079	+5.26
P5	W65C-C	N/A	N/A	N/A	0.426	1150	+12.19	0.401	1082	+5.53	0.390	1054	+2.82
P6	W45FA130-A	0.393	1062	+1.43	0.393	1062	+1.43	0.388	1048	+0.06	0.388	1048	+0.06
P7	W55FA130-A	0.407	1098	+4.89	0.407	1098	+4.89	0.406	1095	+4.58	0.406	1095	+4.58
P8	W45FA230-A	0.398	1074	+2.55	0.392	1059	+1.18	0.392	1059	+1.18	0.403	1088	+3.86
P9	W45FA150-B	0.408	1112	+5.12	0.411	1121	+6.04	0.411	1121	+6.04	0.405	1103	+4.34
P10	W45LP110-B	0.397	1083	+1.02	0.397	1083	+1.02	0.393	1071	-0.15	0.400	1090	+1.67
P11	W45LP210-B	N/A	N/A	N/A	0.407	1110	+3.47	0.405	1104	+2.92	0.405	1104	+2.92
P12	W45LP220-B	0.424	1157	+7.87	0.419	1143	+6.62	0.414	1128	+5.20	0.409	1115	+3.98

Table B2 Result of Image analysis of concrete sample cored existing structure

Notation	Sample	CA/C*	kg./m^3**
P13	A	0.315	850
P14	B	0.334	901
P15	C	0.360	973
P16	D	0.364	981

* CA/C is average ratio by volume of coarse aggregate to concrete

** Content of analytical result of coarse aggregate per concrete 1 m^3 at SSD state

Appendix C

Degree of hydration and Pozzolanic reaction

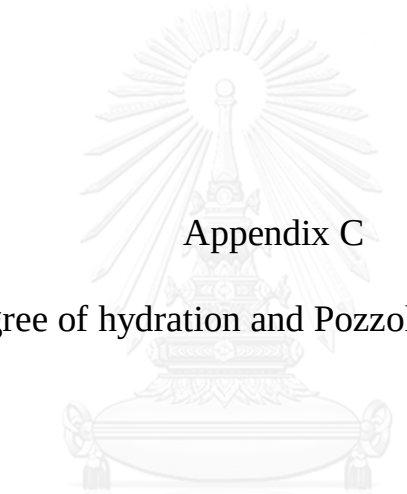

Table C1 Degree of cement hydration and Pozzolanic reaction of sample

Sample	Degree of hydration (α_c)			Degree of Pozzolanic reaction (α_f)		
	14 days	28 days	91 days	14 days	28 days	91 days
W45C-A	-	93.62	96.45	-	-	-
W45C-B	-	93.89	96.76	-	-	-
W45C-C	91.09	-	96.76	-	-	-
W55C-C	96.67	-	99.38	-	-	-
W65C-C	98.57	-	99.77	-	-	-
W45FA130-A	-	93.17	96.78	-	31.00	45.48
W55FA130-A	-	96.89	98.21	-	33.01	59.95
W45FA230-A	-	93.17	96.77	-	23.98	35.17
W45FA150-B	-	92.81	97.91	-	23.34	34.23
W45LP110-B	-	93.82	96.78	-	-	-
W45LP210-B	-	93.82	96.78	-	-	-
W45LP220-B	-	93.65	96.89	-	-	-

VITA

Thidaporn Chuosavasdi was born in Thailand. She graduated B.Eng in Civil Engineering from Burapha University, Thailand, in 2006. Afterwards she was granted a scholarship to study doctoral degree under AUN/SEED-Net program in the field of Structural Engineering, Department of Civil Engineering, Chulalongkorn University, Thailand, 2007-2015. Her interests include durability, inspection, repair, and maintenance of concrete structures.

To contact Thidaporn, please email thidaporn.ch@gmail.com or krati_yam@hotmail.com